Universitat Autònoma de Barcelona

Differences in soil zinc availability as a driver of natural selection in Arabidopsis thaliana and rhizosphere bacteria

Miquel Llimós Turet

Differences in soil zinc availability as a driver of natural selection in *Arabidopsis thaliana* and rhizosphere bacteria

By

Miquel Llimós Turet

Doctoral Thesis

Doctoral Program in Plant Biology and Biotechnology

Universitat Autònoma de Barcelona

Departament de Biologia Animal, Biologia Vegetal i Ecologia
Unitat de Fisiologia Vegetal

Single thesis jointly supervised by:

Dr. Charlotte Poschenrieder

Dr. Soledad Martos

_____ _____

Dr. Charlotte Poschenrieder Dr. Soledad Martos

_____

Miquel Llimós Turet

Universitat Autònoma de Barcelona

September 2017

Declaration:

I declare that this thesis was composed by myself and has not been submitted for any other degree. The work described is my own, unless otherwise indicated.

Miquel Llimós Turet,

28th September 2017

“The ultimate goal of farming is not the growing of the crops,

but the cultivation and perfection of human beings”

Masanobu Fukuoka, 1975

Dedicat als meus pares, Mª Teresa Turet Capellas i Lluís Llimós Roca.

Pel seu constant suport i per haver forjat en mi

les bases de la persona que sóc avui.

Acknowledgements

This work was funded by the Spanish government (project BFU2013-42839-R and BFU2016-75176-R) and by the UAB (PIF pre-doctoral and short stay abroad scholarship).

This thesis covers a broad spectrum of subjects and would not have been possible without the help of many people.

First of all, I would like to thank my supervisors Charlotte Poschenrieder and Soledad Martos for the PhD opportunity, their guidance and many learning opportunities during this years.

Technical support is also greatly acknowledged to Rosa Padilla, Benet Gunsé and Salvador Bartolomé.

I also want to thank Peter Schröder and all his team from EGEN group at the Helmholtz Zentrum from Munich, for their support during the stay. Specially thanks to Andrés Sauvêtre for the help, the guidance and the good atmosphere in the lab office.

Also, my gratitude to Olga Sanchez and Eloi Perladé from the Department of Microbiology, and Joaquim Martí from the Department of Cytology and Histology for their support in some experiments.

Alhora, vull agraïr a tot el department de Fisiologia Vegetal i a la secretaria del BAVE el seu suport durant aquests anys. Principalment a la Joana Terés i a la Sílvia Busoms per la seva ajuda incondicional i pels bons moments compartits. A la Berta Gallego i a la Maite Rosselló per el seu suport. Als estudiants Cristina Cianfanelli, Alonso Agüera, Nicolás Fernandez, Laura Pérez i Laia Moles, per la seva ajuda. Tot això no hagués sigut possible sense l'ajuda de les meves directores, Charlotte i Sole, per això vull agraïr novament la seva paciència i proximitat durant tots aquests anys.

No hauria sigut possible arribar a aquest punt sense l'ajuda dels meus pares, avis, i de la meva familia, que sempre hi ha sigut. També a la Laura per haver-me fet costat, ajuda't i anima't en els bons i els mals moments. Als meus amics, especialment a l'Ignasi, en Sergi, la Laia, l'Aleix, en Pau, en Repu i l'Emma, per ajudar-me i compartir tants bons moments plegats durant aquest camí.

A tots vosaltres, i a molts més, que heu fet possible que arribi fins aquí, gràcies!

Abstract

Increasing world population requires the improvement of problematic soils for agricultural use. Zinc is an essential micronutrient in all organisms, while excess Zn inhibits growth. The transformation through soil microorganisms of non-available Zn to available forms contributes to the improvement of nutrition and growth of plants on Zn-deficient soils. Promotion of Zn mobilization in polluted soil may further be required for enhanced phytoextraction in soil remediation.

The objective of this thesis was to characterize soil Zn as a factor of natural selection in both the model plant *Arabidopsis thaliana* and soil and rhizosphere bacteria. The complex plant-bacteria-soil system was approached as a single interrelated entity with the purpose to get useful information for future applications in both sustainable crop production and phytoremediation.

This thesis is divided into three chapters 1) response of natural *A. thaliana* populations to differences in substrate Zn availability, 2) characterization of soil and rhizosphere bacteria able to promote plant growth and to mobilize Zn, Fe and P, 3) genome wide association analysis on 360 natural populations of an *A. thaliana* collection for the identification of major SNPs related to rosette growth and ionome on a Zn-contaminated mine soil.

The natural variability in soil Zn availability in NE Catalonia was explored and related to Zn accumulation in *A. thaliana* demes from these habitats. Soil and hydroponic culture experiments showed that the demes have locally adapted to these different soil conditions. RT-qPCR analysis revealed distinctively higher expression of genes involved in Zn transport in LLAM, the deme from a site with relatively high soil Zn and carbonate levels. The natural adaptation to carbonate was inheritable as revealed in the F1 generation obtained by crossing more tolerant LLAM with the highly carbonate sensitive deme T6. A Hap map collection of 360 *A. thaliana* populations revealed large differences in Zn and Pb-tolerance on a mine soil exhibiting huge differences in survival, growth and leaf ionome. GWAs revealed that leaf ionomic variations of the metal-tolerant survivors were related to SNPs associated with pathogen resistance genes. This agrees with the important role of Zn and Fe homeostasis in plant pathogen defense.

Soil Zn is a driver for natural selection also in soil and rhizosphere bacteria. Most Zn tolerant bacteria were found in the Zn-polluted mine soil. The rhizoplane of *A. thaliana* CALA, the deme with highest leaf Zn, was the only non-polluted site where Zn-tolerant bacteria were found. Based on Zn and Cd-tolerance, Zn and P mobilization ability, and phytosiderophore and IAA production, best candidates for future application in phytoextraction were: *Pseudomonas fluorescens* (strain uab9) with excellent Zn tolerance and mobilization, *P. antarctica* (uab7) combining Zn-tolerance with excellent P-mobilization, Cd-tolerance and IAA production, and *Serratia marcescens* (uab10) with Zn and Cd-tolerance combined with highest IAA production. Excellent bacterial candidates for plant growth promotion and enhancement of Fe and Zn availability to crop plants on carbonated soils, are *P. rhodesiae* (uab 4/5) and *S. marcescens* (uab1). Both were high siderophore producers, able to solubilize Zn and P, as well as to produce IAA.

In conclusion, the natural variation of soil Zn and carbonate, even within a small range, drives local adaptation of *A. thaliana* plants. Best source of Zn tolerant bacteria able to solubilize Zn is mine soil with high metal burdens. However, plants can strongly influence the presence of rhizosphere bacteria and plants with high Zn uptake efficiency, like CALA, can favor the establishment of Zn-tolerant bacteria in the rhizoplane. Future research will explore the potential application of these results to both sustainable production of crops on Zn deficient soil and phytoextraction of Zn from polluted soil.

Resum

El creixement de la població crea la necessitat de millorar els sòls problemàtics per usos agrícoles. El Zinc és un micronutrient essencial, mentre que en excés inhibeix el creixement. La transformació per microorganismes de formes no disponibles a disponibles de Zn, contribueix a millorar la nutrició i promoure el creixement de plantes en sòls deficients en Zn. La mobilització de Zn en sòls contaminats pot ser necessària per millorar la fitoextracció en remediació de sòls.

Els objectius d'aquesta tesis, son caracteritzar un sòl de Zn com a factor de la selecció natural en la planta model *Arabidopsis thaliana*, i en bacteris rizosfèrics. Entendre el complex planta-bacteri-sòl com una sola entitat interrelacionada amb el propòsti d'obtenir información útil per futures aplicacions en el producció de cultius sostenibles i en fitorremediació.

Aquesta tesis es divideix en tres capítols: 1) resposta de poblacions de *A. thaliana* a substrats amb diferent disponibilitat de Zn, 2) caracterització de bacteris del sòl i rizosfèrics, capaços de promoure el creixement de plantes i mobilitzar Zn, Fe i P, 3) *genome wide association analysis* en 360 poblacions naturals d'una col·lecció de *A. thaliana* per a la identificació de SNPs relacionats amb el creixement de la roseta i nutrició, d'un sòl contaminat provinent d'una mina de Zn.

Es va explorar la variabilitat natural de disponibilitat de Zn de sòl situats al nord-est de Catalunya, i es va relacionar amb l'acumulació de Zn en *A. thaliana* d'aquests hàbitats. Els experiments en cultius de sòls i hidropònics van demostrar que les plantes es van adaptar localment a aquestes diferents condicions del sòl. L'anàlisi de RT-qPCR va revelar una expressió més alta de gens implicats en el transport de Zn en LLAM, el *deme* d'un lloc amb sòl relativament alt de Zn i nivells de carbonat. L'adaptació natural a sòls carbonats era hereditària, tal com es revela a la generació F1 obtinguda mitjançant l'encreuament de LLAM, varietat més tolerant, amb T6, varietat més sensible a carbonats. Una col·lecció de Hapmap de 360 poblacions de *A. thaliana* va revelar grans diferències en la tolerància a Zn i Pb en el sòl de la mina, mostrant grans diferències en la supervivència, el creixement i la ionometria de les fulles. El GWAs va revelar que les variacions ionòmiques foliars dels supervivents tolerants a metalls, estaven relacionades amb SNPs associats amb gens de resistència a patògens. Això coincideix amb l'important paper de l'homeòstasi del Zn i el Fe en la defensa dels patògens vegetals.

El sòl ric en Zn és un motor per a la selecció natural també en bacteris de sòl i rizosfera. La majoria de bacteris tolerants a Zn es van trobar en el sòl de la mina contaminada per Zn. En el rizoplà del *deme* de *A. thaliana* CALA, va ser l'únic lloc no contaminat on es van trobar bacteris tolerants a Zn. Els millors candidats per la seva futura aplicación en base a la tolerància a Zn i Cd, la capacitat de mobilització de Zn i P i la producció de fitosteròfors i IAA, van ser: *Pseudomonas fluorescens* (soca uab9) amb excel·lent tolerància i mobilització de Zn, P. antarctica (uab7) que combina tolerancia a Zn amb excel·lents mobilizació de P, tolarància al Cd i producción de IAA, i Serratia marcescens (uab10) amb tolarància al Zn i Cd, combinades amb la màxima producció de IAA. P. rhodesiae (uab 4/5) i S. marcescens (uab1) són excel·lents candidats per a la promoció del creixement vegetal i la millora de la disponibilitat de Fe i Zn a les plantes, de cultiu en sòls carbonats. Tots dos sent bons productors de sideròfors, capaços de solubilitzar Zn i P i produir IAA.

En conclusió, la variació natural de Zn i carbonat en sòl, fins i tot dins d'una petit rang, condueix a l'adaptació local de plantes de *A. thaliana*. El sòl de la mina amb elevat contingut de metalls, és la millor font de bacteris tolerants a Zn capaç de solubilitzar-lo. Tanmateix, les plantes poden influir en la presència de bacteris de rizosfera. Plantes amb una alta eficiència d'absorció de Zn, com CALA, poden afavorir l'establiment de bacteris tolerants a Zn en el rizoplà. Treballs futurs, exploraràn la

possible aplicació d'aquests resultats tant a la producció sostenible de cultius sobre el sòl deficient de Zn, com a la fitoextracció de Zn en sòls contaminats.

Abbreviations

ANOVA: Analysis of variance

BLAST: Basic Local Alignment Search Tool

BNF: Biological nitrogen fixation

DNA: Deoxyribonucleic acid

GO: Gene oncology

GWAS: Genome-wide association study

IAA: Indole-3-acetic acid

IC's: Indolic compounds

ICP-MS: Inductively coupled plasma mass spectrometry

LD: Linkage disequilibrium

LPH: Les Planes d'Hostoles

NCBI: National Center for Biotechnology Information

OD: Optical density

PCR: Polymerase Chain Reaction

PGPB: Plant growth promoting bacteria

qRT-PCR: quantitative Reverse Transcription Polymerase Chain Reaction

rDNA: Ribosomal DNA

SCF: Santa Coloma de Farners

SNP: Single Nucleotide Polymorphism

TAIR: The Arabidopsis Information Resource

Document presentation

This thesis is the result of 4 years of work (2013-2017) at the Universitat Autònoma de Barcelona (Departament BAVE, Unitat de Fisiologia Vegetal) and a 3-month stay at the *Helmholtz Zentrum* in Munich (EGEN group).

The thesis work has been divided into three chapters with different topics but with a common target and trajectory. Important to say that another chapter related to Next-generation sequencing of the endophytic and rhizospheric microbiome from different natural populations of *A. thaliana*, are still under progress and will be added in a future publication. This experimental work has been performed at the Helmholtz Zentrum, where also the sequencing was done. The bioinformatic and statistical analysis are still in progress.

The thesis chapters are preceded by a general introduction summarizing important general background information. Moreover, each chapter contains a brief introduction of its specific topic. The first chapter concerns the adaptation of natural populations of *A. thaliana* to Zn deficiency, high carbonate, and Zn excess, including physiological and genetic traits of different selected *demes* (group of plants from the same family in relatively homogeneous ecological conditions and separated from other groups by at least 35 m (Busoms et al., 2015)). Chapter two is focused on the extraction, phenotypic and genotypic characterization and phylogenetic analysis of different isolated strains of bacteria in relation to Zn solubilization and plant growth promotion. Chapter three reports the results from a Genome-Wide Association Analysis (GWA) characterizing SNPs related to plant adaptation to Zn contaminated soil.

Each chapter contains a specific discussion of the results. While a concluding remarks and outlook of the work can be found after the last chapter.

Contents

1. Introduction

1.1. Plant mineral nutrition: the importance of plant-soil interactions

Soil is the reservoir and source of water and mineral elements required for plant growth and development. All plants need at least 17 elements in different proportions. Macronutrients are the essential elements required in mM range (C, H, O, N, P, S, K, Ca, Mg), and micronutrients required in the µM range (Fe, Mn, Zn, Cu, B, Mo, Cl, Ni).

The nutrient availability in the soil is affected by different factors like soil properties, plant characteristics and the interaction between roots and microorganisms (Jones et al., 2004). Plant productivity and growth depends considerably on the availability of nutrients in the rhizosphere (soil-root interface), influenced by a wide range of factors including the soil type, its physical and chemical characteristics, the plant species and genotype, the soil's microorganism communities, and the prevailing climatic conditions. Biological activities of both roots and microorganisms play an important role (Marschner 2011).

For plant-soil-microbe interaction studies three different soil portions are distinguished: bulk soil, rhizosphere and rhizoplane. Rhizosphere (or more appropriately the rhizospheric area) was first defined by Hiltner (1904) as the volume of soil influenced by plant roots and their exudates. Bulk soil, in turn, corresponds to the area located outside of the rhizosphere, therefore non-adhering to roots and not under its direct influence. Rhizoplane is defined as the thin layer of soil covering the roots and strongly adhering to them (Cleyet-Marel and Hinsinger, 2000). It forms an interface between roots and rhizosphere.

The nutrient availability differs between the rhizosphere and the bulk soil (Marschner et al., 2003). For this reason, the total nutrient availability in the bulk soil is only an approximation about what is the real nutrient availability on the root surface. Significant differences can be registered between plant species and genotypes. For these reasons, the analysis of nutrient elements in the soil using a variety of chemical extractants is a limited method to know the plant available nutrients.

It is in the rhizosphere where the plant root releases chemical compounds to mobilize nutrients and to communicate with the neighboring soil organisms. These compounds may inhibit pathogenic microorganisms and attract beneficial ones. Different compounds are involved in attracting beneficial organisms. These compounds include amino acids, aromatic acids, aliphatic

acids, fatty acids, sterols, phenolics, enzymes, proteins, sugars, polysaccharides, plant growth regulators and secondary metabolites (Kidd et al., 2009). Important to say that this rhizosphere region is highly dynamic and can be altered by addition or loss of any of the players (Badri et al., 2009).

Root exudates can also induce positive and negative plant-plant interactions and these interactions may also be mediated by indirect effects on soil resources. The soil nutrient availability can be increased or decreased by root exudations (Bais et al., 2006). Moreover, the bacteria living in this rhizosphere area secrete specific substances for both mobilizing nutrients and promoting plant growth. The capacity of some bacteria to solubilize nutrients from insoluble sources is even stronger than that of plants and bacteria may play an important role for providing plants with nutrients in available form (Pii et al., 2015).

1.2. Micronutrient Zinc

Zinc (Zn) is an essential chemical element with atomic number 30. It is the 24th most abundant element in the Earth. The normal oxidation state of Zn is +2 and it has five different isotopes. Zinc is considered as an essential micronutrient and has important physiological functions in all living systems. Zinc is involved in the maintenance of structural and functional integrity of biological membranes, synthesis of proteins and gene expression. Zinc is typically the second most abundant transition metal in organisms after iron (Fe), and the only metal represented in all six enzyme classes (Enzyme Commission number, EC 1–6; (oxidoreductases, transferases, hydrolases, lyases, isomerases, ligases (http://www.chem.qmul.ac.uk/iubmb/enzyme/). These enzyme activities decrease under Zn deficiency conditions.

Zinc-binding proteins make up nearly 10 % of the proteomes in eukaryotic cells, and 36% of the eukaryotic Zn-proteins are involved in gene expression (Andreini et al., 2006). Many enzymes integrate Zn in their structure. Usually they have only one Zn atom; an exception is alcoholdeshydrogenase which contains two atoms of zinc, one with a structural function and other with a catalytical function (Marschner 2012). Zinc forms numerous soluble salts, including halides, sulphates, nitrates, thiocyanates, perchlorates, fluorosilicates, formates, acetates, cyanides, alkali metal zincates and Zn-ammonia salts. Sparingly soluble compounds include Zn hydroxide, Zn-ammonium phosphate and Zn carbonate. Moreover, Zn forms a range of soluble and insoluble organic complexes (Lindsay, 1979; Barak and Helmke, 1993).

Zinc is required for the normal, healthy growth and reproduction of plants, microorganisms, animals, and humans. Inadequate Zn availability to plants affects both crop yields and quality of the crop products. So finally, consumer health, both human and animal, can get disturbed due to Zn deficiency (Alloway, 2004).

1.3. Zinc deficiency and contamination

Zn deficiency is one of the most widespread micronutrient deficiencies in crops and pastures worldwide and causes large losses in crop production and crop quality (Alloway., 2004) (Fig. 1.1). For this reason, Zn deficiency in humans is considered a widespread problem, effecting one-third of the world's population, ranging from 4 to 73% in different countries (Hotz and Brown, 2004) (Fig. 1.1). Zinc deficiency is currently listed as a major risk factor for human health and cause of death globally. It has been estimated that one-third of the world's population obtains insufficient zinc for adequate nutrition (Cakmak, 2008; White and Broadley, 2011). This can be alleviated by increasing the dietary Zn intakes through a number of interventions (White and Broadley, 2009). Some of the most affected countries are Turkey, India and China with the 50% of the arable lands with Zn deficiency. Even higher percentages values are reported for Iran (60%) and Pakistan (70%).

The principal causes of this zinc deficiency are low total zinc in the soil, high soil pH (carbonated soil), high rates of phosphate fertilizer application, salinity, waterlogging/flooding of soil, low manure application and high soil organic matter content (Alloway, 2004). Notably, 50% of cultivated soils in India and Turkey, a third part of the cultivated soils in China, and most soils in Western Australia are classed as Zn-deficient. Zinc deficiency in crop production can be ameliorated through improved agronomic management and/or crop breeding. Crop plants differ in Zn mobilization and requirements. Adequate Zn leaf concentrations usually range from 20-30 to 70-80 mg/kg dry weight. Leaf Zn levels below 20 mg/kg dry weight are deficient for most crop plants (Bergmann, 1993).

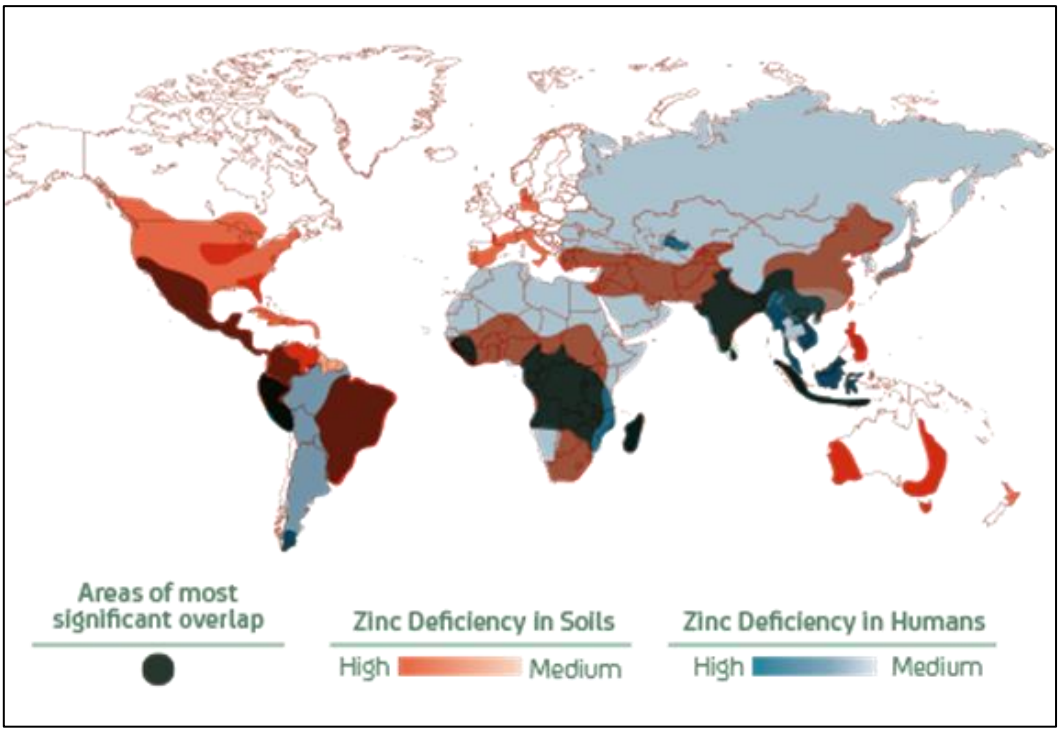

Figure 1.1: Zinc deficiency in soil and in human population. The overlap, represented in black color, is the area where soil Zn deficiency and Zn deficiency in humans coincide. (http://www.zinc.org)

Contrastingly, Zn toxicity may occur in contaminated soils basically due to mine tailings, application of sewage sludge or Zn-rich municipal waste compost. Zn toxicity inhibits root growth, impairs photosynthesis and photoassimilate translocation, and alters ion homeostasis (Ruano et al., 1987 and 1988). Phosphorus and or iron deficiency can be secondary stresses induced by excess Zn (White et al., 1979). Zn leaf concentrations reaching 300 to 1000 mg/kg are considered toxic for most plant species (Chaney 1993).

Excess Zn may affect plant-microbe interactions due to either or both differences in the toxicity threshold between plants and their colonizing microbes and changes in defense signaling and activation of organic defenses in the plant. For example, recent studies (Martos et al., 2016) show that the adequate Zn supply in *A. thaliana* enhance the resistance to the pathogenic fungus *Alternaria brassicicola.*

1.4. Mine tailing soil and carbonate soil.

Carbonate-rich soils and mine tailings represent the extreme values of the range of Zn availability to plants. During this study, we paid special emphasis to these extreme conditions; carbonated soils where low Zn availability is to be expected and mine soils with high Zn burdens.

Anthropogenic activities like mine tailing to extract different mineral influence can cause direct contamination of the Earth surface. Generally, mine soils are chemically, physically, mechanically and biologically unstable and present problems of both nutrient deficiency and ion toxicity (Vega eft al., 2006). Moreover, they have low content of nutrients and organic matter and hugh amounts of heavy metals and other potentially toxic trace elements (He et al., 2005). For this reason, they are unstructured and texturally unbalanced. Frequently, mine spoils have strong acidity due to rapid and intense oxidation (Vega et al., 2005), resulting in high availability of cations (Al^{3+}, Fe^{2+}, Mn^{2+}, Pb^{2+}, Cu^{2+}, Zn^{2+}, Cd^{2+} etc.), thereby creating an unfavorable environment for biological development. Both plants and microorganisms able to colonize these soils must have evolved tolerance to the excess of metal cations, as well as mechanisms for acquisition of essential anions such as phosphate (Kidd et al., 2009; Sessitsch et al., 2013)

Another problematic soil for plant growth are carbonated soils, also known as alkaline soils or calcareous soils, which have a high pH. Calcareous soils cover around 30% of the earth's land surface (Chen and Barak, 1982) and their $CaCO_3$ content varies from a few percent to 95% (Marschner, 1995). They normally contain sodium carbonate (Na_2CO_3), sodium bicarbonate ($NaHCO_3$), calcium carbonate ($CaCO_3$) among others.

Carbonate minerals, due to their relatively high solubility, reactivity, and alkaline character, act as pH buffers; the pH values of most calcareous soils are within the range of 7.5 to 8.5. It is because of these properties that carbonates play an important role in pedogenic, chemical and rhizosphere processes in the soil (Loeppert and Suarez, 1996).

Due to the high pH, carbonated soils use to have low availability of iron and zinc. Papadopoulos and Rowell (1988) postulated that cadmium was retained by the formation of an ideal surface solution with CaCO3, whereas zinc and copper were precipitated as tri-hydroxides or hydroxicarbonates. Both excess HCO^{3-} and Zn deficiency inhibit photosynthesis and PSII activity, which influences photosynthetic and chlorophyll fluorescence parameters (Mohsenian, 2015). Bicarbonate, which is considered the key factor that influences Fe deficiency chlorosis (lime-induced chlorosis) and Zn deficiency in many plant species (McCray, 1992) is the major anion found in calcareous soils, especially in karst regions. In addition, iron, boron, zinc, and

manganese deficiencies are common in soils that have a high $CaCO_3$ due to reduced solubility at alkaline pH values (Marschner, 1995; Brady and Weil, 1999).

1.5. Role of rhizobacteria and endophytic bacteria in mineral nutrition.

1.5.1. Microbe-plant interaction

During the last decades, the use of rhizobacteria to promote plant growth started to be a technique of scientific, ecological and economic interest. The microbiota living in the rhizosphere (immediately surrounding the root) or the endophytic microbiota (within the plant) not only may contribute to promote plant growth and crop yield, but also may be a tool phytoremediation and carbon sequestration (Rodriguez et al., 2008; De Deyn et al., 2008; Vangronsveld et al., 2009; Kolbas et al., 2015). On the other hand, the root influences the rhizosphere by different processes: changes in the soil pH and texture, alteration of the concentrations of antimicrobial substances, production of carbon-rich exudates and quorum-sensing mimicry (Marschner et al., 2010). The bacterial communities in each compartment (bulk soil, rhizosphere, endophytic compartment) are mainly influenced by the soil type, but also by the developmental stage of the plant and its genotype (Lundberg, 2012).

During the last 25 years, the development of different new techniques and methods has substantially enhanced the study of the microbial communities in soils and plants and has allowed quantifying the microbial diversity in genetic, taxonomic or functional terms. One of these methods is the use of sole carbon sources tests to measure the functional diversity (Zak and Willig, 1994). Garland and Mills (1991) describe for the first time a method using a commercially available microtite plate (Biolog®) which can be used to test different substrates as sole carbon sources. Color development of a redox indicator dye, and changes in the overall patters of carbons source utilization rates indicate differences in community composition. With this tool, the metabolic potential of the microbial communities and the capacity of these microorganisms to contribute to the turnover of chemical elements in an ecosystem can be known. Most important, the fast development of DNA sequencing technology now allows the exact identification of microorganisms and changes in microbe communities at affordable costs.

1.5.2. Plant growth promoting bacteria

Plant-microbe interactions can be either mutualistic or pathogenic. Mutualistic interactions provide benefits to the plant and the microbe, while pathogenic relations undermine plant health. Promoting the beneficial interactions and avoiding the harmful ones is of high agronomic interest. Plant growth promoting bacteria (PGPB) are a heterogeneous group of beneficial microorganisms that can be found inside the root, on the root surface or in the rhizosphere. These microorganisms have the capacity to enhance growth of plants and protect them from both biotic and abiotic stresses (Dimkpa et al., 2009a; Grover et al., 2011; Glick, 2012).

Many Gram-positive and -negative PGPB have been reported to colonize the plant rhizosphere and confer beneficial effects by various direct and indirect mechanisms, which can be correlated with their ability to form biofilms, chemotaxis, and the production of exopolysaccharides, indole-3-acetic acids (IAA), and aminocyclopropane-1-carboxylate (ACC) deaminase (Glick., 1995).

These PGPB can facilitate plant nutrient uptake using different direct mechanisms such as nitrogen (N) fixation, solubilization of phosphate (P) and synthesis of siderophores for iron chelation making different nutrients more available to plants (Pii et al., 2015). Though a variety of nitrogen fixing bacteria so called biofertilizers like *Rhizobium*, *Azotobacter*, *Bacillus*, *Pseudomonas*, *Azospirillum* and *Acetobacter* have been isolated from the rhizosphere of various crop plants (Steenhoudt and Vanderleyden, 2000). The interest in the beneficial nitrogen-fixing, growth-promoting rhizobacteria-plant association has increased recently due to their potential effect for replacing chemical N-fertilizer (Vessey, 2003; Mahanty et al., 2017).

Production of indolic compounds (IC's), like indole-3-acetic acid (IAA), is one of the principal traits that promote plant growth (Spaepen et al., 2007). Souza et al. (2013) studied the production of these compounds in the rice rhizosphere and the result shows that around 80% of the isolated bacteria have the capacity to produce ICs. In fact, this capacity is widely-distributed in plant-associated bacteria. Khalid et al (2004) demonstrated that the rhizospheric bacteria produce more IC's than the bacteria found in the bulk soil. Such high IC production has also been shown in endophytic bacteria from the Enterobacteriaceae family (Costa et al., 2014).

Among others, L-tryptophan is the main precursor for the IC's production in bacteria; but the study of the intermediate compounds revealed different pathways using this precursor. Five different pathways are described for IAA production using tryptophan as a precursor. These pathways to produce IAA in bacteria show a high degree of similarity to the biosynthesis ways

of IAA production in plants (Fig. 1.2) (Spaepen et al., 2007). In bacteria, the catabolism of IAA is also well-studied. Bacteria can use this compound as a source for carbon, nitrogen and energy (Jensen et al., 1995). Pathogenic bacteria can also use plant IAA and the capacity to catabolize IAA is a good strategy for PGPB to prevent pathogen attack (Leveau and Lindow, 2005).

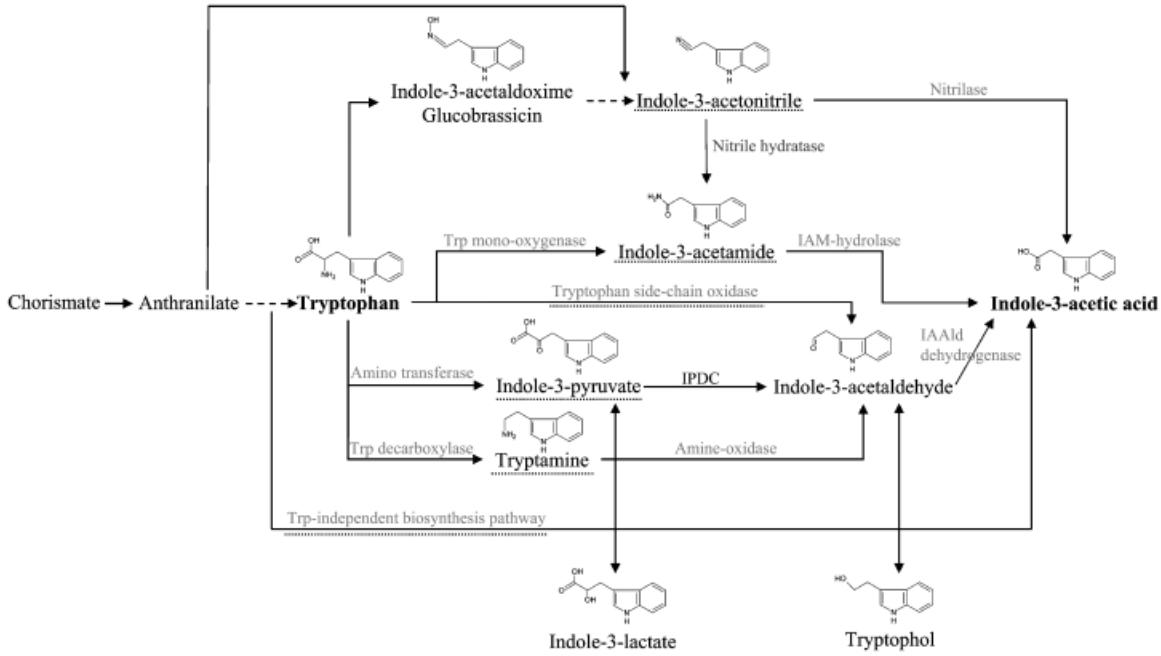

Figure 1.2: Different pathways for IAA biosynthesis in bacteria (Spaepen et al., 2007)

Phosphorus is considered one of the major plant nutrients limiting plant growth (Hinsinger, 2001). Most of the soil phosphorus is present in insoluble forms. Moreover, a large portion of inorganic phosphates applied to soil as fertilizer is rapidly immobilized after application and becomes unavailable to plants (Yadav, 1997). Thus, the release of insoluble and fixed forms of phosphorus is an important aspect of increasing soil phosphorus availability. Seed or soil inoculation with phosphate-solubilizing bacteria is known to improve solubilization of fixed soil phosphorus and applied phosphates resulting in higher crop yields (Jones, 1994). Several authors attribute the solubilization of inorganic insoluble phosphate by microorganisms to the production of organic acids and chelating acids from sugars (Leyval, 1989). Phosphate solubilizing microorganisms are routinely screened by a plate assay method using Pikovskaya (PVK) agar (Pikovskaya, 1948). The test of the relative efficiency of isolated strains is carried out by selecting the microorganisms which are capable to produce a halo/clear zone on plate due to the production of organic acids into the surrounding medium (Katznelson,1962).

The solubilization of phosphate is considered also a PGPB trait. Phosphorus (P) is an essential nutrient for plants and his health. Phosphorus has multiple essential functions: ATP production, structural component of nucleic acids and phospholipids, and important roles in biochemical and metabolic pathways such as photosynthesis and biological nitrogen fixation (BNF) (Khan et al., 2009; Richardson and Simpson, 2011). Two different forms can be taken up by plants: the monobasic ($H_2PO_4^-$) and the dibasic (HPO_4^{2-}) (Glass, 1989). The total amount of available P depends on the solubility of this element that, in turn, is influenced by plant root exudates and the microorganism's activity in the soil (Souza et al., 2015). The bacteria transform insoluble phosphorus compounds such as $Ca_3(PO_4)_2$, $FePO_4$, and $AlPO_4$, through the production of organic acids, siderophores, and hydroxyl ions by PGPB in agricultural soils (Jones, 1998; Chen et al., 2006; Rodríguez et al., 2006; Sharma et al., 2013). Production of organic acids such as gluconic and other carboxylic acids is a well-known mechanism used by microorganisms to solubilize inorganic phosphorus (Rodriguez and Fraga, 1999, Uroz et al., 2009).

Iron (Fe), like Zn, is also an essential micronutrient for plants and microorganisms Iron is required for many different biological functions, redox processes like respiration and, photosynthesis, chlorophyll biosynthesis, and enzyme activities (Kobayashi and Nishizawa, 2012). Under aerobic conditions and in calcareous soils (high pH) the solubility of iron is low, because of the predominance of Fe III, typically observed as oxyhydroxide polymers, (Andrews et al., 2003; Lemanceau et al., 2009). To make Fe available, bacteria produce siderophores. This small (< 1,000 Da) organic compounds are classified by the ligands used to chelate the ferric iron with high specificity and affinity, allowing the transport and deposition of iron within the bacterial cells (Neilands, 1995; Krewulak and Vogel, 2008). This bacterial capacity can contribute to plant growth either directly by stimulating plant nutrition or indirectly by sequestering Fe required by phytopathogenic microbes hampering their infection strategies (Dimkpa et al., 2009b).

1.5.3. Zn solubilization and gluconic acid

The adequate release of Zn in crop soils is of essential importance for achieving high yield of excellent quality. The use of fertilizers with insoluble forms of Zn is the principal strategy to supply Zn to soils with low Zn contents due to geochemical factors (Alloway, 2009). But the major reason for the widespread problem of Zn deficiency in crop plants and subsequently to human deficiency is attributed to low Zn solubility in soils rather than a low total amount of Zn (Cakmak, 2008). The use of bacterial strains with ability to mobilize plant available Zn from insoluble

sources can be a good approach to increase plant productivity on such soils. Especially, problematic in this context, are the alkaline and calcareous soils due to their high pH and, hence low Zn solubility. Zinc mobilizing bacteria could contribute to ameliorate this agronomic problem. Moreover, metal dissolution produces excretion of H^+ that produce positive influence in ammonia assimilation and other metabolic activities, as described for *Pseudomonas* spp. (Illmer and Schinner, 1992).

Gluconic acid, and its 2- and 2,5-keto-derivatives, are produced by fungi and bacteria as a result of an external oxidative pathway effective on glucose and other aldose sugars (Whiting et al., 1976; Babu-Khan et al., 1995; Williams et al., 1996; Ramachandran et al., 2006) (Fig. 1.3). The gluconic acid is subsequently taken up by cell transport systems and used by cellular metabolic pathways. The external oxidation of glucose therefore usually produces only transient increases in the concentration of gluconic acid (Drosinos and Board, 1994). In some conditions, however, the external accumulation of gluconic acid results in acidification of the medium, which may possibly contribute to the solubilization of metal phosphates (Babu-Khan et al., 1995).

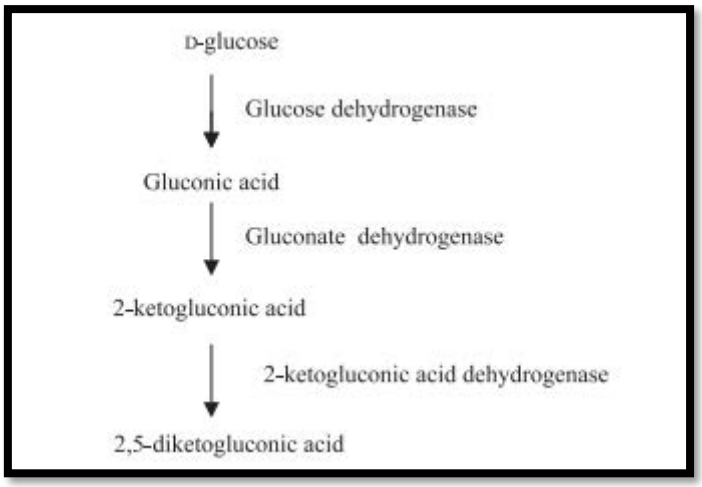

Figure 1.3: Specific pathway for oxidation of glucose (Ramachandran et al., 2006)

Bacteria are also able to immobilize nutrients. Precipitation and absorption are a well-known strategy used by bacteria for metal immobilization. The activity of sulphate-reducing bacteria produces the formation of highly insoluble metal sulphide bio-precipitates in anoxic environments (Gadd, 1996; White et al., 1997). This bio-precipitation has potential for the remediation of polluted waters and soils, also in aerobic environments (Diels et al., 1995; Gadd, 1996; White et al., 1997; Chen and Cutright, 2003).

1.6. *Arabidopsis thaliana* as a model plant

The genus *Arabidopsis*, from the mustard family (Brassicaceae family), contains nine species and eight subspecies that can be distinguished by morphological characteristics such as fruit and seed shape.

The specie *Arabidopsis thaliana*, (L.) Heyhn (2n = 10) is an herbaceous flowering plant commonly named thale cress or mouse-ear cress. The species is annual or biannual and mostly reproduces by selfing in nature. The small size (adults approximately 20 cm tall), short reproduction time (Fig. 1.4), and well-known genome (The Arabidopsis Genome Initiative, 2000) makes *A. thaliana* an ideal model for functional genetics studies (Koorneef and Meinke, 2010). Moreover, this species shows important genetic and trait variation among natural populations or accessions (Shindo et al., 2007). The large phenotypic and genetic differences displayed by these natural accessions allow their use in investigations of the molecular and genetic mechanisms underlying the differences in chosen characteristics.

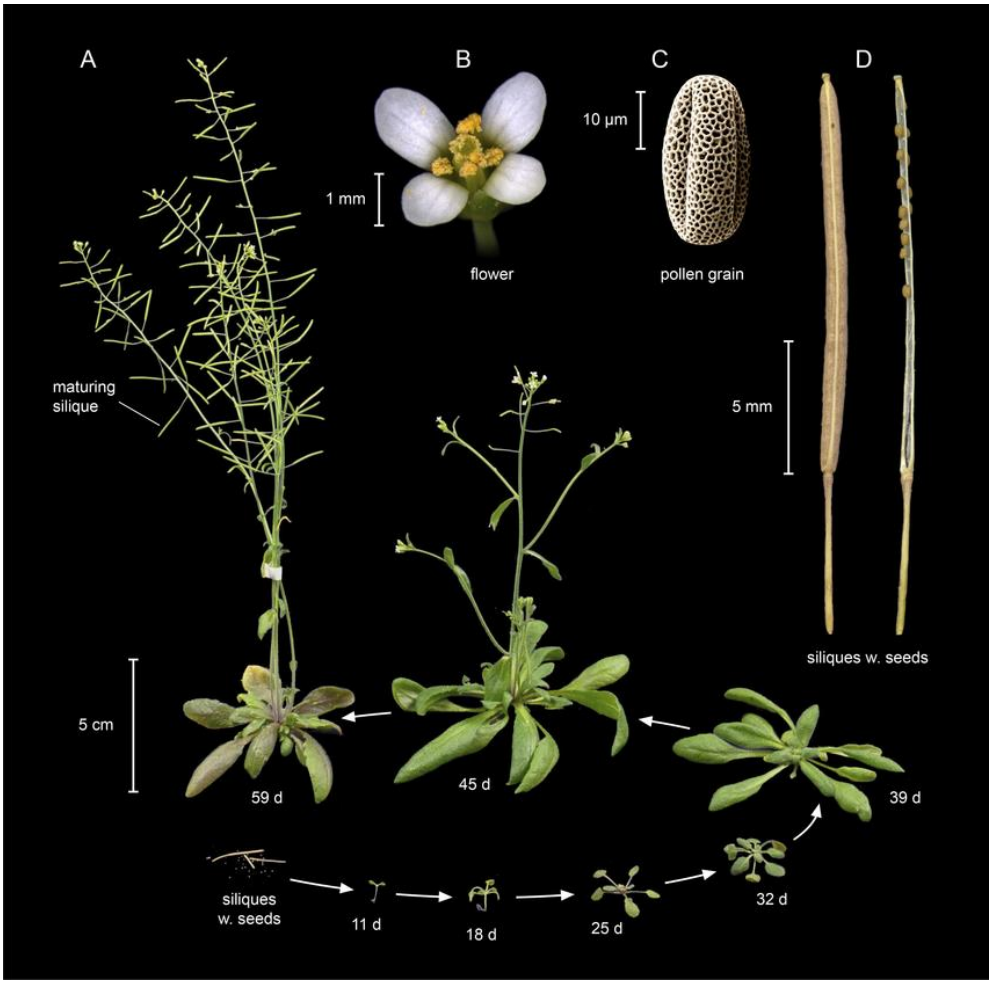

Figure 1.4: Life cycle of Arabidopsis thaliana. (A*) A. thaliana* of the accession Columbia (Col) at different stages of its life cycle, from seed (bottom left) to seedling (11 days), to vegetative growth (39 days), and to reproductive growth (45 days). Photographs of (B) a flower, (C) a pollen grain (scanning electron micrograph), and (D) mature siliques (seed pods; left: closed; right: open with a few remaining unshattered seeds) at higher magnification. (from Krämer, 2015)

The site of origin of *A. thaliana* is not clearly known. Two main hypotheses suggest the middle Asian's mountains or Europe and the North part of Africa as the origin of the specie. However, none of these two hypotheses have been confirmed (Beck et al., 2008). Sharbel et al. (2000), and François et al. (2008), suggest that glacial refugia were sources of postglacial recolonization. Hoffmann (2002) describes the wide climatic amplitude of *A. thaliana* current habitats as follows: low temperatures during autumn-spring seasons and high and dry climate during summer. *A. thaliana* occurs in disturbed or open habitats, sandy soils, river banks, rocky slopes, road sides, meadows, waste places, cultivated grounds, slightly alkaline flats, under shrubs, open areas and until to 4250 m in altitude (Al-Shehbaz and O'Kane, 2002). Over 750 natural accessions of *A. thaliana* have been collected from around the world (Fig. 1.5) and are available from the two major seed stock centers, ABRC and NASC (TAIR). *A. thaliana* also was the pioneer plant for ionomic studies initially developed in Purdue (Salt et al., 2008) with now more than 200,000 samples in the ionomic hub database at University of Nottingham (http://www.ionomicshub.org/arabidopsis/piims/showIndex.action). A recent local survey revealed that the biogeographic distribution of *A. thaliana* is largely conditioned by edaphic factors, especially high soil carbonate content (Busoms et al., 2015). The species clearly prefers siliceous over carbonate substrates (Terés, 2017).

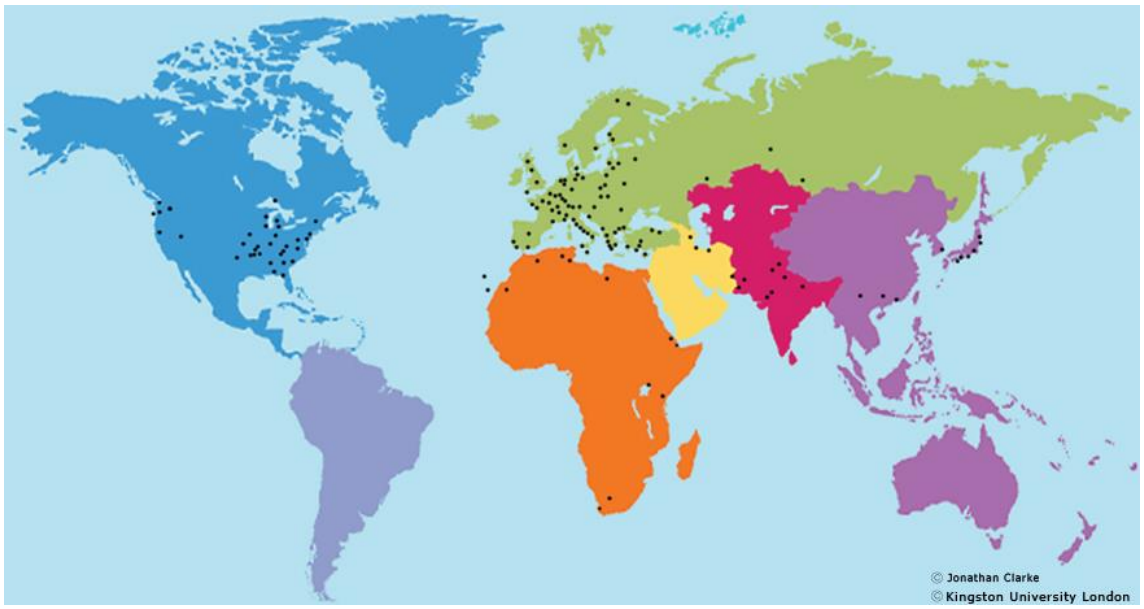

Figure 1.5: Geographical distribution of ecotypes of *Arabidopsis thaliana* (Heynh).

As other Brassicaceae, *Arabidopsis* is not a good niche for arbuscular mycorrhizal fungi, and for this reason other microorganisms may fill this niche (Artursson et al., 2006; Fesel and Zuccaro, 2016).

1.7. Genome wide association analysis using *A. thaliana* Hap-map population

Genome wide association (GWA) analysis is a good strategy to link phenotype with genotype taking advantage of natural variation. For the first time, this technique was used for human genetics (Hirschhorn et al., 2005) where obtaining synthetic mapping populations is impossible. GWA mapping use many genetically characterized individuals to evaluate the statistical significance between the genetic polymorphisms and differences in quantitative phenotype. Polymorphisms are identified using linkage disequilibrium (LD). This LD is based on non-random association between alleles and phenotypes. Genome-wide association studies (GWAS) have been even more successful in plants (Brachi et al., 2010). GWA mapping has some important advantages over traditional linkage mapping using synthetic mapping populations. The natural accessions have experienced more recombination events than mapping populations such as real isogenic lines (RIL) and GWA allows mapping with greater precision. Moreover, GWA mapping takes advantage of a much larger range of genetic variation. This approach, however, brings some disadvantages as well. Not all variants are equally likely to be discovered in GWAS. Rare alleles on the scale of the used population are less likely to be discovered comparing to frequent ones, due to smaller statistical power (Asimit and Zeggini, 2010; Gibson, 2012). Rare alleles usually do not play a key role in the plant adaptation on the scale of the whole species. However, there are some cases where they may play a significant role in adaptation on the local scale. Rare alleles might become more frequent, for example, in the habitats that most plants perform poorly if such variants improve fitness of the organisms in these difficult environments (Kawecki and Ebert, 2004). Heterogeneity also poses a problem for GWA mapping. Genetic heterogeneity takes place when certain alleles of different genes produce the same phenotype. Allelic heterogeneity is observed when different alleles occurring in one gene lead to the same phenotype. It makes the associations of each of these genetic factors weaker. Furthermore, population structure can cause false positive as well false negative results (Zhao et al., 2007).

Genome wide association studies (GWAS) have been used for other economically important species like rice (*Oryza sativa*), wheat (*Triticum vulgare*), maize (*Zea mays*) among others (Cockram et al., 2010; Hao et al., 2011; Yang et al., 2013; Long et al., 2013). With *Arabidopsis,* the first work using GWAS was the study of Atwell et al. (2010), investigating the architecture of 107 different traits in relation to development, flowering time, resistance to pathogens and element composition. The genetic information was obtained through microarray platform analyzing 250,000 single nucleotide polymorphisms (SNP).

2. Aims and Objectives

The overall aim of this study was to explore the mechanisms underlying natural variation in the response of both *Arabidopsis thaliana* and soil microbiome populations to differential soil availability. The ultimate goal of this study is the aplication of this knowledge to enhance Zn acquisition by plants in the context of both Zn deficient crops and phytoextraction at Zn-pollutes sites.

The specific objectives were:

- Exploration of possible local adaptation of *A. thaliana* to soils with different Zn availability conditions (Zn deficiency in carbonate soil and Zn excess in soil contaminated by mining activities), studying the performance on these contrasting soils of natural populations of this species found in the north-eastern region of Catalonia.
- Characterization of bacteria with capacity to solubilize Zn, and to promote plant growth from both natural stands of *A. thaliana* and Zn-rich mine spoils.
- Possible identification of single nucleotide polymorphisms (SNPs) underlying tolerance to excess soil Zn using GWAS on a Hap-Map population of *A. thaliana* with world-wide distribution.

3. Response of *A. thaliana* natural populations to different zinc availability in the substrate.

3.1. Introduction

Zinc (Zn) is an essential micronutrient for plant growth and normal health development in all kind of soils. It is an important structural component of many catalytic enzymes and transcription factors, so that specific dysfunctions and diseases are related to its deficiency (Broadley et al., 2007; Marschner, 2011; Chasapis et al., 2012). The Zn bio-availability in many natural soils is low, often as a result of high $CaCO_3$ content and alkaline soil pH. Consequently, many food products are low in Zn, causing malnutrition in humans (Cakmak, 2008).

Zn influences different biological processes like cell proliferation, carbohydrate metabolism, and phosphorus-Zn interactions (Rengel, 2015). The typical range of Zn concentrations in soils is 10-300 mg/kg with a mean of 50 mg/kg Zn (Kiekens, 1995). Zn plays a key role in the function of different enzymes such as alcohol dehydrogenase, carbonic anhydrase and glutamate dehydrogenase (Rehman et al., 2012). For this reason, Zn deficiency causes inhibition of plant growth and abnormal development. This may be consequence of decreased net photosynthesis and photosynthetic electron transport (Zhao and Wu, 2017), but also caused by interference with auxin metabolism and functioning.

Since micronutrient availability is controlled by pH, Zn toxicity depends on it. Low pH induces Zn availability and, in consequence, Zn toxicity increases. The general symptoms are shoot stunting, curling and rolling young leaves, death of leaf tips and chlorosis (Ye et al., 1997).

Zinc deficiency is caused by different soil factors as low Zn content, high $CaCO_3$ content, low amount of organic matter, low soil moisture, high soil pH, sandy soil, and high amount of phosphorous in soils (Marschner, 1995; Cakmak, 2008). Plant symptoms in Zn deficiency conditions show smaller leaf size, stunted growth, chlorosis in young leaves and thin stems. Severe Zn deficiency may result in leaf wilting and curling with attenuated chlorosis and necrosis. Young leaves are the first to show these symptoms due to a reduced mobility of Zn through the phloem from older to younger leaves (Hacisalihoglu and Kochian, 2003).

Zn availability usually is low in alkaline soils with high pH, such as calcareous and carbonate-rich soils. Carbonated soils, normally contain sodium carbonate (Na_2CO_3), sodium bicarbonate

($NaHCO_3$) and calcium carbonate ($CaCO_3$) among others. Bicarbonate (HCO_3^-) is the product formed in the catalysis of carbon dioxide (CO_2) hydration by carbonic anhydrase (CA). Bicarbonate can be used by plants as an inorganic carbon source to supplement CO_2 in leaf cells (McConnell et al., 2012). Also, HCO_3^- is an important constituent of the water-oxidizing complex of photosystem II (PS II). However, excess of HCO_3^- is harmful to plant growth principally due to the inhibition of both protein synthesis and respiration and the decrease of nutrient uptake (Alhendawi et al., 1997). Severe Zn deficiency is characterized by root apex necrosis ('dieback'), whilst sub-lethal Zn deficiency induces spatially heterogeneous or interveinal chlorosis ('mottle leaf'), the development of reddish-brown or bronze tints ('bronzing'), and a range of auxin deficiency-like responses such as internode shortening ('rosetting'), epinasty, inward curling of leaf lamina ('goblet' leaves) and reductions in leaf size ('little leaf'). In most crops, the typical leaf Zn concentration required for adequate growth approximates 15–20 mg Zn/kg dry weight (Marschner, 1995).

The zinc homeostasis network is related to various processes including sensing of the tissue zinc status, zinc transport, uptake, trafficking and sequestration, thus providing an adequate amount of zinc to all the cells, at all stages of development and under different environmental conditions. Therefore, plants control zinc homeostasis using a tightly regulated network where the coordinated expression of zinc transporters plays a major role in zinc acquisition from soil, in mobilization between organs and tissues and in intracellular sequestration. (Clemens, 2001; Assunçao et al., 2013).

In this chapter, the adaptation of different *Arabidopsis thaliana* demes to problem soils with either high or low Zn availability was investigated. Using the demes recently identified in our group (Busoms et al., 2015), a dual experimental approach (pot and hydroponic) was developed to know the adaptation of different natural populations. The selection of three demes with different adaptation and characteristics was important to carry out further analysis.

3.2. Material and methods

3.2.1. Soil and plant sampling

The *A. thaliana* demes used in this study were selected according to a previous extensive survey of *A. thaliana* distribution in the area of NE Catalonia (Busoms et al., 2015). In this work, the

term “deme” is used to describe a group of plants from the same family (in this case *A. thaliana* spp.) in relatively homogeneous ecological conditions and separated from other groups by at least 35 m (Busoms et al., 2015).

Based on this previous study, five sites with different soil Zn availability and natural demes of *A. thaliana* were selected. Fruit-bearing plants were collected between March-May of 2014-2016.

For the pot experiment, three different soils with variable Zn concentration were selected. A natural soil with extremely high Zn concentrations, was collected close to an ancient lead mine (Mina d’en Nadal). The mine is located at the coastal mountain range, in the Gavarres region at 293 m altitude, in the Northern region of the littoral ridge, between the populations of Calonge and La Bisbal d’Empordà.Furthermore, soil samples were collected at Sta. Coloma de Farnés (SCF) and at Les Planes d’Hostoles (LPH), used as a carbonate-poor (control soil) and carbonate-rich test soils, respectively. Sta. Coloma de Farnés is located in a valley in ”La Selva” region between the mountains of “Les Guilleries” and “Massís de les Cadires”. Les Planes d’Hostoles is located in “La Garrotxa” region, a volcanic region in the valley of “Cogolls” and “Hostoles”.

All sampling sites are located on the map in Figure 3.1. Coordinates of the sites are given in corresponding Table 3.1.

Soils were collected from the first 20-30 cm depth (discarding the first 5 cm of the top layer). Ten g of each collection were kept and stored at -20 ºC to analyze biological properties; the rest was air-dried under laboratory conditions and finally passed through a 2-mm sieve for future uses.

For analysis of mother plants, whole plants with the underlying soil were excavated from the natural stands and placed into plastic planting pots. Plants were irrigated and brought to the lab where they were immediately processed. Mature seeds were collected and stored in Eppendorf tubes over silica gel in sealed boxes until use. After washing part of the plant samples were immediately frozen in liquid N_2 and part were oven dried for posterior mineral analysis.

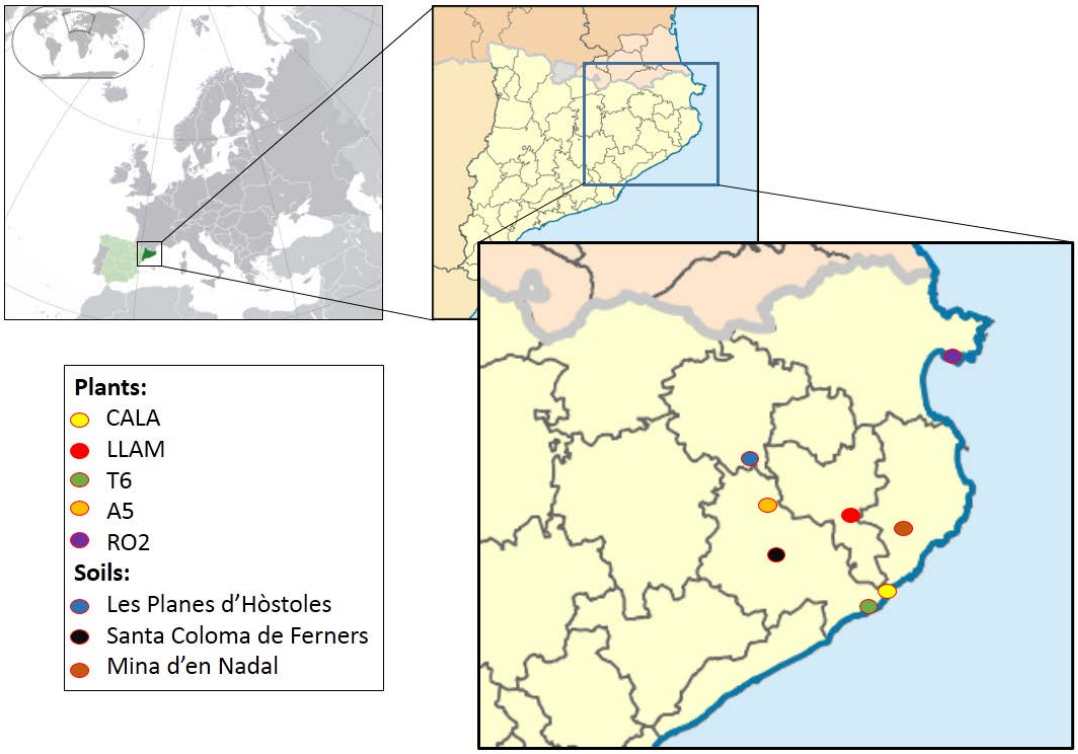

Figure 3.1: Plant and soil sampling sites. Plants: CALA (Tossa de Mar), LLAM (Llambilles), T6 (Tossa de Mar), A5 (Anglés), RO2 (Roses). Soils: Les Planes d'Hostoles (LPH), Santa Coloma de Ferners (SCF), Mina d'en Nadal (Mine soil).

Table 3.1: Coordinates (UTM) of sampled A. thaliana demes and soils

Demes/Soil	UTM (longitude)	UTM (latitude)
T6	496641	4621417
CALA	495575	4619864
LLAM	488354	4641151
RO2	515998	4680193
A5	470427	4643878
LPH	461620	4656602
Mine	501725	4638395
SCF	472172	4634689

Soils were analyzed for pH, carbonated content, organic matter, water-holding capacity, soil texture and global nutrient content. The biological differences among soils were studied by the Biolog® test.

The water-holding capacity and texture of fresh soil was analyzed using the methods described by Reynolds and Topp (2008). The concentration of soil organic matter was determined according to Black et al. (1965).

The pH of was measured following the method of Peech (1965) and Conyers and Davey (1988). In brief, ten g of air-dried mineral soil (< 2 mm) were added into 30 mL beaker and 20 mL of 0.01 M CaCl2. During 30 min, the suspension was stirred intermittently. After 1 h of waiting and the solution was measured with the electrode immersed in the solution using pHmeter (Crison pH basic 20, Hach LPV2000.98.0002).

The concentration of soil carbonate was measured using the method of Loeppert et al. (1984). A standard curve was prepared weighting accurately pure calcite ($CaCO_3$) ranging from 5 to 500 mg (5, 10, 25, 50, 100, 200, 300, 400, 500) into individuated 50 mL polypropylene centrifuge tubes. For exactly neutralizing all the CaCO3 in the standard sample with the highest $CaCO_3$ standard content (500 mg) twenty-five mL of 0.4 M acetic acid was added. After shaking tubes on a rotatory platform for 8h, and centrifugation (1000 g) the pH of the supernatant was recorded to two decimal places after 4 min. Finally, the standard curve of pH was calculated. To measure the carbonate content in the soil, 2 g of sieved soil (2 mm) containing up to 400 mg $CaCO_3$ are mixed with the 25 mL of 0.4 M acetic acid, the other steps are the same as for standard curve. Finally, the pH value recorded was determined using the standard curve and calculate the weight of $CaCO_3$ (mg) in the soil sample. The total carbonate content so determined is referred as the percent of calcium carbonate equivalent.

$$\%\ CaCO_3\ \text{equivalent} = \frac{\text{mg } CaCO_3}{\text{mg sample}} \times 100$$

To characterize the elemental composition of soil, analyses were performed on the 2-mm fraction samples. Five grams of soil was dried for 42 h at 60 °C in 50-mL Falcon tubes. Extraction method (adapted from Soltanpour and Schwab, 1977) consisted of a digestion with 20 mL of 1 M NH_4HCO_3, 0,005 M diaminetriaminepentaacetic acid, and 5 mL of pure water during 1 h of shaking on the rotary shaker at low speed. Each sample was gravity filtered through qualitative filter papers until obtaining approximately 5 mL of filtrate, which was transferred into Pyrex tubes. HNO_3 was added and digested at 115 °C for 4.5 h. Each sample was diluted to 6.0 mL with MQ water and analyzed for As, B, Ca, Cd, Co, Cu, Fe, K, Li, Mg, Mn, Mo, Na, Ni, P, Rb, S, Se, Sr and Zn content (ppb) on an Elan DRCe ICP-MS (PerkinElmer Sciex). National Institute of Standards and Technology traceable calibration standards (ULTRAScientific) were used for the calibration.

Biolog® ECO plates were used to analyze the capacity of the microbial communities of the three different soils to metabolize 31 different carbon sources. The 31 carbon sources are repeated

three times for the replicates of the data. Ten grams of soil was added to 100 mL of a sterile sodium pyrophosphate solution (0.1%) in a 250-mL flask and was shaken at 200 rpm for 20 min. The resulting mixture was diluted 100-fold with a sterile NaCl solution (0.85%). Thereafter, the dilution was used to inoculate wells of the Biolog® Ecoplate. Plate was incubated at 25 ºC and absorbance at 595 nm was measured at 1 hour, 2 days and 7 days. The metabolism of microorganisms in the different wells reduces tetrazolium and change from the colorless state to purple formazan.

3.2.1.1. Climatic characteristics

Tables 3.2 and 3.3 show climate at the sampling sites in Baix Empordà, Gironès and la Selva. Providing data were obtained from http://www.meteo.cat. Parameters like altitude, annual average, maximum and minimum temperature during the year 2015 were included, along with the pluviometry during the month of plant and soil collection.

Table 3.2: Temperature (ºC) from Baix Empordà, Gironès and la Selva regions. Information of the weather station site of each region. Data from 2015. http://www.meteo.cat.

Temperature							
Region	**Weather station site**	**Altitude** (meters over the see level)	**Annual average** (ºC)	**Average maximum temperature** (ºC)	**Average minimum temperature** (ºC)	**Maximum temperature** (ºC)	**Minimum temperature** (ºC)
Baix Empordà	la Bisbal d'Empordà	29	15.4	22.4	9	40.3	-4.8
Gironès	Girona	72	14.9	23	7.7	41.2	-7.3
Selva	Anglès	150	14.8	22.7	8	42.9	-6.6

Table 3.3: Pluviometry (mm) from Baix Empordà, Gironès and la Selva regions during the months March, April and May of 2015. http://www.meteo.cat.

Pluviometry			
Region/month	**March**	**April**	**May**
Baix empordà	87.9	26.7	13.8
Gironès	71.6	13.4	18
Selva	136.9	19.4	29.3
Average 3 sites	98.8	19.83	20.36
Standard deviation	30.40	5.96	7.17

3.2.2. Experiments with field-sampled plants and soils

3.2.2.1. Pot experiments

The pot experiments were conducted with *A. thaliana* demes CALA, LLAM and T6.

Soil was air-dried under laboratory conditions and finally passed through a 2-mm sieve, after that, the soil was homogeneously mixed with perlite (2:1) to increase soil pore size for better aeration. To create a control soil, commercial soil (COMPO SANA® SEMILLEROS) was combined with SCF soil and perlite (1:1:1). For each soil, three different planting trays containing each 4x6 (24) cells with a volume of 80 mL per cell were used. Eight planting cells were used for each deme in each soil (Figure 3.10).

Seeds for all experiments, excepting for endophyte studies (see section 5), were sterilized by soaking in 70% (v/v) ethanol for 1 min, in bleach 30% (v/v) and 1 drop of Tween-20 for 10 min, and finally rinsed 3 times in sterile Milli-Q water. Then seeds were vernalized 4 ºC for 48 hours in the dark and then allowed to germinate on contrasting soils. Seedlings were grown in a growth chamber under controlled environmental conditions of light intensity 100 mmol/m^2s, photoperiod 8 h day/16 h night, and temperature 25 ºC day/20 ºC night. Plants were watered to water holding capacity as needed using Milli-Q water. The whole experiment was repeated twice (or three times) to assure reproducibility.

3.2.2.2. Hydroponic experiments

For seed germination, Eppendorf lids filled with sterilized bacteriological agar (0.7 %) (Scharlau, Barcelona, Spain) were used as a germination holder. These holders were prepared as follow. Lids of black 1.5 mL Eppendorfs were separated and pierced in the middle with a 2-mm borer. Once autoclaved (4002517 AUTESTER ST DRY PV III, Sant Cugat del Vallès, Spain, 121 ºC 15 min), lids were stacked on tape for being filled with the liquid agar and the tape was removed when the agar become solidified (Fig. 3.2 A). After that, filled lids were located on racks (Fig. 3.2 B) and the rack was filled with sterile Milli-Q water. Seeds were sterilized (using the sterilization protocol explained before); to promote the germination, seeds were mixed with a solution of gibberelic acid (0.01 mM) and vernalized during 4-5 days at 4 ºC before the sawing. Surface-sterilized seeds were placed individually on the hole of the filled lids with a toothpick. The rack

was covered with hermetic plastic bag and stored at 4 ºC without light. Passed two days, racks were kept under the conditions explained for the pot experiment. Water was re-filled to racks when it was necessary. Once the root grew out of the agar and touched the water, seedlings were transferred to the hydroponic system this is approximately when root system was 2-3 cm long and the rosette diameter was approximately 1.5 cm (Fig. 3.2 C).

Two different hydroponic methods were used. One for large experiments of more than 3 weeks with 20 plants per container (9L) and the plants individualized in cut falcon tubes to avoid entangling of the root systems (from now hydroponic A, Fig. 3.2 D). The other system for smaller plants and shorter experiments used 100 ml plastic pots containing a single plant (from now, hydroponic B, Fig. 3.2 E).

In both systems, modified half-strength Hoagland solution (pH 7.0) (Hoagland and Arnon, 1950) containing 10 µM Fe in the form of EDTA was used. Solutions were changed every 4-5 days to maintain a consistent concentration of nutrients in the solution. The nutrient solution was modified for each treatment: Zn control treatment (2 µM Zn), Zn-deficiency treatment (0.05 µM Zn), excess Zn treatment (5 µM Zn) and high carbonate treatment (2 µM Zn, 10 mM $NaHCO_3$). The treatment was initiated after 7 days of plant adaptation to hydroponic conditions.

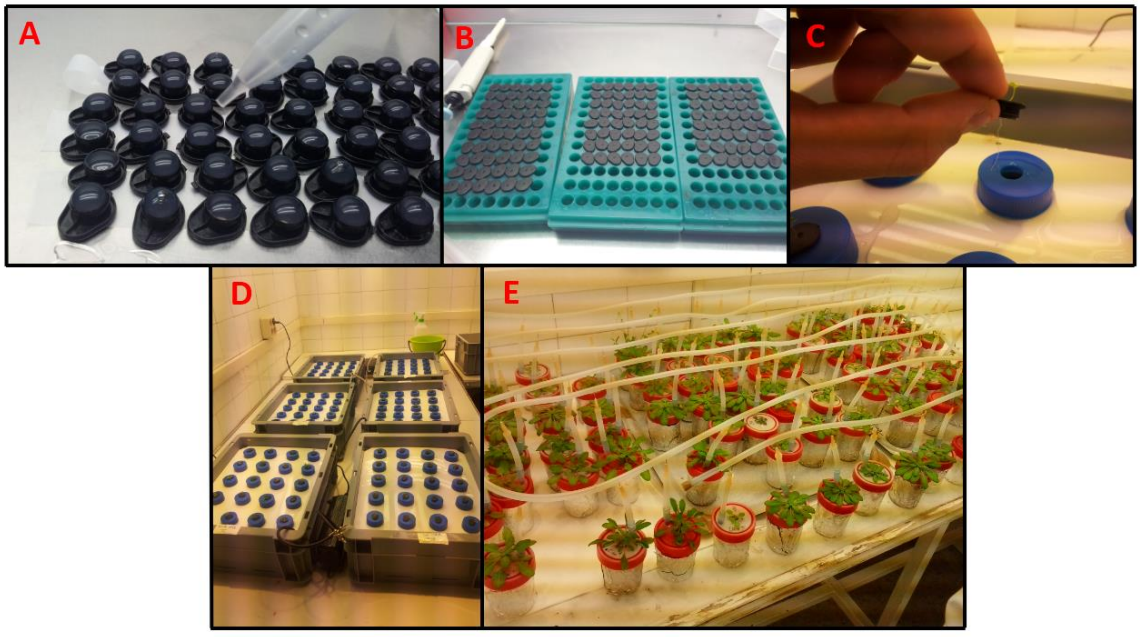

Figure 3.2: Hydroponic culture: A, Filled Eppendorf lids with 0.7% Agar. B, Racks with prepared lids. C, Seedlings grown on lids transferred to the hydroponic system. D, Hydroponic box system (hydroponic A). E: Hydroponic pot system (hydroponic B).

3.2.2.3. Plant performance

ICP analyses was performed to detect differences among the nutrient compositions of the demes exposed to different treatments. Dry material (0.1 g) of different tissues was pre-digested overnight in H_2O_2 30% HNO_3 69% (v/v) (2:5) and then digested during 4 h at 110 ºC (HotBloc model 154-240, Environmental Express, Charleston, South Carolina, USA). After that, the final volume was adjusted to 25 mL with Milli-Q water and ion concentration was analyzed by inductively coupled plasma mass spectrometry (PerkinElmer, Elan-6000).

Fresh and dry weight: Plants were removed from the growing medium (normally soil); all loose soil was washed off. After gently dry-blotting with paper towel, the plants were immediately weighed to determine the fresh weight. Then the plant samples were dried in an oven during 2 days at 60 ºC to achieve constant dry weight.

In hydroponically grown, plant root length was measured with a ruler. Other parameters like root mass, lateral roots, number of root tips were analyzed on scanned roots using software WinRHIZO™ (Pro, 2004).

Largest rosette radius was measured with the help of a ruler from the perimeter to the rosette centre.

Leaf chlorophyll concentrations were measured with a SPAD (SPAD-502Plus Konica Minolta®)

The two extreme demes, LLAM (carbonate-resistant) and T6 (carbonate-susceptible), were grown in the carbonate-rich (LPH) and carbonate-poor (SCF) soils. After that, the two selected demes were crossed. The first generation (F1) were obtained making 16 crossings (8 pairs of crossing) using the same deme as a male and female (e.g. T6 x LLAM and LLAM x T6). These crossings were also grown on the two soils (LPH, SCF) and rosette diameter and total number of siliques was calculated.

3.2.3. Gene expression analysis (RT-qPCR)

Three selected demes of *A. thaliana* plants (CALA, LLAM, T6) were grown under control (2 µM) and Zn-deficient (0.05 µM) conditions, in hydroponics (Fig. 3.2 E) for 3 weeks. The relative expressions of the main Zn transporters (MTP1, HMA3, MTP3, HMA2, ZIP1) in leaf tissue were studied. For this purpose, leaves were collected in plastic tubes, finely pulverized in liquid nitrogen, and stored at −80ºC. Total RNA was extracted using the Maxwell® RSC Plant RNA Kit

from Promega® according to manufacturer's indications. Extracted RNA was quantified with a Nanodrop2000 (Thermo Scientific, DE, USA) and quality was checked by the OD A260/A280 (1.8–2.0) and OD A260/A230 (> 1.8). One microgram of RNA was used for reverse-transcription to cDNA using the cDNA Synthesis kit (Bio-Rad, CA, USA) according to manufacturer instructions. Quantitative real time PCR was performed on a CFX384 or a CFX 96 Real-Time System (Bio-Rad, CA, USA). Each reaction contained 5 µL of iTaqTM Universal SYBR®Green Supermix (Bio-Rad, CA, USA), 2 µl of the sense and antisense primers (Tab. 3.4) at a final concentration of 2 µM and 3 µL of a dilution 1:10 or 1:50 of cDNA. The amplification program was performed by pre-incubating the cDNA for denaturation at 95 ºC for 10 min, followed by 40 cycles of a denaturation, annealing, and extension steps. After each cycle, fluorescence was measured at 72 ºC. A negative control without a cDNA template was run in each assay. Standard curves from serial dilutions of sample cDNA were used to determine primer efficiency. Expression of all studied genes was normalized by the tubulin gene of *A. thaliana*. Expression of the target gene relative to the expression of the reference gene was calculated using the $2^{-\Delta\Delta Ct}$ method (Livak et al., 2001). Three technical replicates were used in all cases per sample, dilution and non-template control.

Table 3.4: Sequences of forward and reverse primers used in the RT-qPCR. Primer design of genes: AtMTP1, AtHMA3, AtHMA2, AtZIP1 by Kawachi et al., 2008. Primer design of gene AtMTP3 by Desbrosses et al., 2005.

Gene	Primer name	Sequence
AtMTP1	MTP1F	5'-ATGGAGTCTTCAAGTCCCCAC-3'
	MTP1R	5'-CCGGAAGCATTCTTAGAATCTG-3'
AtHMA3	HMA3F	5'-GGCGGAAGGTGAAGAGTCAA-3'
	HMA3R	5'-GAAACCTCCGATGAACAGCA-3'
AtHMA2	HMA2F	5'-AGAAGATGACCAAGAGTTACTTCG-3'
	HMA2R	5'-GCTTGGTTCAGTGCTTTAACG-3'
AtZIP1	ZIP1F	5'-GTGCCTCGAGTGATTGTACAAGTC-3'
	ZIP1R	5'-CGGCTACAAGAAGTAAAGCTATCG-3'
AtMTP3	MTP3F	5'-GCGATTACTGTCGGCAAACTTT-3'
	MTP3R	5'-AAACCATATCTGCCTCTGCCTC-3'

3.2.4. Statistical analysis

Continuous data were analyzed by the JMP software (Cary, NC, USA). Normal distribution was checked and data not adjusting to normal distribution were transformed with logarithm and sinus correction, before applying parametrical tests, ANOVAs followed by Turkey HSD.

3.3. Results

3.3.1. Field-sampled soils and natural demes of *A. thaliana*

Main characteristics of the soils from the different sampling sites are summarized in Table 3.5 Soils T6, CALA, LLAM, RO2 and A5 correspond to the sites where *A. thaliana* demes had been sampled (see map in Fig. 3.1). LPH and SCF are the soils from the field experimental sites, and Mine corresponds to the soil from the Zn-Pb mine. Part of the soils had already been characterized in a previous study (Busoms et al., 2015). Here, we include a more detailed description of the soils from the mining site that, because as far as we know, this has not previously been analysed. Soils from LPH, SCF and Mine were further analysed for microbiological characteristics using Biolog® ECO plates. Moreover, selected soils from the natural habitats of *A. thaliana* demes were used to quantify and isolate cultivable bacteria (see section 4).

Table 3.5: Characteristics of soil from the different sampling sites. Zn values for mine soil corresponds to EDTA extractable fraction (*).

SOIL	pH	% O.M.	% $CaCO_3$	WHC (mL/g)	µg Zn/ g soil	Texture	%Sand	%Clay	% Silt
T6	6.30	2.17	1.36	5.4	6.33	Sandy-Loam	71	11	18
CALA	5.72	4.11	1.20	6.5	4.25	Sandy	90	5	5
LLAM	7.28	3.14	8.15	19.3	11.6	Loam	37	18	45
RO2	6.29	3.14	1.48	11	5.38	Sandy-Clay-Loam	52	28	20
A5	6.76	4.18	12.26	16.5	10.2	Sandy-Clay-Loam	50	25	25
LPH	7.86	3.84	33.25	21.05	9.84	Silty-Loam	20	20	60
Mine	5.72	2.40	2.22	30.42	410*	Sandy-Loam	65	10	25
SCF	7.32	2.88	4.81	13.8	1.68	Loam	45	22	33

Although the analysed soils are relatively close to each other, notable differences were observed in their texture, composition, pH, carbonate content and Zn concentrations. As expected, soil from the mining site has the highest Zn concentration. On the other hand, the soil from LPH has the highest carbonate contents.

Soil Zn concentrations considerable vary both among the sampling sites and between the collection periods of March and May (Fig. 3.3). While in early spring Zn concentrations in soils from *A. thaliana*'s natural habitats were relatively high at the inland sites from Anglés (A5) and Llambilles (LLAM), as well as at the coastal site (CALA), in late spring Zn concentrations were low at all sites excepting A5. Lowest Zn concentrations were found at the coastal sites in Roses (RO2) and Tossa de Mar (T6).

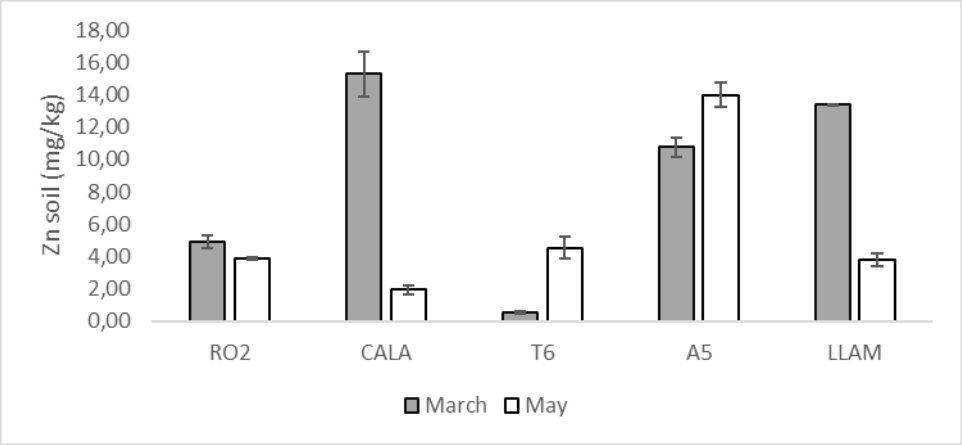

Figure 3.3: Differences in Zn concentration (DTPA extraction) during two periods of soil collection.

Figure 3.4 shows the leaf Zn concentrations in the *A. thaliana* demes collected in late spring at the different sites from soils with Zn concentrations shown in Figure 3.3. As expected, plants from the sites with lowest Zn extractability, RO2, A5 and T6 had lowest leaf Zn concentrations, while plants from LLAM and CALA had considerably higher Zn leaf concentrations. An extremely high variability in leaf Zn concentrations was observed in plants from deme CALA. This was coincident with the large variation in soil Zn extractability over time at this location (Fig. 3.3). We cannot exclude that the population at this site contains individuals with different Zn accumulation efficiencies.

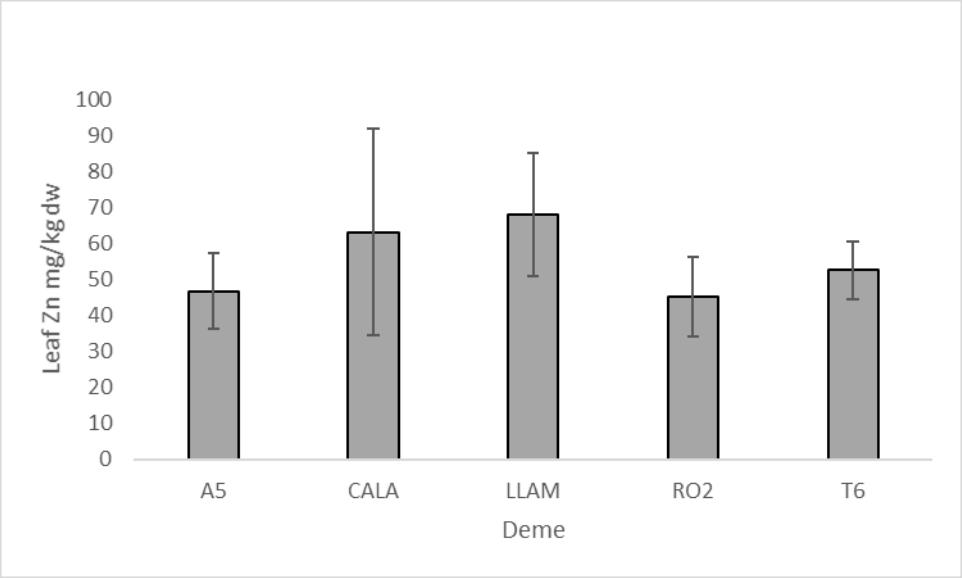

Figure 3.4 Zinc in shoots of *A. thaliana* demes from soils differing in Zn concentrations. Error bars on columns are standard deviations.

As expected, highest Zn concentrations in soils were found close to the mine. The "Mina d'en Nadal" was a poorly yielding, now abandoned mine, explored in the 50ies of the last century. Both pseudototal and EDTA-extractable Zn concentrations decreased with the distance to the mine entrance (Tab. 3.6 and 3.7). Similar concentration changes were also observed for the other *accompanying* metals, namely Pb, Cd, Cu, and Co. *Arabidopsis thaliana* was not found at this location neither on the highly contaminated soils close to the mine entrance or at the two more distant sampling sites with moderate metal concentrations located approximately 1.6 km North (Can Bancells) and 0.95 km South-East (Can Vergeli) from the mine entrance (Fig. 3.5). The mine soil was used in two types of pot experiments; a comparison study with selected natural deme using soils with high and low Zn availability (see section 3) and Genome-wide association study to explore Zn tolerant traits in *A. thaliana* (see section 5).

Table 3.6: Total (aqua regia) metal concentrations in soil samples from different sites around the mine entrance. Mine 1m, 2m and 3m indicate the distance (in meters) to the mine entrance. The distance to the main entrance at Can Vergeli was 0.95 km and at Casa Bancells 1.6 km.

Soil	µg Cd/ g soil	µg Pb/ g soil	µg Zn/ g soil	µg Cu/ g soil	µg Co/ g soil
Mine 1 m	12.9	1158	1062	111	28
Mine 2 m	7.62	3810	903	304	32
Mine 3 m	4.16	816	591	75	17
Casa Vergeli	0.38	50	106	40	9.3
Casa Bancells	0.30	32	96	32	10

Table 3.7: EDTA extractable metal concentrations in soil at different sites around the mine entrance (see legend to Tab. 3.6) and at Santa Coloma de Farners (SCF, non-carbonate) and les Planes d'Hostoles (LPH, carbonate-rich).

Soil	µg Cd/ g soil	µg Pb/ g soil	µg Zn/ g soil	µg Cu/ g soil	µg Co/ g soil
Mine 1 m	7.9	247	410	8.2	8.6
Mine 2 m	3.6	873	215	17	1.1
Mine 3 m	1.7	260	61	3.1	0.61
Can Vergeli	0.18	9.4	10	0.95	0.31
Casa Bancells	0.15	7.1	12	2.9	0.61
LPH	0.09	1.7	6.6	4.2	0.32
SCF	0.03	4.3	2.2	0.85	0.06

Figure 3.5: Views of sampling sites around the mine A; Can Bancells B; Can Vergeli.

Figure 3.6: Plants located around mine. A; *Hedera helix B; Quercus suber C; Arbutus unedo D; Rubia peregrina E; Arbutus unedo F; Smilax aspera*.

Vegetation around the mine is typically for the Gavarra area with Mediterranean climate. Observed species are *Pinus halepensis*, *Pinus pinea*, *Quercus pubescens*, *Quercus ilex* subsp. *ilex*, *Quercus suber*, *Smilax aspera*, *Hedera helix*, *Arbutus unedo*, *Viburnum tinus*, *Asparagus acutifolius*, *Pistacia lentiscus*, *Phillyrea latifolia*, *Ruscus aculeatus*, *Cistus monspeliensis*, *C. salviifolius*, *Erica aborea*, *Ulex parviflorus*, *Clematis flammula*, *Lavandula latifolia*, *Rosmarinus officinalis* and *Lonicera implexa* subsp. *implexa*, among others. (Fig. 3.6). Any *A. thaliana* plant was found around the mine.

The soil polluted by mining activity was selected for its high Zn content (Tab. 3.7); but also, the concentration of Pb, Cd, Cu and Co were enhanced in comparison to the other two soils selected for low and high carbonate (SCF, LPH) (Tab. 3.8)

Biolog® ECO plates analysis. The average well-color development allows to differentiate soil microorganisms based on their ability to process different carbon sources. In figure 3.8 the results 7 days after the inoculation are shown. There are clear differences between the carbonated soil (LPH) and the two other soils (Mine soil and SCF) in almost all of the different carbon sources. Exceptions were D-mannitol, Tween 40, and arginine with hardly no differences among the soils.

The soil from SCF, is the soil with more activity in all of the carbon sources; this was a further reason to use it as a reference control. Surprisingly, the metal-polluted mine soil, is the second more active soil in relation to carbon metabolizing activity and in some cases, it's is similar to

the control soil (SCF). However some significant differences were found (D-xylose, glucose-1-phosphate, D,L-α- glycerol phosphate, phenylethylamine and glycyl-L glutamic acid) specially in all the carboxylic and ketonic acids (less in itaconic acid and D-malic acid). In general, the mine soil has a profile similar to the control soil with some significant differences in specific sources. The carbonate-rich soil from LPH has clearly lower carbon metabolizing activity than the carbonate-poor control from SCF and the mine soil. Microbes metabolizing carbohydrates (excepting D-mannitol), carboxylic and ketonic acids had 2-3 times less activity; also, those metabolizing, polymers and amino acids were less activity in comparison to the control soil (SCF). Carbon metabolism is clearly less active in LPH, and probably this is due to the high carbonate content.

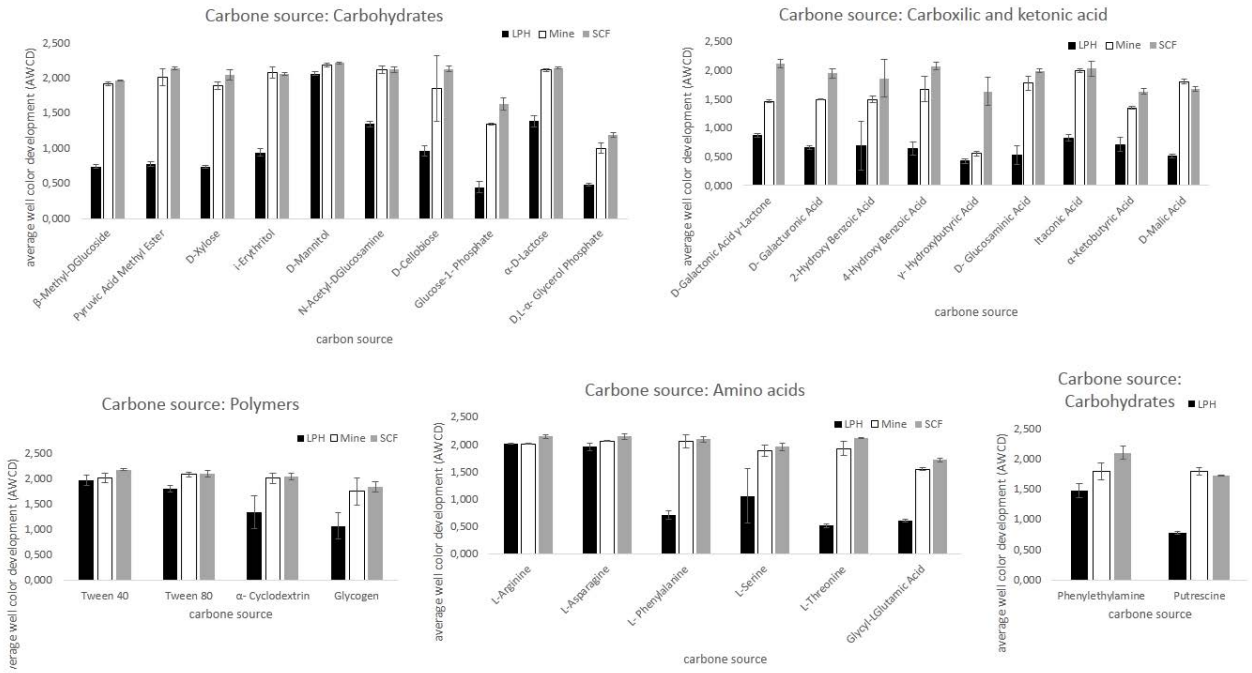

Figure 3.7: Biolog analysis results of 3 different soils (LPH, Mine, SCF). Results expressed in, average well color development (AWCD). 7 days post inoculation.

3.3.2. Pot experiments for Zn efficiency and tolerance

Pot experiments using carbonate-rich soil from Les Planes d'Hostoles (LPH), low carbonate soil from Santa Coloma de Farnérs (SCF) and Zn–rich mine spoil soil were performed with selected *A. thaliana* demes. Plants were grown from seeds collected from demes that in their natural habitat differ in shoot Zn concentrations: LLAM and T6 with high and low Zn shoot

concentrations, respectively; as well as CALA with a highly variable Zn accumulation pattern (Fig. 3.4).

Surprisingly, the pot experiments were unable to reveal differences in the capacity of the demes to accumulate Zn in the shoots when grown on the same soil type. All three demes had highest shoot Zn concentrations on the mine soil and similar low concentration at LPH and SCF. Only on the carbonate-poor SCF soil with extremely low Zn content T6 accumulated somewhat higher Zn shoot concentrations than CALA (Fig. 3.8). This was not observed at LPH, with an almost 6-time higher soil Zn concentration. Probably the high carbonate content of the LPH soil hampered the acquisition of Zn by the plants.

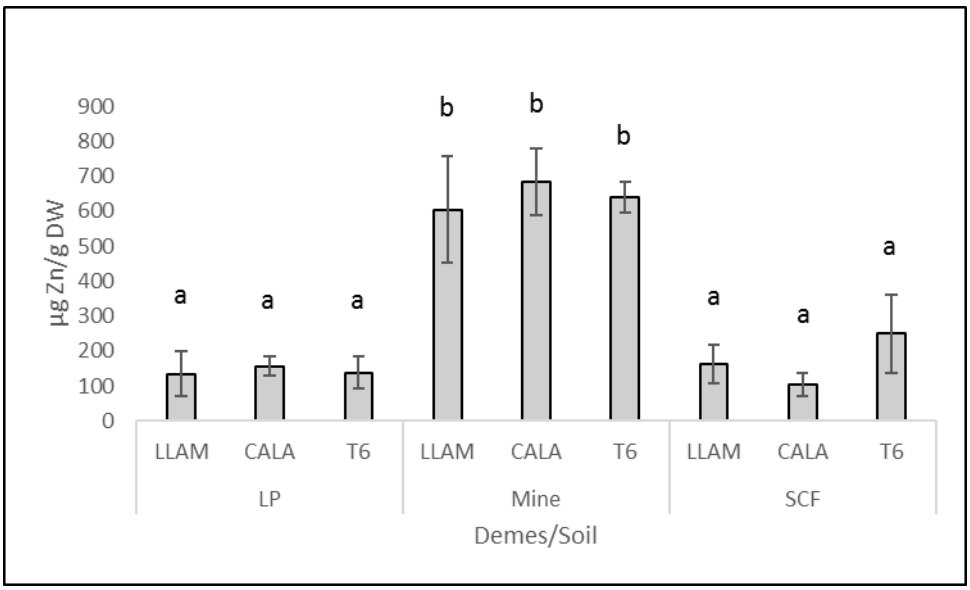

Figure 3.8: Zn content (µg Zn/g DW) in the three demes on different soil conditions. LPH (carbonated soil), Mine (Zn polluted soil), SCF (control soil). Error bars on columns are standard deviations based on ICP-MS analysis from different plants. Columns with the same letter are statistically not different (Tukey test $p < 0.05$).

However, further growth chamber experiments comparing plant performance on Zn-rich mine spoil soil and Zn-poor SCF soil after 4 weeks exposure, revealed clear differences among the demes in tolerance to the high and low Zn concentrations, respectively (Fig. 3.9). T6 performed best on SCF without foliar symptoms, while CALA and LLAM exhibited violet colour, especially in the older leaves, when grown on this Zn-poor substrate. Purple leaf colour development is a usual leaf symptom in *Arabidopsis* plants under stress. Enhanced anthocyanin biosynthesis, which is responsible for this leaf symptom, may contribute to enhanced antioxidant defence under stressful conditions (Shao et al., 2008). On the metal-rich mine spoil soil, LLAM was clearly

the best performing deme, while CALA suffered severe growth inhibition and T6 hardly germinated and only one plant survived on this soil (Fig. 3.9).

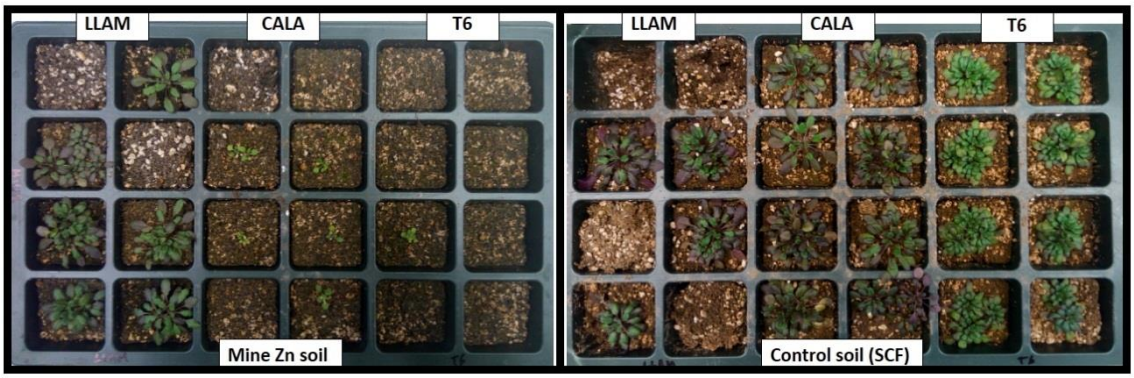

Figure 3.9: Three selected demes grown during 4 weeks in Mine Zn polluted soil and a control soil. Soils previously described in table 3.5.

Comparing Zn accumulation in plants in their natural habitat with those cultivated in pot experiments clear differences are observed. In their natural habitat, Zn shoot concentrations of the demes mainly reflect Zn concentrations in the substrate. Highest soil Zn was found at LLAM followed by A5, T6, RO2 and CALA. In the demes, highest Zn shoot concentrations were found in LLAM, followed by CALA, A5 T6 and RO2. The different behavior of CALA may be due to the highly variable Zn availability with time in its natural habitat.

When grown in the growth chamber on soils with highly different Zn availability, clear differences in leaf Zn concentrations among plants on mine spoil and the other soils were observed. However, there were no clear differences neither between plants on the carbonate - rich and carbonate poor soils or among the demes on the three soils. The fact that demes in their natural habitat display differences in leaf Zn accordingly the Zn availability in the soil, but not in the pot experiment on soils with different Zn availability from outside the natural habitat, can have different causes related to either or both cultivation system and soil properties. Restriction of root development in the pots, hampering exploration of large soil volume to acquire nutrients, and extreme soil chemical factors on the non-habitat soils may account for this. All demes accumulated similar high shoot Zn concentrations when growing on mine spoil soil. This suggests that soil conditions were too extreme to reveal differences among Zn acquisition mechanisms among the demes. High carbonate content at LPH may have hampered Zn uptake in T6, a deme less adapted to carbonate soil than LLAM. In contrast, T6 accumulated

somewhat higher Zn concentrations than the other demes on SCF, the soil with low carbonate, but extremely low Zn availability.

Due to the complex interactions on factors in soil studies, we further analyzed Zn efficiency and tolerance in the demes using a hydroponic culture system.

3.3.3. Hydroponic experiments

The new method developed for the hydroponic cultivation is advantageous for different reasons. First of all, it allows to work easily with each plant individually, even so if the plant was grown in big containers along with other plants due to the separation of root systems by the Falcon tubes. The system allows easy calculation of germination rates, yet the performance of each individual seed can be visualized. Moreover, the system avoids manipulation or movement of the seeds after germination as it only is necessary to move the Eppendorf cap to the pot or box with the nutritive solution. A further advantage is that the root structure can be easily assessed using the WinRHIZO analysis system.

Clear differences among treatments and demes in Zn accumulation in roots and shoots were detected in hydroponic conditions. As it was expected, Zn tissue concentrations were highest under excess Zn supply (Fig 4.8 A, B). CALA exhibited highest root and shoot Zn concentrations, followed by LLAM and T6. Lower Zn concentrations were observed for RO2, A5 and Col-0. Shoot/root Zn concentration ratios were highest for Col-0 and T6.

Under normal Zn supply (2 µM) CALA and LLAM had the highest shoot Zn concentrations followed by Col-0, T6, RO2 and A5 had the lowest Zn shoot concentrations without differences among them. Root to shoot transfer of Zn was lowest in T6 and A5.

Under Zn deficient conditions in solution without carbonate T6 accumulated highest Zn levels in the shoots, followed by CALA and LLAM; T6 exhibited the highest root to shoot Zn transfer. Contrastingly, in solutions supplemented with $CaCO_3$ Zn translocation form roots to shoots was worst in T6, while LLAM clearly accumulated the highest shoot Zn concentrations.

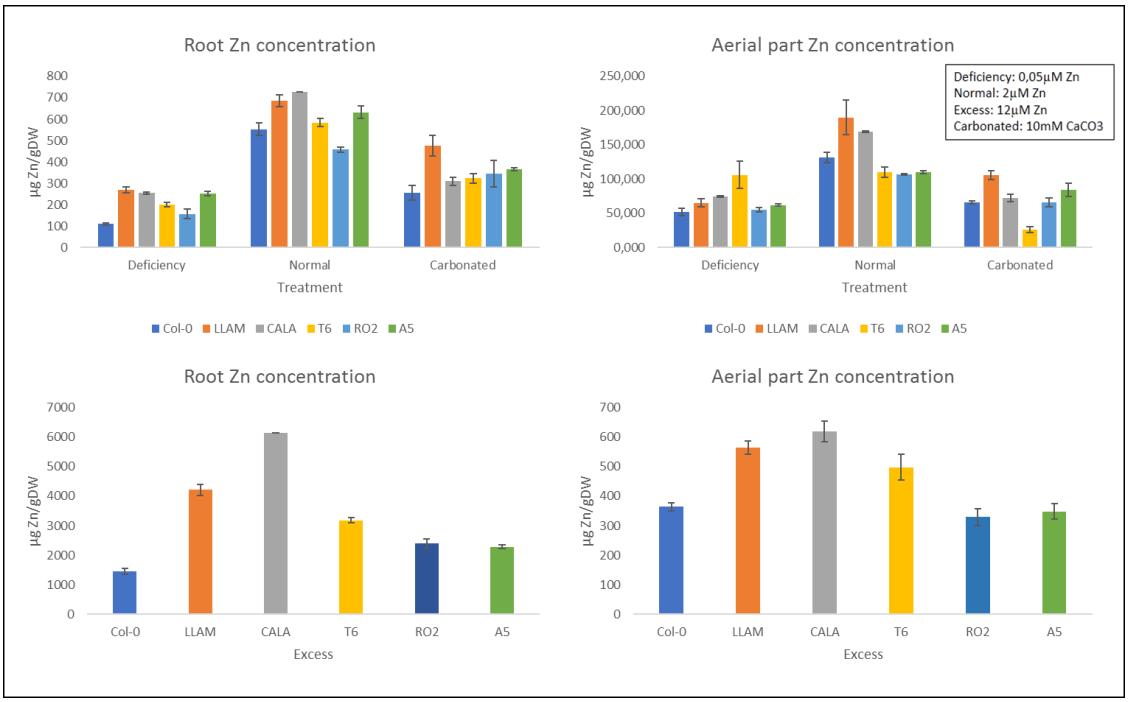

Figure 3.10: Zn concentrations in root and aerial part of hydroponically grown *A. thaliana* demes. The graphics show the three selected demes (LLAM, CALA, T6), also 2 new demes (A5, RO2) described by Busoms S. et al., 2015 and the Col-0. Error bars on columns are standard deviations based on ICP-MS analysis from different plants.

To further characterize the response to different Zn availability, other hydroponics with the selected demes (LLAM, CALA, T6) were developed. As before, CALA deme showed more capacity to translocate Zn to the shoot under both normal and excess Zn supply (Fig. 3.11).

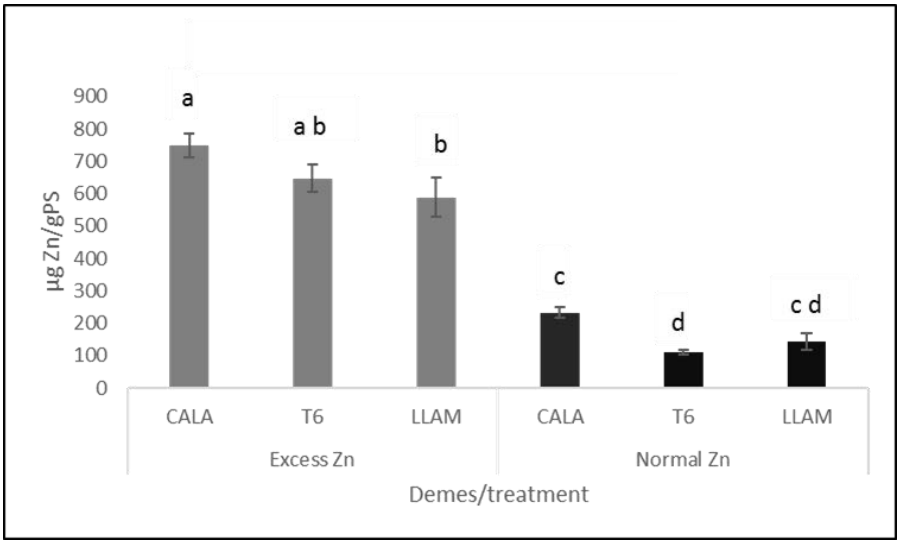

Figure 3.11: Zn concentrations in aerial part of hydroponically grown *A. thaliana* demes. The graphics show the three selected demes (LLAM, CALA, T6). The nutritive solution was supplied with normal (2 µM) and excess (12 µM) of ZnSO4. Error bars on columns are standard deviations based on ICP-MS analysis from different plants. Columns with the same letter are statistically not different (Tukey test $p < 0.05$).

To further characterize the differences in response of the most distinctive demes to carbonate a further hydroponic experiment was performed comparing LLAM, CALA and T6 in nutrient solution with and without $CaCO_3$ using hydroponic box system (Fig. 3.12). Clearly visible differences in mortality and growth appeared between the treatments due to the carbonated effect (Tab. 3.8 and Fig. 3.12 to 3.15).

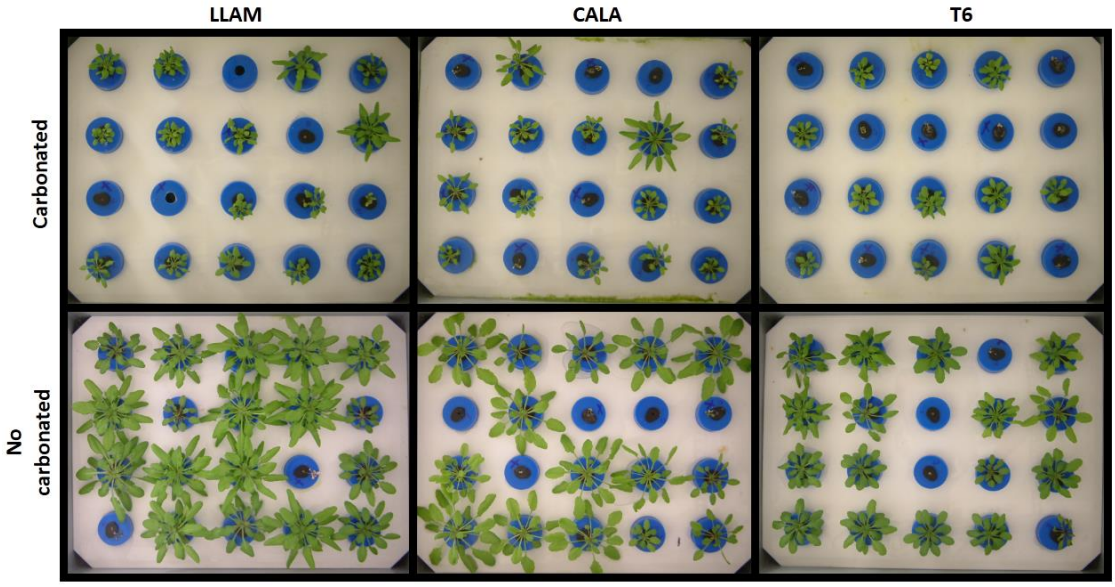

Figure 3.12: Plant growth of the three demes (CALA, LLAM, T6) grown in half-strength Hoagland solution supplemented with 10mM $CaCO_3$ (carbonated) or without (non-carbonated).

Rosette diameter and root length were severely affected by the 10 mM $CaCO_3$ treatment (Tab. 3.8) in all demes without statistically differences among them.

Table 3.8: Growth measurements of three demes on hydroponic experiment under different treatments. Percentage of mortality, root length and rosette diameter ± standard deviations from different plants in root length and rosette diameter. Same letter is statistically not different (Tukey test $p < 0.05$) for the specific parameter.

Treatment	Demes	% mortality	Root lenght	Rosette diameter
CARBONATED	CALA	25	8.64 ± 1.39 **b**	3.5 ± 1.37 **c**
	LLAM	20	7.82 ± 1.71 **b**	3.22 ± 1.1 **c**
	T6	45	7.82 ± 1.03 **b**	3.09 ± 0.48 **c**
NO CARBONATED	CALA	5	23.6 ± 3.63 **a**	7.4 ± 1.94 **a**
	LLAM	10	22.06 ± 3.38 **a**	7.52 ± 1.57 **a**
	T6	15	20 ± 2.48 **a**	5.35 ± 0.99 **b**

Fig. 3.14 shows the average Zn concentrations average of the demes. There was a clear inhibitory effect of carbonated on Zn acquisition. There is tendency but not significant differences in root tissue but significant differences appear in aerial part between the carbonated and non-carbonated treatment.

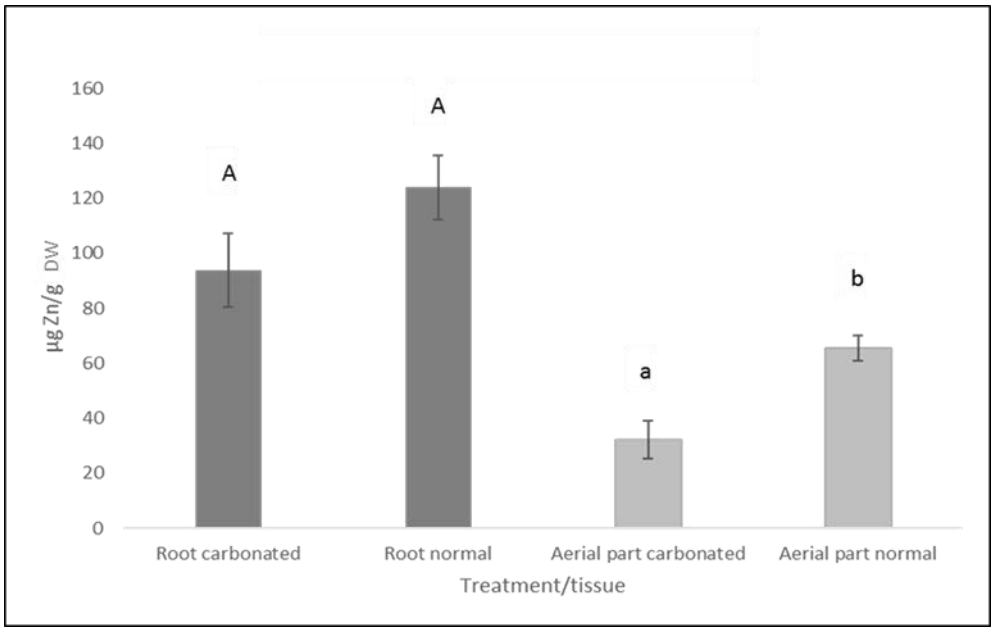

Figure 3.13: Concentration of Zn (µg Zn/g dry weight) in root and aerial part. Average of zinc concentration of the three selected demes (CALA, LLAM, T6) grown in hydroponic conditions, nutritive ½ Hoagland solution (Normal) and supplemented with 10 mM of $CaCO_3$ (Carbonated). Error bars on columns are standard deviations based on ICP-MS analysis from different plants. Columns with the same letter (capital for root and lower case for aerial part) are statistically not different (Tukey test $p < 0.05$).

Dry weight (Fig. 3.14) and root structural features (Fig. 3.15) were determined under control and carbonate-rich conditions. Although 10 replicate plants per deme and treatment were analyzed, no significant differences among the demes were observed under control conditions, due to large standard deviations. All the measured parameters were severely affected by the exposure to 10 mM carbonate, but no differences among the demes were observed.

Other analyzed growth parameters, like chlorophyll content, germination taxa or ferric reductase capacity, also did not showed statistically significant differences among the demes (data not shown).

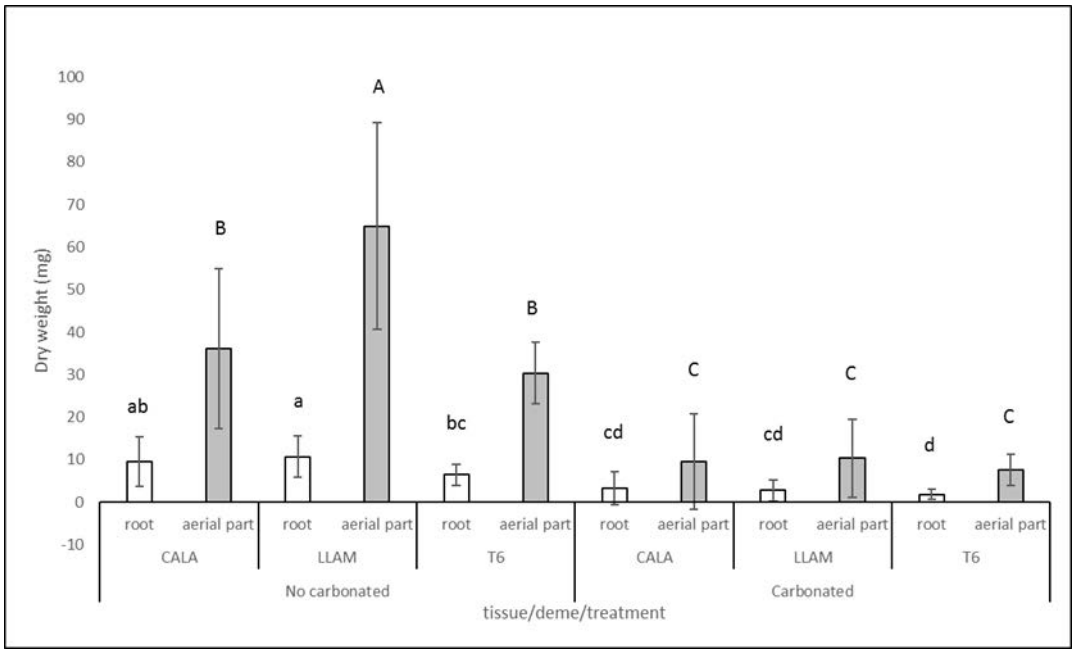

Figure 3.14: dry weight of *A. thaliana* plants grown in hydroponic conditions. Root dry weight (white bars) and aerial part dry weight (grey bars) of the different demes in carbonated and non-carbonated treatment. Error bars on columns are standard deviations. Columns with the same letter (capital for aerial part and lower case for root) are statistically not different (Tukey test p < 0.05).

Winrhizo® analysis was done after see the differences in the root length and with the software other important parameters were analyzed. This protocol was developed at the end of the hydroponic due to the manipulation of the plant material.

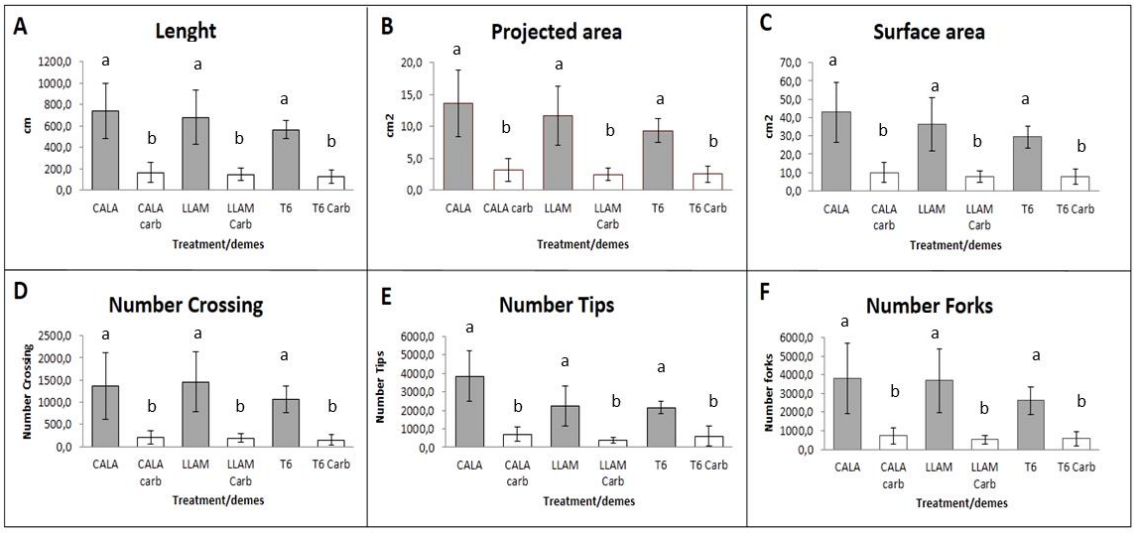

Figure 3.15: Winrhizo analyzed parameters. A; Root Length. B; Projected area. C; Surface area. D; Number Crossing. E; Number Tips. F; Number Forks. Error bars on columns are standard deviations based on diameter measurements from different plants. Columns with the same letter are statistically not different (Tukey test p < 0.05).

3.3.4. Gene expression (RT-qPCR)

This analysis was developed to know the differences among the demes (CALA, LLAM, T6) in the expression of selected genes related to Zn homeostasis (Fig. 3.16) when growing in hydroponics under normal (2 µM) and deficient (0.05 µM) Zn conditions.

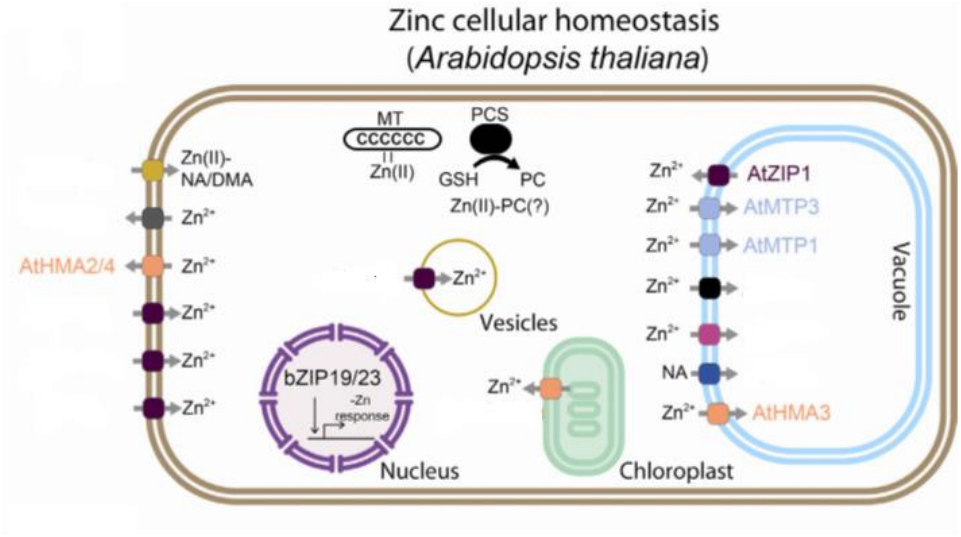

Figure 3.16: Transporters and Zn-binding molecules involved in Zn homeostasis are shown in a schematic plant cell. Arabidopsis thaliana. Modified from Ricachenevsky et al., 2015.

Under control conditions, there were significant differences between LLAM and CALA on one side and T6 on the other in relation to the expression of *AtHMA3*. LLAM and CALA had higher constitutive expression of this gene. (Fig. 3.17).

Clear differences appeared between LLAM and the other two demes (CALA and T6) under deficient conditions. The expression of *AtMTP1* gene in deficiency was highly increased (5-fold more) in LLAM compared to CALA and T6. The expression of *AtHMA2* and *AtZIP1* was also 4-fold higher in the Zn deficient treatment for LLAM.

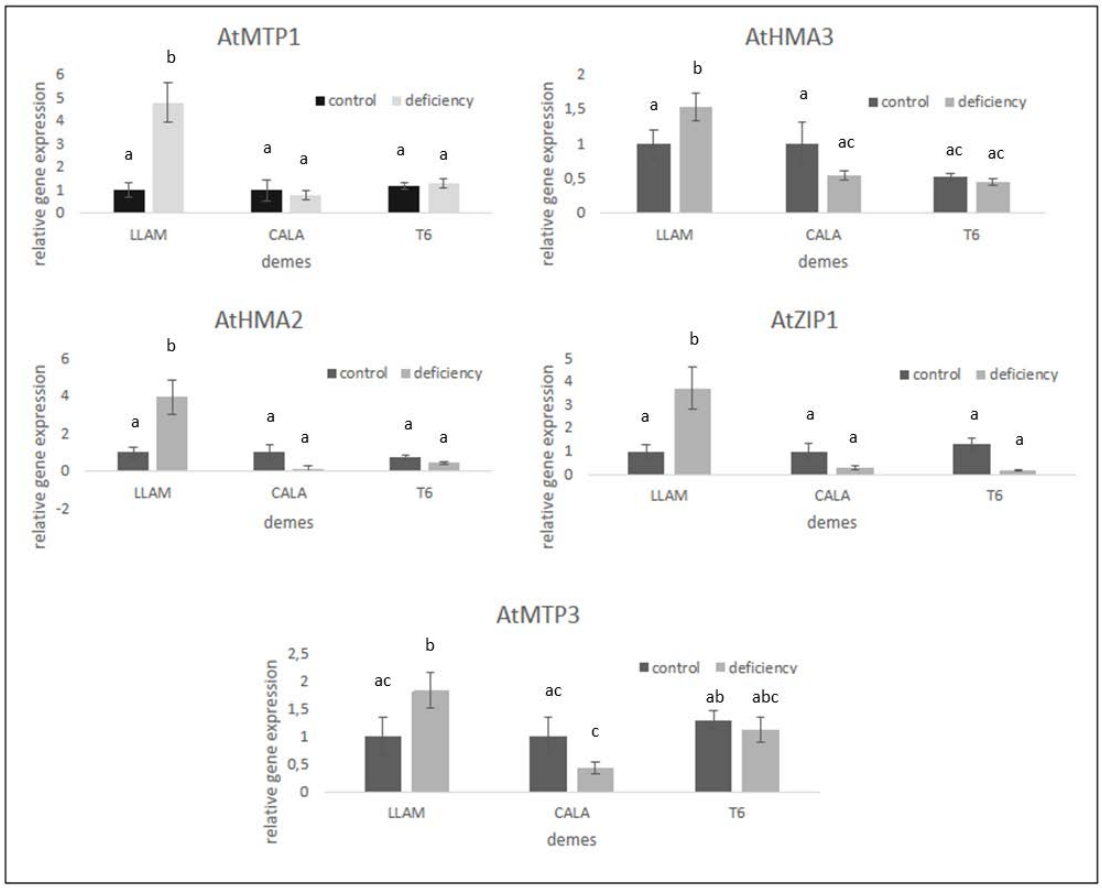

Figure 3.17: Relative expression of five Zn transporter genes (*AtMTP1, AtHMA3, AtMTP3, AtHMA2, AtZIP1*). Error bars on columns are standard deviations based on values from three different plants. Columns with the same letter are statistically not different (Tukey test p < 0.05).

3.3.5. Performance of T6 x LLAM intercross on carbonate soil

Our hydroponic experiments comparing the performance of the *A. thaliana* demes revealed lower root to shoot Zn transfer (Fig. 3.13) and higher mortality of T6 than in LLAM (Fig. 3.9) when exposed to carbonate supplemented nutrient solution. This better carbonate tolerance in LLAM than in T6 is in line with the difference in carbonate concentrations in the soils of the respective natural habitats, with a 6 times higher carbonate content at Llambilles (LLAM) (8.15 % carbonate) than at Tossa de Mar (T6) (1.36 % carbonate).

To see both whether this differential carbonate tolerance is sufficiently expressed to allow differences in performance under field conditions on soils with a considerably higher carbonate concentration and whether this characteristic is inheritable further experiments were conducted comparing T6 x LLAM intercross on carbonate-rich soil at LPH (33 % carbonate) along with the parental demes. Performance of parental demes was further compared in field

experiments on carbonate-rich soil in LPH and at SCF with a carbonate poor (4.8 % carbonate), siliceous soil (Tab. 3.5).

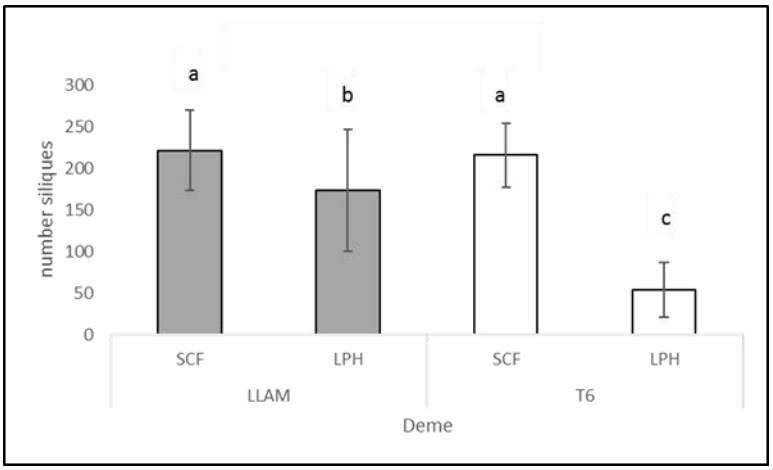

Figure 3.18: Number of siliques of LLAM and T6 demes grown on SCF (non-carbonated soil) and LPH (carbonated soil). Error bars on columns are standard deviations. Columns with the same letter are statistically not different (Tukey test $p < 0.05$).

On the siliceous soil at SCF, both parental demes performed well, displaying T6 a somewhat lower, inherent, production of siliques (Fig. 3.18). LLAM showed the same fitness in terms of silique production on the carbonate soil at LPH than on the siliceous soil at SCF. Contrastingly, T6 performed much poorer at LPH suffering an almost 60% decrease in fitness according to the number of siliques per plant.

Intraspecific crosses between the carbonate sensitive T6 and the more carbonate tolerant LLAM showed an intermediate carbonate tolerance both considering the maximum rosette diameter (Fig. 3.19) and the number of siliques (Fig. 3.20). These results, indicates that carbonate tolerance is inheritable and, probably not a dominant trait in LLAM deme.

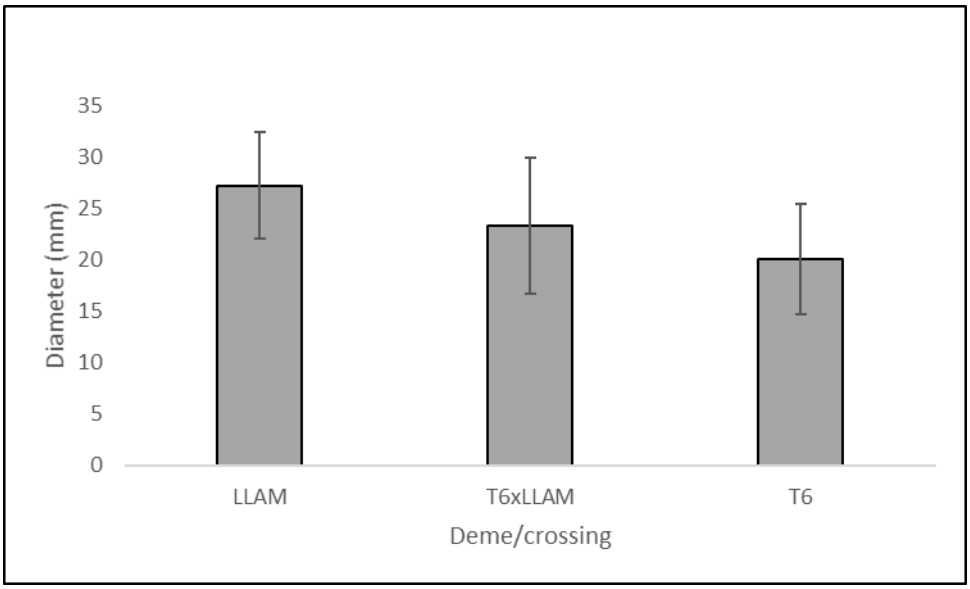

Figure 3.19: Maximum rosette diameter of demes LLAM and T6 and the crossing of the two demes (F1). Error bars on columns are standard deviations based on diameter measurements from different plants.

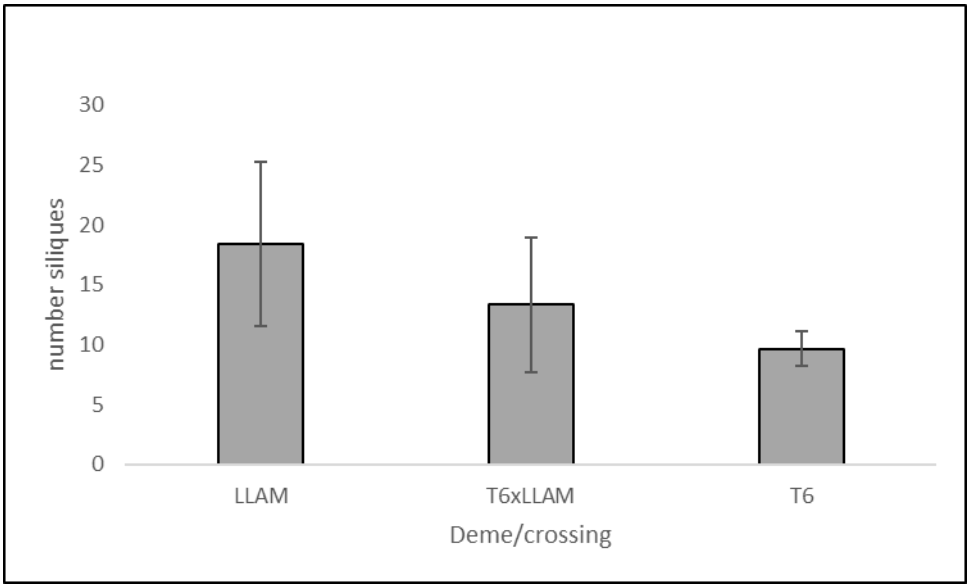

Figure 3.20: Number of siliques of demes LLAM and T6 and the crossing of the two demes (F1). Error bars on columns are standard deviations based on diameter measurements from different plants.

3.4. Discussion

Essential micronutrients have a relative small range of tissue concentrations that allow optimum plant performance. Both below the critical deficiency and above the critical toxicity concentrations plants suffer dysfunctions that limit their fitness and competitivity (Epstein and

Bloom, 2004). In the case of Zn, the range of optimal leaf concentrations lay between 20 to 80 μg/g dry weight for crop plants of the Brassicaceae family (Bergmann, 1993). This is coincident with our results from *A. thaliana* growing in their natural habitat, where rosette Zn concentrations ranged from around 40 to 70 μg/g dry weight(Fig. 3.4). The leaf Zn concentration depends on both soil and plant-related factors. Moreover, the activity of rhizosphere microorganisms may play a crucial role (Rengel, 2015).

The natural habitats of *A. thaliana* in the sampling zone in NE Spain revealed considerable variation in extractable Zn both among the sampling sites and the time of the year (Fig. 3.3). The solubility of Zn in soils at pH below 7 is governed by adsorption and desorption processes. At pH above 7 precipitation-dissolution reactions may take place (Brümmer et al, 1983). Besides the total Zn content of the mother rock, pH is a main factor determining Zn availability (Sims, 1985). However, in our experimental soils no clear correlation between extractable soil Zn and soil pH could be established (Tab. 3.5). Other factors, especially texture and organic matter may play an important role. Sandy soils are more prone to Zn deficiency than soils with heavier texture and higher cation exchange capacity (Alloway, 2004). Low-molecular weight and soluble organic matter favor Zn solubility. However, Zn adsorption onto organic matter can reduce Zn availability (Duffner et al., 2014). In fact, in the non-contaminated soils of this study highest EDTA-extractable Zn concentrations were observed for LLAM, A5, and LPH, the soils with the lowest sand content. (Tab. 3.5). A surprising observation was the large difference in extractable soil Zn concentrations between March and May samples for CALA and LLAM. It is unlikely that lixiviation is responsible for this; March had 4 to 5-times higher rainfall than April or May. No huge differences in pluviometry occurred at both sites and, even in sandy soils and high rainfall Zn lixiviation is rather low (Drissi et al., 2016).

The different demes and soils were analyzed for their ionomic content and other parameters, showing clear differences among demes and their respective original soils. The maximum distance in the geographical distributions of the different demes was between T6 and LLAM populations, being approximately 23 km. Nonetheless, the distances among the different demes were sufficient to observe notable differences among the soils and the plants in their natural habitat. Among the soils of the *A. thaliana* natural demes, soil at LLAM has the highest carbonate content (8.15 % and pH (7.3), but also the highest Zn concentration (11.6 μg Zn/ g soil), while at CALA and T6 soil carbonate and Zn contents are substantially lower.

The question here was whether these differences in soil characteristics have led to differential tolerance to imbalanced Zn availability (deficiency or toxicity) and/or high soil carbonate among these demes.

Arabidopsis thaliana is a preferential model for functional genetic studies and the variability of natural population of this species is providing important information linking functional genetics and evolution. However, it is also considered that the use of *A. thaliana* for trait identification is limited to the conditions where these natural populations have evolved and that other related species occurring in extreme habitats are better models for characterizing important adaptation mechanisms, especially to extreme stress situations (Roosens et al., 2008). In fact, important information on metal and salt tolerance mechanisms has been obtained using extremophiles like *A. halleri* (Dräger et al., 2004; Becher et al., 2004) and *Thellungiella halophila* (Inan et al., 2004, Taji et al., 2010), respectively.

Common garden experiments are highly useful tools for characterizing deme/habitat interactions, for studying phenotypic plasticity and for detection of local adaptation (Kawecki and Ebert, 2004; Dorman et al., 2009; Busoms et al., 2015). Frequently, common garden experiments are designed to be less stressful than the natural habitat of the contrasting population so to avoid strong effects on survival rates and confounding effects in the quantitative genetic analysis (Villemereuil et al., 2016).

The use of both mine spoil soils with excess Zn and enhanced levels of other potentially toxic metals (Pb, Cd) and high carbonate soil (LPH) represent strongly challenging conditions for all the selected demes. Nonetheless, such hard selection conditions can help to identify traits that are essential for maintenance of Zn homeostasis and survival under either Zn toxicity or deficiency. Here we show that natural populations originally growing in habitats with different Zn availability display huge differences in Zn toxicity tolerance when growing on mine spoil soil. No natural population of *A. thaliana* was found at the mining site. However, under lab conditions with no other stress factors (drought, competition, herbivory etc.) LLAM, the deme originally growing at the site with the highest soil Zn concentration, performed much better on the mine soil than demes from habitats with lower soil Zn (Fig. 3.9). In fact, our study shows clear differences in survival on mine spoil with excess Zn among the demes (Fig. 3.9) allowing to classify the demes according to their tolerance to metal toxicity in the following order LLAM >> CALA >> T6.

Unfortunately, we have no survival data of the demes on carbonate-rich soils. However, under field conditions at LPH where soil carbonate content was higher than 30%, a soil carbonate concentration much higher than those described for any habitat where *A. thaliana* occurs in nature, LLAM grew better and had higher fitness based on siliques formation than T6 (Fig. 3.18). Less sensitivity to carbonate soil conditions of LLAM than of T6 is in agreement with the higher carbonate content in the LLAM native soil (8.15 %) than in soil at Tossa de Mar (1.36 %), where

T6 comes from (Tab. 3.5). Further support for better carbonate tolerance in LLAM comes from the mortality rates observed in hydroponics with 10 mM CaCO3 (Tab. 3.9).

Although LLAM is less sensitive to carbonate than T6, all demes suffered severe growth inhibition when exposed to 10 mM $CaCO_3$ in hydroponics (Figs. 3.14, 3.15). In this open system at pH 8, carbonate forms a solid phase maintaining a rather constant bicarbonate concentration in the solution. Several investigations have revealed huge differences in carbonate/bicarbonate sensitivity of different plant species. While in different ornamental species the critical level ranged from 2-10 mM (Valdéz-Aguilar and Reed, 2007), for several Brassicaceae species no growth inhibition was observed at 10 mM (Zhao and Wu, 2017). In this context, all of our natural *A. thaliana* demes were carbonate sensitive under hydroponic conditions, but differences were revealed when cultivated in carbonate–rich soil. This contrasting behavior could be related to rhizosphere processes such as root–induced lowering of rhizosphere pH (Valentinuzzi et al., 2015), exudation of phenolics (Fourcroy et al., 2014; Schmid et al., 2015; Terés, 2017) and microbial activity (Kidd et al., 2013).

The observation that deme LLAM performed better both on slightly acidic (pH 5.7) mine spoil soil with excess Zn burdens and on carbonate–rich soil with alkaline pH and considerably lower Zn concentrations was surprising and suggests more efficient Zn homeostasis under extreme conditions in this deme. In their native habitats plants from CALA and LLAM accumulated higher average rosette Zn concentrations than T6 (Fig. 3.10) but the large differences among individuals at each site did not allow to establish statistically significant differences. Pot studies were also unable to reveal differences among demes in rosette Zn accumulation, probably due to the spatial limitations for root development in the small planting trays (Poorter et al., 2012).

Contrastingly, the hydroponic approach, where neither root development or water and nutrient supply are restricted, provided interesting differences in rosette Zn accumulation in relation to the stress treatments: Zn deficiency, bicarbonate treatment, and excess Zn (Fig. 3.10). As expected, leaf Zn was usually lower under Zn deficiency and carbonate treatment than under control conditions. However, while T6 maintained higher leaf Zn than CALA and LLAM under Zn deficiency, carbonate supply affected Zn translocation from roots to shoots much more intensively in T6 (Fig. 3.10). This result confirms the carbonate sensitivity of T6. While this deme more efficiently transports Zn from root to shoot under both Zn deficient and excess conditions, carbonate severely inhibits this process. Under all treatments, LLAM accumulated higher root Zn concentrations than T6, but carbonate had less influence on Zn translocation to the rosette than in T6 (Fig. 3.10).

The differences in Zn rosette concentrations among the demes when growing under the same hydroponic conditions indicate differences in metal ion transporter activities (Olsen and Palmgreen, 2014). To make a first approach to this, q-PCR analysis was performed to characterize the relative expression levels of selected metal transporter genes (Fig. 3.17) in rosettes of the different demes under Zn deficiency in comparison to control Zn supply. Selection based on current literature included the plasma membrane efflux transporter AtHMA2/4, the tonoplast transporters AtHMA3, AtMTP1, and AtMTP3 responsible for metal vacuolar storage, and AtZIP1 a tonoplast located transporter of Zn and probably manganese that seems responsible for Zn export from the vacuole to the citoplasm (Millner et al., 2013; Ricachenevski et al., 2015).

The plasma membrane located AtHMA2 and AtHMA4 are metal ATPase proteins involved in root xylem loading of Zn (Kisko et al., 2015). Contrastingly, HMA3, a P-type ATPase similar to HMA4 is located in the tonoplast. The fusion protein AtHMA3:GFP (green fluorescent protein) has been localized at the vacuole, consistent with a role in the influx of cadmium into the vacuolar compartment. In *A. thaliana*, the mRNA of *AtHMA3* was detected mainly in roots, old rosette leaves and cauline leaves. But zinc transport could not be proven and in *Arabidopsis* the expression of the gene is not affected by exposure to zinc (Gravot et al., 2004). Other works (Van de Mortel et al., 2006) show the up-regulated expression under Zn deficiency. *MTP1* and *MTP3* genes, encode vacuolar transmembrane transporters which are involved in Zn sequestration in the vacuole, under conditions of Zn excess and iron deficiency (Kobae et al., 2004; Desbrosses-Fonrouge et al., 2005; Arrivault et al., 2006; Gustin et al., 2009). The cell vacuoles are important sites for Zn remobilization during periods of Zn deficiency and for Zn storage and detoxification when Zn is present in excess (Sinclair and Kramer, 2012). Under Zn deficiency ZIP1 the tonoplast efflux transporter is characteristically upregulated (Grotz et al., 1998).

Figure 3.17 shows the relative expression of these genes under control and Zn deficiency in the three selected *A. thaliana* demes. Under adequate Zn supply, expression was the same for all demes, excepting deme T6 with a constitutively lower expression of *AtHMA3.* Overexpression of *HMA3* coding for a Zn and Cd vacuolar transporter is essential for the extreme tolerance to excess Zn and Cd in the hyperaccumulator *A. halleri* and *Noccaea caerulescens* (Becher et al., 2004; Ueno et al., 2011). The HMA3 protein is also functional in *A. thaliana* (Morel et al., 2009). The low constitutive expression of *AtHMA3* in T6, as well as the decreased relative expression under Zn deficiency in CALA may help these demes to avoid sequestration of Zn in the vacuoles favoring transport to the leaves. In fact, among the studied demes T6 and, to a lesser extent, CALA maintained highest rosette Zn concentrations under Zn deficient conditions (Fig. 3.10).

Furthermore, in both demes expression of the vacuolar transporters AtMTP1 and At MTP3 were also maintained low under Zn deficient conditions.

In LLAM, the deme with best tolerance to carbonate all the analyzed genes related to metal transport were upregulated under Zn deficiency (Fig. 3.17). Highest enhancements were observed for *AtMTP1*, *AtHMA2* and *AtZIP1.* The high expression of *AtZIP1* and *AtHMA2* may favor the release of Zn from the vacuolar storage compartment and favor Zn translocation to the shoots, respectively. Surprisingly, however, the expression of *AtMTP1* coding for a vacuolar influx metal transporter was also strongly (5-fold) enhanced under Zn-deficient conditions. Furthermore, *AtMTP3* expression was enhanced (around 2-fold). MTP1 is involved in the tolerance to excess Zn and it has been proposed that the histidine-rich loop of the MTP1 tonoplast transporter acts as a sensor for cytoplasmic Zn (Tanaka et al., 2014). Both MTP1 and MTP3 are Zn transporters located at the tonoplast. However, both have opposite effects on Zn shoot accumulation probably due to differences in tissue specific expression levels. While MTP3 reduces Zn translocation to the shoots, probably by sequestering Zn in the roots, MTP1 favors Zn transport to the shoots (Sinclair and Krämer, 2012).

This first approach to the molecular mechanisms behind the differential responses of *A. thaliana* demes from sites with contrasting soil Zn revealed a distinctive expression pattern of Zn transporter genes in LLAM. LLAM, the deme with the highest soil carbonate and Zn in its native habitat had the best tolerance to extreme soil conditions (namely high carbonate or Zn-contaminated mine spoil soil) requiring efficient regulation of Zn homeostasis. Furthermore, results on the fitness of the F1 generation of a cross between the more carbonate tolerant LLAM and the sensitive T6 demonstrate that the carbonate tolerance is an inheritable trait. Heritability of traits related to carbonate tolerance have mainly been considered in grapevine and fruit breeding indicating a polygenetic character (Bert et al., 2013). In *A. thaliana* tolerance to moderate soil carbonate also seems due to multiple traits. Here we found intermediate tolerance to carbonate soil in the F1 offspring when parental were LLAM (moderately tolerant to carbonate soil and Zn efficient) and T6 (sensitive) (Fig. 3.19, 3.20). Contrastingly, when T6 had been crossed with the iron efficient deme A1, fitness of the F1 generation on carbonate -rich soil was inherited in dominant fashion (Terés, 2017). Our result supports the view of natural selection and inheritance of vegetative functional traits (Gebber and Griffen, 2003) leading to better carbonate tolerance in *A. thaliana*.

3.5. Conclusions

- Level of carbonate in the soils is the main factor related to the tolerance to carbonated in the selected natural populations of *A. thaliana*.
- Zinc content in the soils is the main factor related to the tolerance to Zn polluted soils in the selected natural populations of *A. thaliana*. Moreover, the differences in the soil during different periods show the capacity of some demes to adapt the genetic expression in relation to Zn metabolisms.
- LLAM origin soil with more concentration of carbonated content and Zn content, for this reason is more resistant to these extreme conditions in the carbonated (LPH) soil and in the Zn mine soil. On the other hand, T6 deme from a poor carbonated soil have less capacity to growth and more mortality in LPH soil.
- Crossing of the two selected demes shows intermediate characteristics in relation to diameter of growth and number of siliques.
- Gene expression in Zn deficiency conditions shows the capacity of LLAM deme to mobilize better the Zn through the cell membrane in compared to the other selected demes.
- Biolog® ECO plates analysis describes the LPH carbonated soil as the soil with less activity in relation to the capacity of the microbiome soil extraction to metabolize different Carbone sources compared to the control soil (SCF).

4. Characterization of rhizospheric bacteria promoting nutrient availability to plants

4.1. Introduction

Zinc is a micronutrient needed for healthy growth and normal reproduction of plants in a range from 5 to 100 mg/kg. Zinc deficiency leads to reduce synthesis of carbohydrates, nucleotides, auxins, cytochromes, chlorophyll. Zinc deficient plants suffer from impaired membrane integrity and develop susceptibility to heat stress (Singh et al., 2005). On the other hand, high applications of zinc fertilizers or metal-contaminated sewage sludge have detrimental effects on both soil microbial communities and crop yields of causing evident toxic effects (McGrath et al., 1995). The solubility of Zn is directly related to the soil pH and moisture and for this reason, a lot of areas around the world like arid and semiarid areas from Asia and the Mediterranean are often zinc-deficient (Goteti et al., 2013). Around 96–99% of Zn applied for crop requirements is converted into different insoluble forms depending upon the soil types and different physicochemical reactions within 7 days of application (Saravanan et al., 2004). Microbes are a potential alternative that could help to satisfy plant zinc requirements by solubilizing different zinc forms in soil. Several genera of rhizobacteria belonging to *Pseudomonas* spp. and *Bacillus* spp. are reported to solubilize zinc (Hughes and Poole 1991). Furthermore, it is well known that these bacteria may have other plant growth promoting traits (PGPT) like IAA production, phosphate solubilization, siderophore production or antibiotic resistance so that they can play an important role in the new biotechnology strategies for agriculture approaches.

The aim of this study was to select and characterize different bacteria from the root-surrounding soil for their ability to solubilize zinc and to promote plant growth. First, the bacterial content was studied for each soil as a starting point to find PGP bacteria. After that, different strains were selected for both their Zn-tolerance and their ability to mobilize Zn from a sparingly soluble solid phase using a growth medium with zinc oxide (ZnO). Other PGPT were also analyzed to know more concretely the capacity of each selected strain to promote plant growth for future application. The analyzed traits were: IAA production, phosphate solubilization, siderophore production and antibiotic resistance. Finally, the production of gluconic acid were detected by HPLC-MS in the solubilization halo from the selected efficient Zn solubilizing bacterial strains.

After the phenotypic characterization, the genetic characterization was done using the region 16S rDNA. Once sequenced the analyzed region, the similarity to already identified strains was compared by MegaBLAST (NCBI).

4.2. Material and methods

4.2.1. Bacteria extraction and quantification

To quantify the total amount of cultivable bacteria in the different soil fractions, the standardized method of Barillot et al. (2012) was used. The natural populations of *A. thaliana* LLAM, CALA and T6 were grown in six different soils: Les Planes d'Hostoles (LPH), Santa Coloma de Farnérs (SCF), an ancient Zn mine and their own field soils. The bacteria from bulk soil of LPH, SCF, mine, LLAM, CALA and T6 soils were extracted as well as the bacteria from the rhizosphere and rhizoplane of LLAM, CALA and T6 plants. The bacteria extraction was the first approach to estimate the total bacterial content in each soil. Each extraction was done in triplicate. The analyzed soils differed on their carbonated content, directly linked with the soil pH and ion availability for plants. These soils were previously described on chapter 3 (3.2.1 Soil and plant sampling).

Due to its special characteristics with a steep gradient of Zn concentrations, the Zn mining site was analyzed in more detail and different points where screened to characterize the best point for the further soil collections. For this reason, samples from different distances in relation to the main entrance of the mine were collected and processed in the lab. Soil was sampled from outside of the mine, following a straight line starting from the entrance (Fig. 4.1).

Figure 4.1: External mine points (1 to 6) where the soils for bacteria extraction were collected.

To obtain the bulk soil fraction, 20 cm depth of soil, discarding the first 5 cm of surface soil, was directly collected with plastic bags. In soils with plant cover, (field collection or pot experiment), selected plants were vigorously shaken by hand for 10 min, without damaging the roots. The soil remaining adherent on the root surface was further analyzed for rhizosphere and rhizoplane fractions. The rhizosphere soil was extracted by hand-shaking the roots submerged in 1 L of sterile 0.9% NaCl during 10 min, to remove adhering soil. Finally, the rhizoplane fraction was collected washing and handshaking the roots vigorously during 10 min in 1 L of a sterile 0.9 % NaCl solution containing Tween 80 (0.01 % v/v).

For quantification of the different rhizosphere and rhizoplane fractions, flasks containing NaCl solutions were weighted before and after rinsing the roots in the solution, the observed difference in weight corresponds to the weight of the soil fraction.

Bulk soil bacteria extraction was following the method previously described. To homogenize the amount of each soil, 100 g of bulk soil were added to 1 L of a sterile 0.9 % NaCl solution. The soils suspensions were incubated to homogenize the bacterial content in an orbital shaker (300 rpm, 90 min, 25 °C) and centrifuged (150 g, Eppendorf 5810-R, 25 °C, 10 min) in 200 mL sterile tubes to concentrate soil particles in the pellet. Supernatants were subsequently roughly filtered on 1 mm sieves to eliminate remaining residuals in suspension. To know the bacterial density of

each soil type, 1 mL of the supernatant was diluted in a sterile NaCl 0.9% solution until 10^{-5}. One-hundred µL of each dilution were spread by surface-scratching the media in triplicate on Luria Broth (LB)-agar Petri-dishes (90 mm), supplemented with cycloheximide (100 mg/L). The number of colony-forming units (CFU) was determined after 3 and 6 days incubating the dishes at 25 ºC in a lab incubator. Plates showing fungal contamination were discarded.

4.2.2. Zn selective medium and morphological type

Prior to select the bacteria in relation to their Zn mobilization capacity, the extracted bacteria were analyzed for their Zn resistance. For this purpose, the number of CFUs and the growth of bacteria was quantified in normal LB plates and the same medium supplemented with 2.5 mM of soluble Zn ($ZnSO_4$). The strains that were able to grow and develop on high Zn media were selected for further studies. The strains confronting 2.5 mM of soluble Zn were also selected based on morphological differences on form, elevation and margin type (Fig. 4.2).

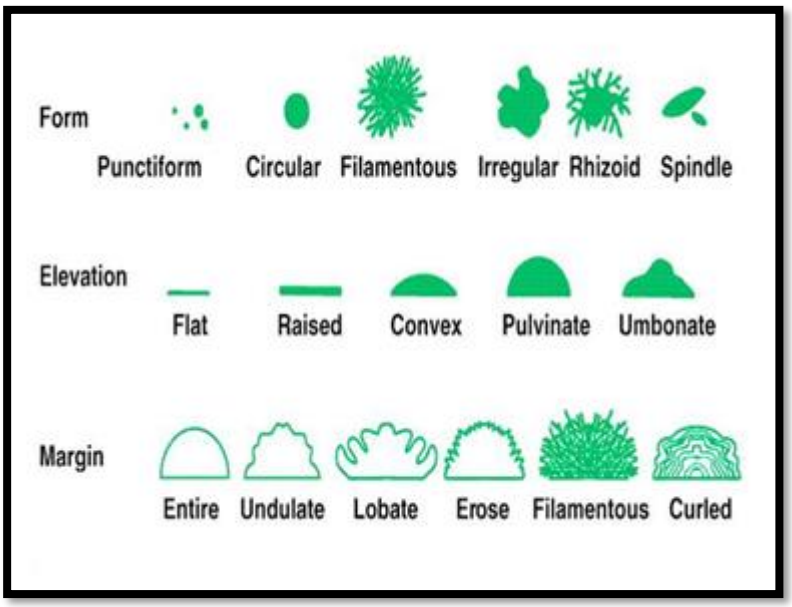

Figure 4.2: Analyzed characteristics of bacterial colonies extracted from soils (http://www.medical-labs.net/wp-content/uploads/2014/03/Bacterial-colony-morphology.jpg).

4.2.3. PGP traits

Different PGP traits were analyzed for the high-Zn-resistant bacteria previously selected. The analyzed traits were those previously described by different authors as tha main characteristics of bacetria relevant for the promotion of plant growth (Ahmad, 2008; Lugtenberg and Kamilova, 2009). Furthermore, this trait characterization was useful to get first information regarding the bacterial family or genus.

4.2.3.1. IAA production

The production of auxins was quantified by determining the absorbance values according to the method originally proposed by Bric et al. (1991) and adapted by Husen (2003). The bacterial isolates were grown in test tubes containing 3 mL of Luria–Bertani culture medium (LB: 10 g/l bacto-tryptone, 5 g/l yeast extract, 5 g/l NaCl, pH 7.5) supplemented with 1 g/L L-tryptophan. The vials containing the bacterial isolates were incubated at 28 ºC for 24 h on a shaker (150 rpm). Afterwards, 1.5 mL of the liquid culture was transferred to microtubes, centrifuged at 9,500 g for 2 min, and 100 µL of the supernatant were transferred to microplate wells together with 100 µL of Salkowski's reagent, consisting of 1 mL of 0.5 mol/L $FeCl_3$ and 49 mL of 35 % $HClO_4$. The absorbance was performed at 530 nm, using a microplate reader Cary 50 (Varian, Walnut Creek, CA, USA), half a minute after addition of Salkowski's reagent. A commercial IAA (Sigma-Aldrich, San Luis, Misuri, USA) was used to obtain the standard curve equation. The development of a reddish pink color in the samples indicates the production of auxin. The test was completed in triplicate for each isolate.

4.2.3.2. Siderophore production

The capacity to chelate iron compounds was checked using the method of Schwyn and Neilands (1997) who developed the assay using chrome azurol S (CAS) and hexadecyltrimethylammonium bromide (HDTMA) as indicators. In brief, CAS-blue agar (1 L) was prepared using 60.5 mg CAS dissolved in 50 mL distilled water, and mixed with 10 mL iron (III) solution (1 mM $FeCl_3.6H_20$, 10 mM HCl). Under stirring, 72.8 mg HDTMA dissolved in 40 mL water was slowly added to this solution. The resultant dark blue liquid was autoclaved at 121 °C for 15 min. Also autoclaved was a mixture of 750 mL water, 15 g agar, 30.24 g Pipes, and 12 g of a solution of 50% (w/w) NaOH

to raise the pH to the pKa of Pipes (6.8). The dye solution was finally poured along the glass wall and agitated with enough care to avoid foaming.

Petri dishes (90 mm) were prepared with 30 mL of appropriate medium for culturing each strain. Briefly, the assay was performed by spotting 10 µL of each exponential bacterial culture previously grown LB liquid medium. The siderophore levels produced by the isolates were recorded as the diameter of the orange halo produced by the colony. Each strain was inoculated in duplicate in three sets of experiments. Un-inoculated CAS-agar plates were incubated under the same conditions as control plates of and no color change was checked even after long incubation periods (15–20 days). The quantification of this capacity was calculated dividing the diameter of the halo in relation to the diameter of the colony.

4.2.3.3. Phosphate solubilization

The capacity to solubilize phosphate was checked in Pikovskaya's (PKV) agar medium (Pikovskaya, 1948) (contained ingredients g/l: 10 g glucose, 5 g tricalcium phosphate (TCP), 0.5 g ammonium sulphate, 0.2 g sodium chloride, 0.2 g potassium chloride, 0.1 g magnesium sulphate, 0.5 g yeast extract, 0.1 µg manganese sulphate, 0.1 µg ferrous sulphate, and 15 g agar. The pH was adjusted to 7.0 ± 0.2 before sterilization. Finally, the rate of phosphate solubilization capacity for each strain was calculated dividing the maximum diameter of the solubilization halo in relation to the maximum diameter of the colony. This result was called as the phosphate solubilization efficiency.

4.2.3.4. ZnO solubilization and organic acid production

The capacity of ZnO solubilization from the different isolated strains was checked using Tris-minimal agar medium supplemented with d-glucose and insoluble zinc oxide following the method described by Fasim et al. (2002). The Tris-minimal medium was separately amended with zinc oxide (ZnO) [1.244 g/L = 15.23 mM] at a concentration equivalent to 0.1% Zn. Tris–minimal salts medium was employed for solid culture, containing the carbon source, usually D-glucose, 10 g/l, and solidified using Agar No.2 (IDG Ltd., Bury, UK), 15 g/l, as appropriate. The Tris-medium contained (in g/L): Tris–HCl 6.06 g; NaCl 4.68 g; KCl 1.49 g; NH_4Cl 1.07 g; Na_2SO_4, 0.43 g; $MgCl_2{\cdot}2H_2O$ 0.2 g; $CaCl_2{\cdot}2H_2O$ 30 mg. The medium was adjusted to pH 7 using HCl. After sterilization and plating, one drop of 10 µl was added to the surface of the Tris-minimal agar medium plate in triplicates. The plates were incubated at 28 ºC for 7 days in dark to observe

clear halo formation around the colonies. The diameter of the halo around the colonies and colonies diameter were measured after 7 days. The solubilization efficiency (SE) of zinc was determined according to Nguyen et al. (1992) as SE = (diameter of solubilization halo/diameter of the colony) × 100. The isolates with the highest SE are considered to be effective zinc solubilizers.

The organic acid production was analyzed by HPLC (LC-MS). LC–MS analysis was carried out on a HPLC system (Varian ProStar 210), coupled to an ion trap mass spectrometer (Varian 500-MS). The HPLC conditions were as follows: the column was a Phenomenex HYDRO-RP column (C18, Polar Endcapped; particle size 4 µm; 50 mm × 2.0 mm ID). Solvents used: Buffer A (H_2O, 0.1% formic acid) and Buffer B (acetonitrile, 0.1% formic acid). Elution gradient: 0–2 min 97% Buffer A (isocratic); 2–5 min 95% Buffer B (linearly increasing); 5–8 min 95% Buffer B (isocratic); 8–9 min 97% Buffer A (linear decreasing); 9–12 min 97% A (isocratic). The flow rate was 0.3 mL/min. All solvents used for LC–MS were of LC–MS grade (Roth, 99.9%), filtered and degassed before use.

A piece of $1cm^3$ of the solubilization halo from the most efficient ZnO solubilizer strain growing on the Tris-minimal medium was introduced in an Eppendorf tube and refilled with MQ ultrapure water. After 24h, the water was used as eluent for the HPLC analysis. The HPLC eluent was introduced to the mass spectrometer using a pneumatically assisted electrospray source. The mass spectrometer was operated in the negative ion mode. The interface was adjusted to the following conditions: capillary voltage, 40 V; needle voltage, - 5,600 V; spray shield voltage, 600 V; nebulizer gas pressure, 50 psi; drying gas pressure, 30 psi; drying gas temperature, 350 °C. A 5 µl aliquot of each sample was directly injected into the HPLC system. MS/ MS spectra were obtained by collision-induced dissociation using helium as the collision gas. The mass transition for gluconic acid was m/z 195→ 129.

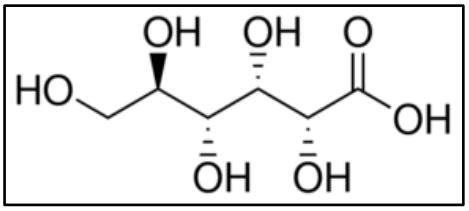

Figure 4.3: D-gluconic acid molecular structure.

4.2.4. Other analyzed parameters

The following parameters were analyzed to better characterize each isolated strain:

- The optimum pH and temperature were estimated using the diameter of the colony as a growth indicator. For this reason, LB plates with different pH between 5 until 8 were prepared with a droplet of 10 µL an isolated strain previously growing on LB medium. Three replicates per strain were inoculated for each pH. For the optimum temperature, LB plates with the optimum pH for each strain were inoculated in a similar way using different stove between 15 and 39 ºC. After that, the diameter of each colony was measured 5 days later and the biggest diameter established the best parameter of pH and temperature.
- The resistance or tolerance to different antibiotics was checked in LB plates supplemented with different antibiotics as ampicillin (0.1 mg/mL), chlorotetracycline (0.025 mg/mL), gentamycine (0.01 mg/mL), kanamycine (0.05 mg/L, streptomycine (0.1 mg/mL), and tetracycline (0.01 mg/mL). Antibiotics were added with a syringe and filtered (0.04 µm) after the medium was autoclaved. If no colony growth was detected, the strain was described as an antibiotic non-resistance for this specific antibiotic. On the other hand, if some colony appeared in the plate, the strain was described as antibiotic resistant.
- The enzymatic activities of the more interesting strain were analyzed using the technology of API ZYM test. The API ZYM system is a semi-quantitative rapid system for the detection of bacterial enzymes applicable to various environments, tissues, cells, body fluids, organisms, among others. The API ZYM (BioMerieux, Marcy-l'Etoile, France) system consists on a plastic gallery of cupules, in the bottom of each of which is a fabric support carrying the substrates and buffer. These substrates detect the following enzymes: alkaline and acid phosphatases, butyrate esterase, caprylate esterase lipase, myristate lipase, leucine, valine and cystine aminopeptidases, trypsin, chymotrypsin, phosphoamidase, α-galactosidase, β-galactosidase, β-glucuronidase, α-glucosidase, β-glucosidase, β-glucosaminidase, α-mannosidase, and α-fucosidase. No aseptic precautions were necessary because the incubation time was limited and the load microbial cells inoculated per well must be important. The support fibers ensure a homogeneous distribution of the insoluble or sparingly soluble molecules in aqueous medium. The API ZYM strips were placed in the incubation boxes and the microtubes are inoculated with the prepared cell suspension. Samples were incubated for 4 to 4.5

hours at 30 °C. After the incubation one drop of reagent A and one drop of reagent B were pipetted into each microtubule. After 5 min, staining was recorded according to the color scheme described in the manufacturer's instructions. The enzyme activity was determined according to the color scale from 0 (no enzyme activity) to 5 (maximum enzyme activity).

- The different selected strains were also characterized in relation to the Cd resistance in LB medium plates supplemented with 200 µM $CdSO_4$. Selected strains were inoculated in this medium and checked after one week. If the colony appeared, it was considered that the strains have the capacity to growth in these conditions. This experiment was developed because some strains come from the mine soil that have a toxic concentration of Cd (see Tab. 4.1).
- The fluorescence when they were exposed to UV light. To detect the capacity of produce fluorescence, the colonies grown on LB medium were exposed to the UV light (Panreac TLC. PANREAC QUIMICA, SA. Barcelona, Spain).

4.2.5. Genetic analysis (16S rDNA amplification) and sequencing

The selected bacteria with the most interesting PGPT and, particularly, thosewith high efficiency of Zn solubilization were genetically characterized. The bacterial DNA was extracted from a culture using the Fast DNATM SPIN kit for soil (MP Biomedicals). The universal primers 27FW (5'-AGAGTTTGATCCTGGCTCAG-3') and 1492R (5'-GTTACCTTGTTACGACTT-3') were used to amplify the 16S rRNA encoding gene from the rhizospheric bacteria. A 50 µL PCR reaction mixture was prepared containing 100–200 ng of extracted DNA, 1 × Top Taq buffer, 200 µM of each dNTP, 200 pM of each primer and 1.25 U of Top Taq polymerase (Qiagen). After initial denaturation step at 94°C for 5 min, each cycle consisted on 1 min denaturation at 94 °C, 1 min annealing at 52 °C and 1.5 min elongation at 72 °C. After 35 cycles, a final extension step was performed at 72 °C for 10 min. PCR products were separated by electrophoresis on 1% agarose gels. Bands corresponding to approx. 1,450 bp were excised and purified using the NucleoSpin® Gel and PCR clean-up kit (Macherey–Nagel). After that, the purified PCR products were used for the sequencing. The primers for the sequencing process were 16S-27f (5'-AGRGTTTGATCMTGGCTCAG-3'), 16S-609f (5'-ACTACYVGGGTATCTAAKCC-3'), 16S-907R (5'-AAACTCAAAGGAATTGACGG-3'), and 16S-1492R (5'- GTTACCTTGTTACGACTT-3') using an ABI 3730 48-capillary sequencer (Applied Biosystems). PCR reactions for the sequencing were

performed using the BigDye® Terminator v3.1 cycle sequencing kit (Life Technologies) following the instructions of the supplier.

Results of the sequencing, were aligned and edited using BioEdit program (Hall, 1999) and included in the BLAST (Basic Local Alignment Search Tool). The sequences were compared using the database from NCBI (National Center for Biotechnology Information) using Megablast tool (Altschul et al., 1997). The information of the alignment was included as maximum score, total score, query cover, E value, identity and the accession with more similarity like a same species.

4.2.6. Phylogenetic tree

The phylogenetic differences between the isolated strains were reproduced by the online platform Phylogeny.fr (Dereeper et al., 2008). Phylogeny.fr is a free, simple to use web service dedicated to reconstructing and analyzing phylogenetic relationships between molecular sequences.

The genotyped sequences were firstly aligned using the software BioEdit (Hall, 1999) and then, the file was upload to the online program. The type strain (strains on which the description of a bacteria species is based) of the identified strains and some of the best-known bacteria species were included in the alignment. The aim was to reproduce a more complete phylogenetic tree and to see if our species are within the same clade of the type strains.

4.3. Results

4.3.1. Bacteria quantification

The analysis of bacterial abundance in soils of natural populations of *A. thaliana* revealed substantial differences in bacterial abundance between rhizosphere and rhizoplane soils for all analyzed *A. thaliana* demes. The average density (Fig. 4.4) of cultivable bacteria, which are directly attached to the root (rhizoplane) of the *A. thaliana* plants, was considerably higher than that of the surrounding root (rhizosphere).

The amount of extracted bacteria from bulk soil of the three demes was very similar (Fig. 4.4). Related to rhizosphere and rhizoplane soils, the deme CALA stood out among the other studied demes.

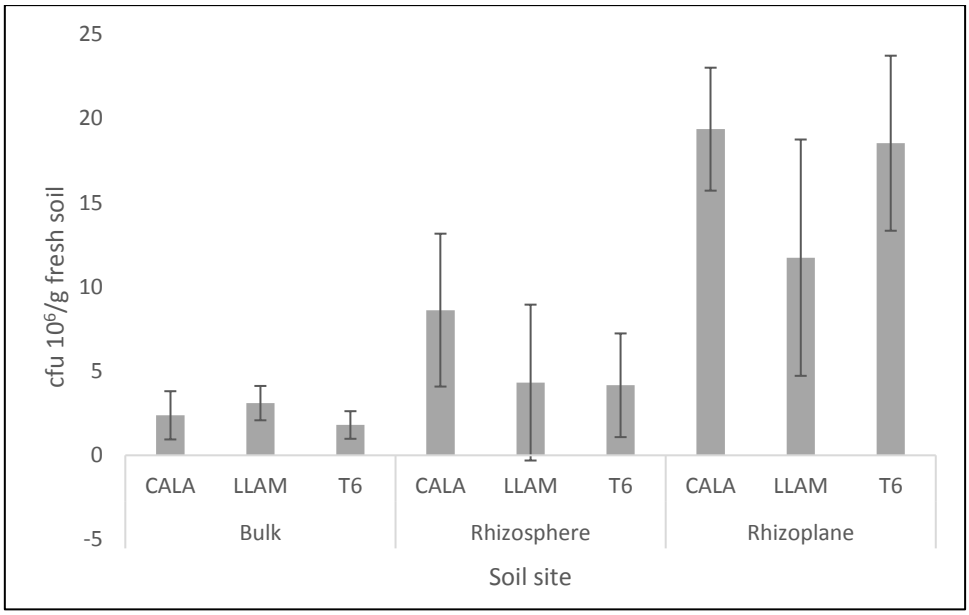

Figure 4.4: Cultivable bacteria extractions from different root distance (bulk soil, rhizospheric soil, and rhizoplane soil). Counts of 3 days post plating at room temperature. Following the protocol of Barillot et al. 2012. Error bars on columns are standard deviations.

In the mine, 6 different extraction points were marked to know the location with more presence of bacteria for the further extractions (see Fig. 4.5). No significant bacteria content was observed inside the mine, neither evidences of plants nor other living organisms (not shown in Fig. 4.5). In relation to the mine entrance, the richest content in bacteria was the point 3 corresponding to the distance of 2.5 meters (Fig. 4.1). Also, this collecting point was near to plants and with proximity to their root structure. According to this result, this place was selected as the best point for bacteria extraction for further experiments.

The three soils used for our pot experiments, LPH, SCF and mine, revealed approximately the same number of bacteria (Fig. 4.6). Based on this, the mine soil can be used to be compared and contrasted to the other two treatment soils (LPH, SCF).

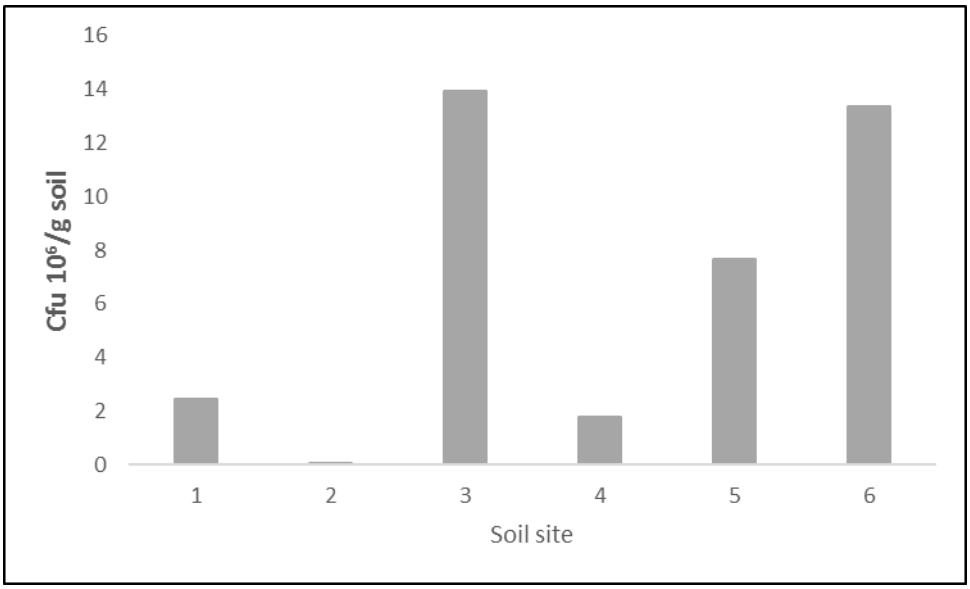

Figure 4.5.: Soil cultivable bacteria counts from different sites around the mine entrance. Counts of 6 days post plating at room temperature. Number of soil sites are referred to in Fig. 4.1.

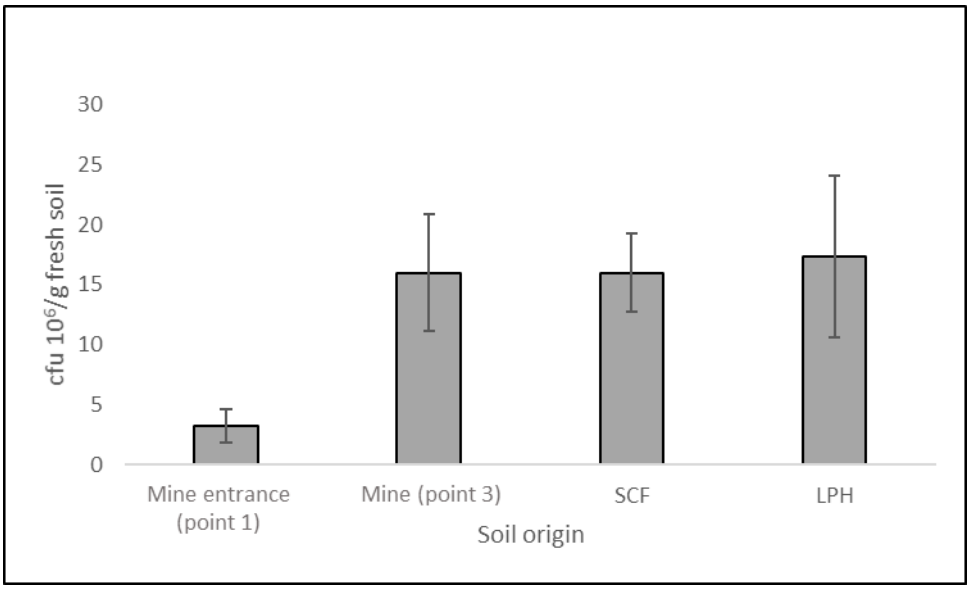

Figure 4.6: Cultivable bacteria counts 6 days post plating of the soils used in pot experiments. Error bars on columns are standard deviations.

4.3.3. Zn selective medium

After quantification, colonies with the different morphological characteristics from bulk, rhizosphere and rhizoplane soils where selected and plated in selective Zn medium (2.5 mM $ZnSO_4$). Important differences were shown in relation to the extracted cultivable bacteria grown

on normal LB medium or on medium supplemented with 2.5 mM $ZnSO_4$. The extractions from the mine were those less influenced by high Zn, probably because the original soil contains high Zn concentrations. Zinc in soluble form completely conditioned the growth and development of bacteria and only some strains from the mine soil (bulk soil) and from CALA (rhizoplane soil) tolerated the supplemented Zn concentration.

Finally, ten different strains were selected for the complete characterization and analysis.

4.3.4. PGP traits

The bacteria strains with high Zn tolerance were further screened for different PGP traits (see section 4.2.3). They were also genetically characterized based on 16S rDNA amplification for identification of genus and species. The results of the 10 pre-selected strains for different PGP and other analyzed traits are presented on Table 4.1.

Table 4.1: Results of tolerant bacteria strains to 2.5 mM $ZnSO_4$ related to PGP and other characterized traits (IAA production; siderophore production (orange halo around the colony growing in CAS agar); P and Zn solubilization efficiency; Cd tolerance (200 µM); fluorescence emission and optimum temperature and pH). Green color is the highest value for a specific parameter, red the lowest and in black the intermediate values.

ID	Origin	MegaBlast identity	IAA (µg/ml)	Siderophore (cm)	P solub eff	Zn solub eff	Cd tolerance	Fluorescense	Optimum temp	Optimum pH
uab1	rhizoplane CALA	*Serratia marcescens*	10.86	3.22	2.50	5.00	yes	yes	30	6
uab2	mine soil	*Bacillus thuringensis*	16.96	1.6	7.00	0	yes	no	28	8
uab3	mine soil	*Serratia liquefaciens*	3.17	1.5	2.40	0	yes	no	28-30	5.4
uab4	rhizoplane CALA	*Pseudomonas rhodesiae*	13.8	3.33	2.80	2.67	no	no	39	5.4
uab5	rhizoplane CALA	*Pseudomonas rhodesiae*	13.12	3.1	3.00	1.75	no	no	39	5.4
uab6	mine soil	*Serratia spp.*	22.62	0	1.33	2.00	no	no	28	9
uab7	mine soil	*Pseudomonas antarctica*	19	0	10.00	3.20	yes	yes	28	5.4-6
uab8	mine soil	*Pseudomonas fluorescens*	16.28	1.3	1.86	3.33	no	yes	28	5.4
uab9	mine soil	*Pseudomonas fluorescens*	9.95	0	1.50	6.00	no	yes	28	5.4
uab10	mine soil	*Serratia marcescens*	37.77	1.18	1.60	2.67	yes	no	30	5.4

In relation to the most important PGP trait, Zn solubilization capacity, different selected bacteria showed good ratio of solubilization capacity. The traits of the different bacteria in relation to selected PGP characteristics and other analyzed parameters are summarized in Table 4.1. Each studied trait is specifically explained bellow.

4.3.4.1. IAA production

All the selected strains produced IAA, although in different quantities. Two extreme strains could be distinguished: uab10 and uab3 with the highest and lowest IAA production, respectively. The rest of strains can be considered intermediate IAA producers. Although there were quite large differences, up to two-fold in their ability to synthesize IAA. Two of these intermediate strains, uab 4 and uab5, had similar morphology and produced about the same quantity of IAA, probably they are the same strain.

4.3.4.2. Siderophore production

The observed differences between the selected strains were transformed in a three-level scale depending on the siderophore production capacity: no production, normal production and large production. Any solubilization was observed in uab6, uab7, and uab9 strains. Normal production was observed in uab2, uab3, uab8, and uab10. Finally, a large siderophore production, that also means a big halo of solubilization, was observed in uab1, uab4, and uab5. The ratio (diameter halo solubilization/diameter colony) is represented in the Figure 4.7.

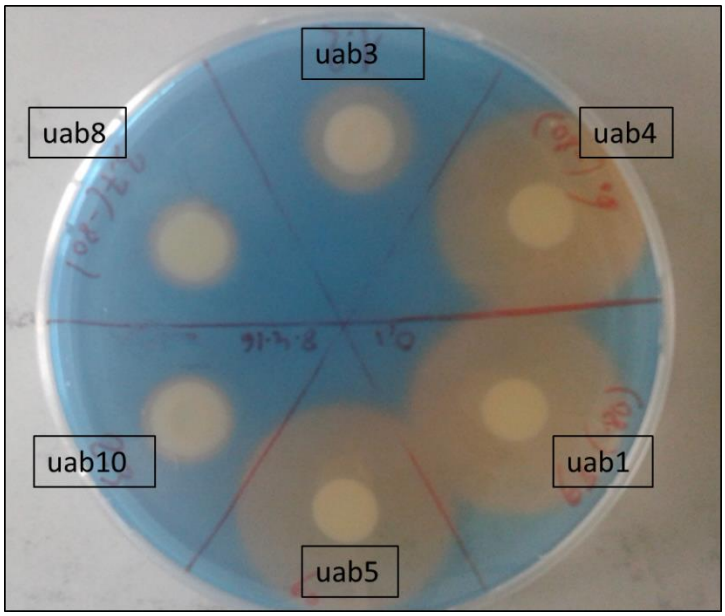

Figure 4.7: CAS agar plate with colonies of 6 selected strains. The solubilization halo (orange circle around the colony) on the blue-color medium are clearly differenced.

4.3.4.3. Phosphate solubilization

After incubation, the colonies with the capacity to solubilize P showed a transparent zone around the colony clearly visible in the opaque medium (Fig. 4.14). The differences were transformed in a three-level scale: low, normal and high efficiency. Two of the selected strains present the highest P solubilization efficiency (uab2 and uab7) (Tab. 4.3). These strains had a reduced growth (lowest colony diameter) but comparatively an enormous halo of solubilization. The strain uab6 displayed the lowest efficiency and the rest of strains presented an intermediate efficiency.

Table 4.2: Phosphate solubilization efficiency of the ten selected strains. The columns represent the name of the colony, the capacity to solubilize, the halo solubilization diameter, colony diameter and the phosphate solubilization efficiency ratio. Green color represents the two selected strains with the highest efficiency and the lowest efficiency is detailed in red.

ID	Halo solubilization diameter (cm)	Colony diameter (cm)	Quantitative solubilization efficiency	P solubilization efficiency (scale)
uab1	10	4	2.50	normal
uab2	14	2	7.00	high
uab3	12	5	2.40	normal
uab4	14	5	2.80	normal
uab5	15	5	3.00	normal
uab6	8	6	1.33	low
uab7	15	1.5	10.00	high
uab8	13	7	1.86	normal
uab9	12	8	1.50	normal
uab10	8	5	1.60	normal

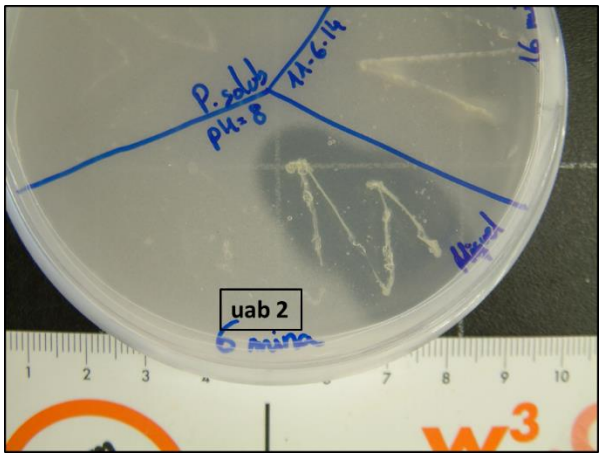

Figure 4.8: Phosphate solubilization of strain uab2 growing in Pikovskaya agar medium at pH 8, and 1-week post plating.

4.3.4.4. ZnO solubilization and organic acid production

Eight of the ten selected strains showed the ability to mobilize Zn from an insoluble source (Tab. 4.3). The differences were transformed in a three-level scale: non-existent, normal and high efficiency. Two of the selected strains (uab1 and uab9) registered the best ratio of ZnO solubilization efficiency and for this reason are the best candidates for future applications as

PGP bacteria. Two strains (uab2 and uab3), that selected due to their ability to grow on a high Zn medium, were although unable to grow in a medium without Zn.

Table 4.3: ZnO solubilization efficiency of the ten selected strains. The columns represent the name of the colony, the capacity to solubilize, the halo solubilization diameter, colony diameter and the zinc solubilization efficiency ratio. Green color represents the two selected strains with the highest efficiency and the lowest efficiency is detailed in red.

ID	Diameter halo Zn solubilization	Diameter colony	Solubilization efficiency	Zn solubilization efficiency
uab1	10	2	5.00	high
uab2	-	-	-	no
uab3	-	-	-	no
uab4	8	3	2.67	normal
uab5	7	4	1.75	normal
uab6	8	4	2.00	normal
uab7	8	2.5	3.20	normal
uab8	10	3	3.33	normal
uab9	12	2	6.00	high
uab10	8	3	2.67	normal

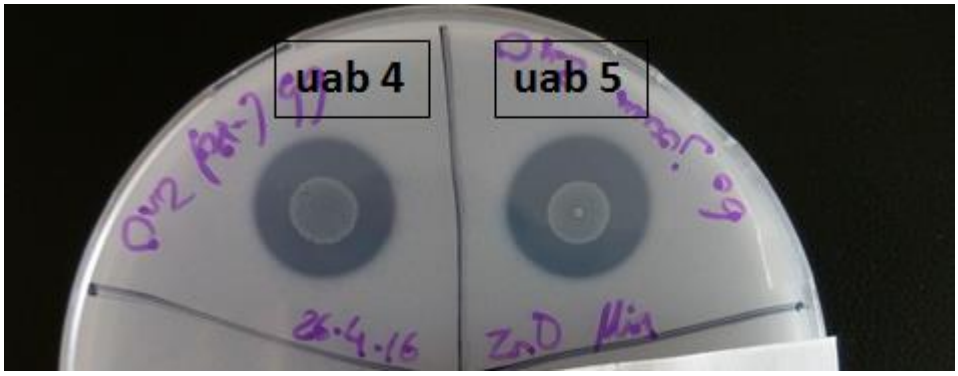

Figure 4.9: ZnO solubilization efficiency of uab4 and 5 after one week.

As expected, strain uab1 produced gluconic. This was detected by HPLC-MS analysis (Fig. 4.10). The strains produced a peak at the same position (m/z 195) as the standard. Moreover, the fragments of m/z 99, 129 and 177, correspond to the same as those found for gluconic acid used as analytical standard (Fig. 4.10D). This production of gluconic acid can be responsible of the ZnO solubilization detected in uab1.

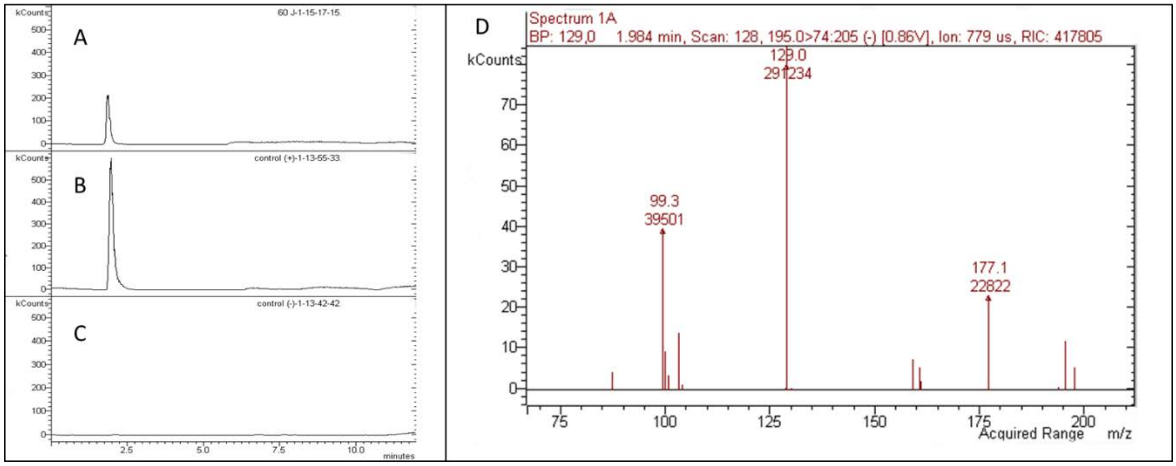

Figure 4.10: Chromatogram of HPLC analysis of gluconic acid with negative ionization at m/z 195. A; Chromatogram of the gluconic acid production by uab1 strain. B; positive control. C; negative control. D; Fragmentation MSMS spectrum of gluconic acid detected as m/z 177, m/z 129 and m/z 99 same as gluconic acid used as analytical standard.

4.3.5. Other analyzed parameters

Other parameters were analyzed to characterize more specifically the properties of the isolated strains. Some parameters were important to classify the species (like fluorescence) and others to define the best conditions for each strain (optimum pH and temperature). Finally, the whole characterization will be useful for future applications or to understand better the metabolism of each isolated bacterial strain.

Optimal temperature and pH

The ten selected colonies were characterized to obtain their optimum temperature and pH. The different optimum ranges of temperature and pH are represented on Table 4.1. As an example, the growth curves in relation to different temperatures of strains uab9 and uab5 are shown in Fig. 4.11. The optimum temperature was 28 ºC for uab9 and 39 ºC for uab5.

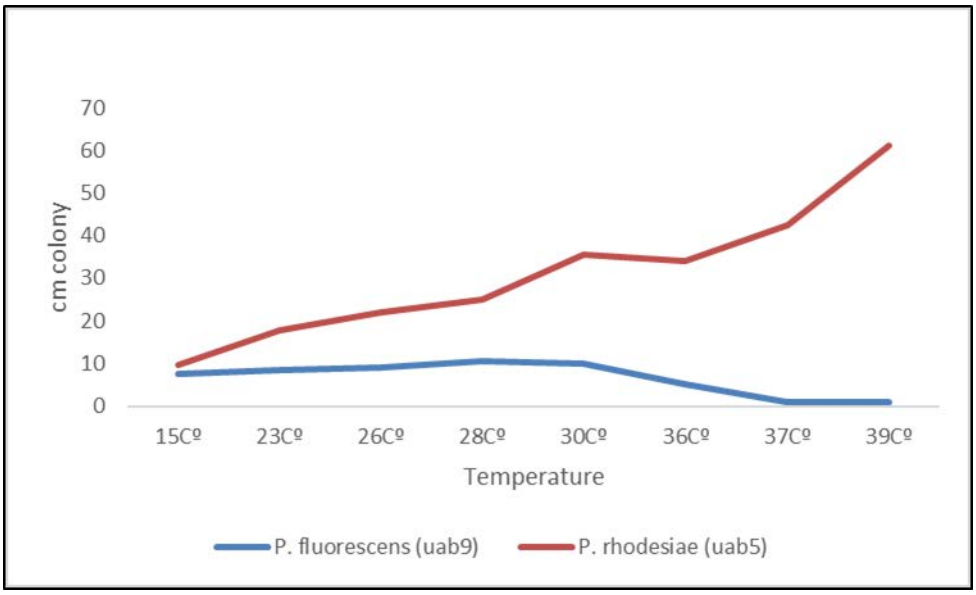

Figure 4.11: Graphic of colony diameter five days post plating at different temperature range (15 to 39 ºC). The uab9 (*P. fluorescens*) show maximum pic of growth at 28ºC and uab5 (*P. rhodesiae*) at 39ºC. The strains were grown on LB 90mm plate.

Antibiotic resistance

The growth of the selected strains related to the antibiotic resistance are represented on table 4.4. There were observed differences among the selected strains, however, those classified as the same species (*P. fluorescence* (uab8 and uab9), *P. rhodesiae* (uab4 and uab5) and *Serratia marcescens* (uab1 and uab10)) showed similar resistance to the studied antibiotics. As it was expected, the antibiotic resistance is specific and two strains from a species have the same profile of resistance. Any of the strains was resistant to either streptomycine or kanamycine.

Table 4.4: Antibiotic resistance capacity of each strain following the concentrations in table X. O, indicates growth in the medium; X, indicates no presence of colony or growth.

Strain\Antibiotic	Tetracycline	Chlorotetracycline	Gentamycine	Ampicilin	Streptomycine	Kanamycine	C+ (LB)
uab1	O	O	O	O	X	X	O
uab2	X	X	O	O	X	X	O
uab3	X	X	X	X	X	X	O
uab4	X	O	X	O	X	X	O
uab5	X	O	X	O	X	X	O
uab6	X	X	X	O	X	X	O
uab7	X	O	X	O	X	X	O
uab8	X	O	X	O	X	X	O
uab9	X	O	X	O	X	X	O
uab10	O	O	O	O	X	X	O

Enzyme activity

The enzymatic activities using API ZYM system was only analyzed for strain uab1 from the rhizosphere of *A. thaliana* deme CALA. The results are represented in Table 4.5. The uab1 strain showed no activities for the enzymes lipase (C14), valine-aminopeptidase, cysteine-aminopeptidase, β-glucuronidase, α-glucosidase, α-manosidase and α-fucosidase. Low enzyme activity (1 corresponding to 5 nmol) for the enzymes lipase (C4), trypsine, α-galactosidase, β-galactosidase, β-glucosidase and α-glucoseaminidase. Other enzymes with more activity (10 nmol to 30 nmol) were alkaline phosphatase, lipase (C8), leucine-aminopeptidase, acid phosphatase and naphtol phosphohydrolase.

Table 4.5: Hydrolytic enzyme activities of strain uab1 grown LB medium and determined by the API ZYM system. The scale of the Api-ZYM® test was used for enzyme quantification.

	Enzyme	Enzyme activity	
1	Control	0	
2	Alkaline phosphatase	3	
3	Lipase C_4	1	
4	Lipase C_8	2	
5	Lipase C_{14}	0	
6	Leucine-aminopeptidase	3	
7	Valine-aminopeptidase	0	
8	Cysteine-aminopeptidase	0	
9	Trypsine	1	
10	Chymotrypsin	0	
11	Acid phosphatase	3	
12	Naphtol phosphohydrolase	4	
13	α-galactosidase	1	
14	β-galactosidase	1	
15	β-glucuronidase	0	
16	α-glucosidase	0	
17	β-glucosidase	1	
18	α-glucoseaminidase	1	
19	α-manosidase	0	
20	α-fucosidase	0	

Cadmium tolerance

The results of the tolerance to 200 µM $CdSO_4$ from each selected strain is represented in Table 4.1. From the ten selected strains: uab1, 3, 7, 10 were able to grow in a media supplemented with high concentration of Cd.

Fluorescence

The capacity to produce fluorescence in presence of UV light were checked in the 10 selected strains. Only the strains uab1, uab8 and 9 showed this capacity. In Fig. 4.18 two fluorescent bacteria are compared to a non-fluorescent producer (uab6). It is important to say that the strains uab8 and uab9 were genetically described as *Pseudomonas fluorescens*, species that commonly shows this trait (Meyer and Abdallah, 1978).

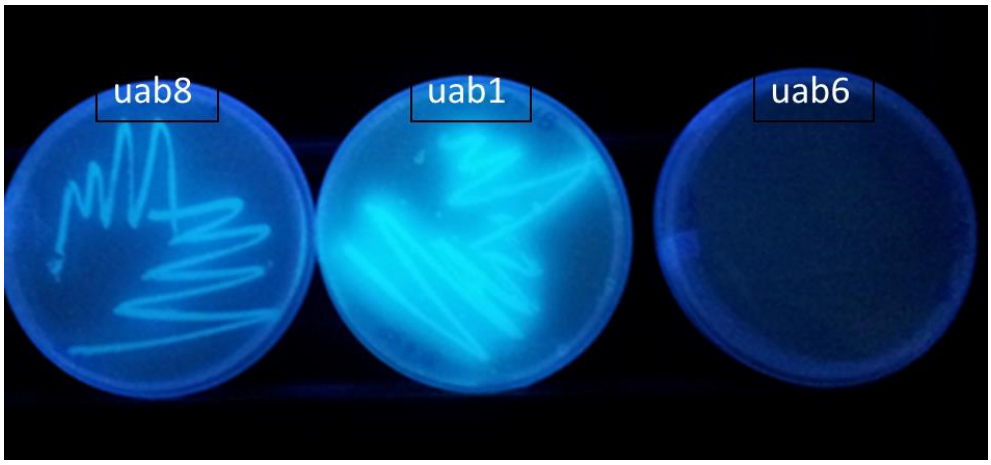

Figure 4.12: Three different colonies (uab8, uab1 and uab6) under UV light conditions. Colonies uab8 and uab1 show fluorescence light.

4.3.6. Genetic analysis (16S rDNA amplification)

The electrophoresis of the 16s rDNA fragments showed a band of 1,500 bp for the 10 selected strains (Fig. 4.13). A strain of *Escherichia colli* was used as a positive control and its 16S rDNA fragment showed a band of identical size.

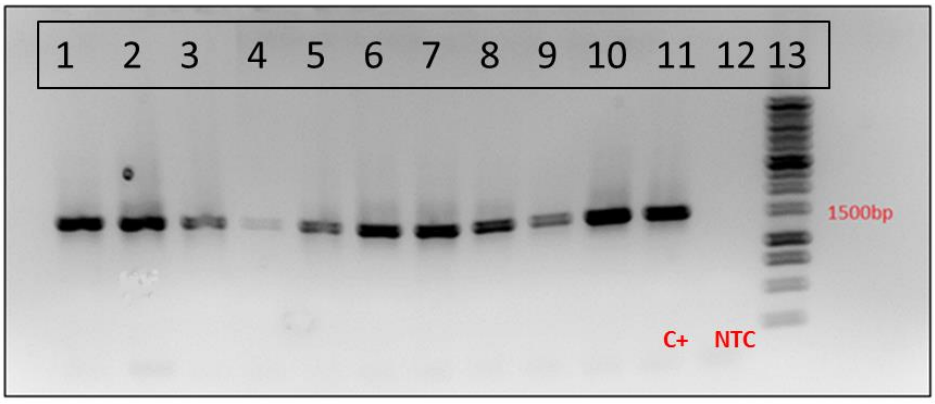

Figure 4.13: Electrophoresis of the 16S rDNA fragments of the isolated strains in a 1%-agarose gel. The positive control (C+) of a *Escherichia coli* strain is in line 11; the non-template control (NTC) in line 12 and the the size-marker in line 13 (1 kb ladder, Promega, Madison, WI, USA)

The edited sequenced were introduced in the NCBI database using the MegaBlast tool to search for the highly similar sequences. The table 4.6 shows the results of this analysis and the similitude of our sequences with the database.

Table 4.6: Results of the MegaBlast (NCBI) for the ten selected strains for highly similar sequences.

ID	Max score	Total score	Query cover	E value	Ident	Accession	MegaBlast identity
uab1	2614	16175	100%	0.0	99%	CP019927.2	Serratia marcescens
uab2	1088	14132	100%	0.0	99%	CP020002.1	Bacillus thuringensis
uab3	1094	7608	100%	0.0	100%	CP014017.1	Serratia liquefaciens
uab4	2634	13166	99%	0.0	99%	LT629801.1	Pseudomonas rhodesiae
uab5	2540	12695	100%	0.0	99%	LT629801.1	Pseudomonas rhodesiae
uab6	1544	1544	100%	0.0	97%	KX928059.1	Serratia spp.
uab7	2490	14920	100%	0.0	99%	CP015600.1	Pseudomonas antarctica
uab8	2639	2639	100%	0.0	99%	KR233795.1	Pseudomonas fluorescens
uab9	2521	2521	100%	0.0	99%	HQ824887.1	Pseudomonas fluorescens
uab10	1072	1072	100%	0.0	100%	KY421549.1	Serratia marcescens

4.3.7. Phylogenetic tree

The phylogenetic tree obtained by the *Phylogeny.fr* software is shown in Figure 4.14. Three main blocks are clearly separated in the construction. A first block containing the *Bacillus thuringensis* type strain grouped with *B. thuringensis* uab2. A second block where uab3 (*Serratia liquefaciens*) and uab6 (*Serratia spp.*) are assigned to *S. liquefaciens* type strain and uab1 and uab10 (both classified as *Serratia marcescens*) to *S. marcescens* type strain. Finally, the third group contains the genus *Pseudomonas* with three type strains species (*P. fluorescences, antarctica and rhodesiae*) together with uab7 (*P. antarctica*), uab4 and uab5 (*P. rhodesiae*), and uab8, uab9 (*P. fluorescens*).

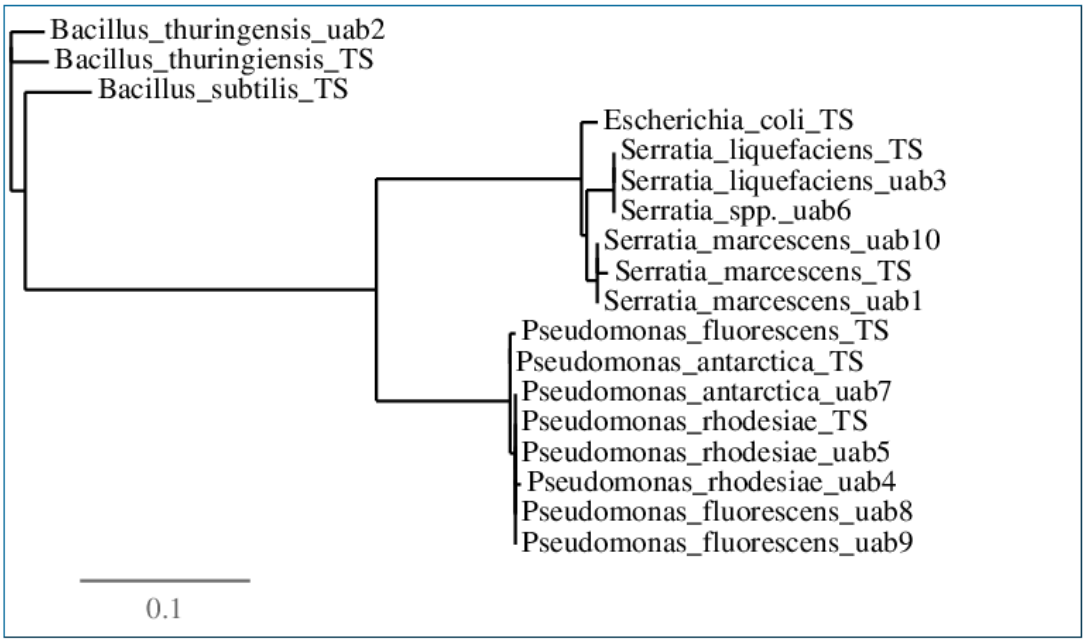

Figure 4.14: Phylogenetic tree of the 10 isolated strains plus the more important type strains (TS). The branch length is proportional to the number of substitutions per site.

Summarizing, *Serratia marcescens* strain uab10 from the mine soil had the highest auxin production combined with Cd tolerance, but relatively low ability of both P and Zn solubilization and siderophore production. Contrastingly *S. marcescens* strain uab 1 from the rhizoplane of *A. thaliana* deme CALA combined high capacity of Zn solubilization with high siderophore production and Cd tolerance. The other bacterial species isolated from CALA rhizosphere, *Pseudomonas rhodesiae* also revealed high siderophore production combined with moderate ability of P and Zn mobilization and IAA production, but no Cd tolerance (Tab. 4.1). Best P mobilization was achieved by two mine-soil bacteria *P. antarctica* (uab7) and *Bacillus thuringensis* (uab2); both were also Cd tolerant, but only *B. thuringensis* produced siderophores.

4.4. Discussion

Soil microorganisms are crucial to the functioning of terrestrial ecosystems. They play a vital role in soil biochemical processes, organic matter cycling, and soil quality maintenance (Giller et al., 1998; Trevors, 1998).

Both soil bacterial densitiy and diversity depend on multiple factors. Soil, vegetation, and climate are most relevant (Classen et al., 2015). Bacterial densities in the bulk soils of our study were quite similar in the carbonate-rich soil from LPH, the silicieous soil at SCF, and even the Zn polluted soil at 3-meter distance to the mine entrance (Fig. 4.6). Therefore, within the range of our study the different physical and chemical soil properties had little influence on the microbial abundance of the soils exposed to quite similar climatic conditions. Only soils with very high metal concentrations at 1 and 2-m distance from the mine entrance (Tab. 3.6) had clearly lower bacterial density. This was probably related to both higher heavy metal burdens and lower root density in the soil.

The negative effects of heavy metal pollution on soil bacteria are well established (Lenart-Boron and Boron, 2014). High concentrations of Zinc, Cd and/or Pb derived from mining or industrial activities may reduce bacterial biomass and activity (Xie et al., 2016). However, the specific metal-induced changes in certain bacterial phyla and genera may be more import than the influence on total bacterial density and activity (Xu et al., 2017).

Plants have a crucial influence on soil microbes. Both increase in the number of bacteria and changes in bacterial types occur in the proximity to the roots (Barillot et al., 2013). Here we also could observe this beneficial effect of roots on soil microbes. Increasing bacterial abundance

with decreasing distance to the roots was found; the highest bacterial density was observed in the rhizoplane of the *A. thaliana* demes. Bulk soil from T6 had around 10 -times lower bacterial density than the T6 rhizoplane (Fig. 4.4.). This is in line with the observations by others on unpolluted soil where 10 to 100-fold higher bacterial density was found in rhizosphere than in bulk soil (Ridder-Duine et al. 2007). Others reported a plant root-induced increase of 197% in microbial biomass (Helal and Sauerbeck., 1986). Also on metal-polluted soil rhizospheric bacterial density is higher than in bulk soil (Dell'Amico et al. 2005; Aboudrar et al. 2007).

Our main objective was to select rhizosphere bacteria combining Zn mobilization ability with Zn tolerance and plant growth promoting characteristics. Therefore, the bacterial characterization was performed on the samples with the highest bacterial density, and considering the soil Zn concentrations also. In the case of the soil from the mining site, samples at a 2-meter distance to the mine entrance were selected for further bacterial characterization (Tab. 3.6; Fig. 4.1; Fig. 4.5.). Long-term metal pollution may have shifted microbial communities to more heavy-metal–tolerant species, save the zinc available fraction in polluted soils is too low to affect microbial metabolic functions (Giller et al., 1998). High throughput sequencing methods are now more and more used to fully characterize metal-induced changes in microbial communities (Xu et al., 2016; Guo et al., 2017). However, in such studies the identification of the bacterial types responsible for beneficial effects on plant performance can be hampered by the complexity of the entire microbiome (Panke-Buisse et al., 2017). As our aim was the isolation of bacteria with potential use in phytoremediation and agriculture here we made a more classical approach to characterize cultivable bacteria using different selective media. The first filter in our experimets was high Zn availability in the medium to select for good bacterial growth under excess Zn. The selected strains were then identified using genetic analysis by 16SrDNA amplification.

With the analysis of the different PGP traits, and other parameters, two of the strains uab4 and uab5 (*P. rhodesia*) had the same profile. After the genetic analysis of the 16S rDNA from the different isolated strains, uab4 and uab5 revealed the highest identity with the same accession (LT629801.1) analyzed with MegaBlast platform (Morgulis et al., 2008). For this reason, at the end of this phenotypic and genotypic characterization, these 2 strains were considered the same species. The other isolated strains were also genotypic analyzed using the amplification of the 16S rDNA. Two of them were *Pseudomonas antarctica* and two *Serratia marcescens* but with identity for different accessions (Tab. 4.6). One of the isolated strains have only 97% of identity and for this reason were described only with the genera *Serratia* spp. Finally, with this genetic information, phylogenetic tree was developed using the online tool Phylogeny.fr (Dereeper et al., 2008) alignment using the program BioEdit (Hall, 1999) see Figure 4.20. This phylogenetic

tree divides the isolated strains in mainly three groups. A group of *Bacillus* spp. (uab2), a group of *Serratia* spp. (uab1, uab,3 uab6, uab10) and group of *Pseudomonas* spp. (uab4, uab5, uab7, uab8, uab9).

The measurement of pollution-induced community tolerance (PICT) has previously been developed by Blanck et al., 1988. The PICT concept considers that at contaminated sites the proportion of species tolerant to the pollutant(s) increases resulting in the increased average tolerance of the community (Blanck, 2002). The increased community tolerance indicates a damaging effect of the pollutant. In tolerant communities, the biodiversity may be decreased (Almås et al., 2004) and the tolerant species may not always be able to perform the same ecological functions as the sensitive ones (Giller et al., 1998; Gong et al., 2002).

In the mine soil, we expected that the bacteria community is more resistant to the Zn than in the other soils and that most of the bacteria isolated on the medium with excess Zn will be found in this soil. In fact, this hypothesis was confirmed and from the mine soil we isolated several bacterial strains with excellent growth on culture medium containing a high, potentially toxic concentration of soluble Zn (2.5 mM $ZnSO_4$) (Tab. 4.1). Surprisingly, however, two Zn-resistant strains (uab1 and uab4/5) were also isolated from the rhizoplane of *A. thaliana* accession CALA, while no Zn-resistant bacteria were associated with other *A. thaliana* demes. All *A. thaliana* demes were from unpolluted soil. Interstingly, while soil from CALA had not the highest extractable Zn concentration among all original soils of *A. thaliana* demes (Tab. 3.5), it presented a high seasonal variability in extractable Zn concentration (Fig.3.3). Moreover, under hydroponic conditions CALA was the deme with the highest shoot Zn concentrations both under normal and excess Zn supply (Fig.3.11). These results suggest both that in the natural habitat Zn availability in the rhizosphere of CALA is relatively high and that CALA has a high ability to mobilize Zn to the shoots. This combination may have favoured the establishment of Zn-resistant bacterial strains in the rhizoplane of CALA demes.

Half of the bacteria able to withstand high Zn were also tolerant to Cd. Zinc and Cd are geochemically related and soil polluted by Zn mining activities frequently are also polluted by Zn. The Cd concentration in the mine soil from which the bacteria had been isolated was clearly enhanced (Tab. 3.6) and may have acted as a selection factor for Cd tolerant bacterial strains. Interestingly, among the Zn-tolerant Pseudomonas species only *P. antarctica* evolved Cd tolerance (Tab. 4.1.). Unexpected was the Cd- tolerance in strain uab1 (*Serratia marcescens*) from the rhizoplane of *A. thaliana* CALA. The unpolluted soil at CALA has low Cd concentrations. A co-tolerance with Zn could be possible. The gram negative *Serratia marcescens* has been found on the rhizoplane of the Cd hyperaccumulating *Solanum nigrum* and its Cd tolerance has been

attributed to high antioxidant activity (Khan et al., 2017). High antioxidant defense in this bacterial species could provide a mechanism for Cd and Zn co-tolerance.

Mechanisms underlying resistance to excess Zn can imply either avoidance by extracellular Zn sequestration through bacterial-produced biopolymers or Zn-tolerance mechanisms based on internal detoxification. Bacterial polymers like exopolysaccharides may become useful for remediation technologies based on sorption and reduction of bio-available metal burdens in contaminated soils and waters (Gupta and Diwan, 2017). However, Zn-avoidance by extracellular immobilizatioin is not a useful trait for achieving enhanced Zn solubilization and availability for plant uptake.

Therefore, a second selection filter in our study was ability for Zn solubilization from a sparingly soluble Zn form (Tab. 4.1). Different insoluble Zn forms as $ZnCO_3$ or $Zn_3(PO4)_2$ have been used to reveal the Zn solubilization capacity of bacteria (Saravanan et al., 2007). Here the sparingly soluble ZnO was used. All strains, excepting *Bacillus thuringensis* (uab2) and *Serratia liquefasciens* (uab3), were able to mobilize Zn from the sparingly soluble zinc oxide. At least *B. thuringensis* ows its Zn and Cd resistance to extracellular metal immobilization. The inability of *B. thuringensis* to mobilize Zn from ZnO seems a general characteristic of this microorganism and is a key factor in the production of *B. thuringensis* coated ZnO nanoparticles used as a biopesticide (Malaikozhunhan et al., 2017). Best Zn mobilization was achieved by *P. fluorescens* from the mine soil (strain uab9) and *S. marcescens* from CALA rhizosphere. *P. fluorescence* has been described before as a metal-resistant plant-growth promoting bacteria (Dell'Amico et al. 2005). Other publications also found strains of *P. fluorescens* and of other Pseudomonas species as good candidates to promote plant growth with Zn solubilizer capacity (Di Simine et al., 1998; Fasim et al., 2002). The excretion of H^+, resulting in metal dissolution, may also promote ammonia assimilation and other metabolic activities, as described for *Pseudomonas* spp. (Illmer and Schinner 1992).

Capacity to produce IAA is a key property of PGPBs. All the selected strains in our study have the capacity to produce this hormone. It has been reported that IAA produced by bacteria differ between species and strains, and it is also influenced by different parameters as culture condition, growth stage and substrate availability (Mutluru and Konada, 2007). Moreover, isolates from the rhizosphere are more efficient auxin producers than isolates from the bulk soil (Sarwar and Kremer, 1995). The strain uab10 (*Serratia marcescens*) was the best IAA producer. The observed IAA production (37.77 µg/ml) can be considered as really high (Erturk et al., 2010).

Contrastingly, *Serratia liquefaciens* (uab3) was the lowest IAA producer. Our results confirm that in the same genera (*Serratia* spp.) the IAA production can largely differ (Mutluru and Konada, 2007). The other strains produced between 9.95 to 22.62 µg/mL. IAA production is one of the most important PGP traits and recent publications proposethat IAA production should be the the first PGP trait for screening bacteria as PGP agents (Etesami et al., 2015). IAA can specifically enhance root growth andbranching, favouring nutrient acquisition by the plant.

Bacterial isolates were assayed for siderophores production on the Chrome azurol S agar medium described by Schwyn and Neilands (1987). Best siderophore production was observed in the bacterial strains isolated from CALA rizoplane. Three of the isolated strains produced the biggest diameter orange halo in relation to the diameter of the colony, uab1 (*Serratia marcescens*), uab4 and uab5 (*Pseudomonas rhodesiae*). The uab6 (*Serratia spp.*), uab7 (*Pseudomonas antarctica*) and uab9 (*Pseudomonas fluorescens*) strains were not able to produce siderophores using Chrome azurol S agar medium. The other isolated strains can produce siderophores but not as the best producers uab2 (*Bacillus thuringensis*), uab3 (*Serratia liquefaciens*), uab8 (*Pseudomonas fluorescens*), uab10 (*Serratia marcescens*). Clear differences appear between the strains and also these differences appeared within the same species (*Serratia marcescens*) isolated from to different sites (mine soil and rhizoplane of CALA deme). This siderophore production in rhizosphere bacteria could enhance plant growth increasing the Fe availability near to the root. Iron availability can be low specially in pH neutral or alkaline soils with high carbonate content. Under such circumstances, siderophore production by bacteria could enhance Fe bioavailability (Kraemer, 2004). Moreover, siderophore producing rhizosphere bacteria can have beneficial influence on plant performance by inhibiting the colonization of roots by plant pathogens (Alexander and Zuberer, 1991). Siderophore-producing bacteria could also be used to improve heavy metal phytoextraction (Rajkumar et al., 2010). In our metal contaminated mine soil, however, spontaneous soil bacteria with Zn mobilization capacity had rather low phytosiderophore production.

Phosphate is one of the most important essential macronutrients in plants and is applied in form of biofertilizers in the soil. However, soluble inorganic phosphate is immobilized rapidly and becomes unavailable to plants (Goldstein, 1986). Phosphate solubilization using Pikovskaya agar medium plates (Pikovskaya, 1948) revealed that uab7 (*Pseudomonas antarctica*) strain had highest phosphate solubilization capacity (SE = 10) followed by strain uab2 (*Bacillus thuringensis*) (SE = 7). Other studies have als shown that phosphate solubilization is most frequently found in *Bacillus* (80%) and *Pseudomonas* isolates (Ahmad et al., 2008). The other isolated strains had low P solubilization ability (between 1.33 to 3) with little differences among them. There have

been a number of reports on plant growth promotion by bacteria that have the ability to solubilize inorganic and/or organic P from soil after their inoculation in soil or plant seeds (Kucey et al., 1989; Kloepper et al., 1988; Datta et al., 1982). Phosphorus deficiency can be a strong limiting factor for plant development on mine soils. Water soluble P is fixed on iron oxides wich are being formed over time in these soils (Sheoran et al., 2010). Bacetria with high P solubilization capacity may both help plants to acquire P and increase metal mobilization from insoluble P forms (Adhya et al., 2015; Arunakumara et al., 2015)

Comparison of the strains with the highest Zn solubilization ability, *P. fluorescens* (uab9) from the mine soil and Serratia marcescens from the A. thaliana rhizosphere reveals clear differences in other important traits. UAB1 in contrast to uab9 produced siderophores on Chrome azurol S agar medium (Schwyn and Neilands, 1987) and was Cd tolerant. We therefore decided to further analyze uab1. Gluconic acid was observed like the principal second metabolite that produce this Zn solubilization (Fig 4.16). Previously studies confirmed the capacity of gluconic acid to solubilize different zinc salts (Fasim et al., 2002). However, is also documented, that the external accumulation of gluconic acid results in acidification of the medium, and contribute to the solubilization of metal phosphates (Goldstein et al. 1993; Babu-Khan et al. 1995). Rhizosphere acidification by organic acid secretion could be important in providing iron to plants specifically which are grown in alkaline soils. In addition to the plant growth promotion by enhancing nutrient availability, organic acid secretion by rhizospheric bacteria could be helpful in the amelioration toxic effects caused by heavy metals (Archana et al., 2012). For this reason, this strain could be an excellent candidate for promoting growth of both crops on soils with low Zn availability and plants used in phytoextraction technologies for remediation of metal polluted soils

4.5. Conclusion

- Three soils with different physico-chemical properties (LPH, SCF and Mine soil) had approximately the same density of bacteria (10^6/g fresh soil). Only in soil with very high metal burdens bacterial density was decreased.

- Bacteria density increase with the root proximity. More bacteria in rhizoplane than rhizosphere or bulk soil were observed.
- The ten isolated, Zn tolerant strains were divided in three genera groups: *Bacillus, Serratia* and *Pseudomonas spp*.
- The mine soil was a good source for zinc tolerant bacteria strains. These bacteria strains were more able to solubilize Zn than the extracted from the non-polluted soil.
- All the selected strains could be a good PGPB, but uab1 (*Serratia marcescens*) and uab9 (*Pseudomonas fluorescens*) were the best in relation to Zn solubilization capacity.
- Zn/Cd tolerant *S. marcescens* with both high Zn mobilization capacity and siderophore production occurs on non-polluted soil in the rhizosphere of an *A. thaliana* deme with high Zn translocation capacity.

These properties make *S. marcescens* an excellent candidate for application in both sustainable agriculture and phytoremediation.

5. Genome-wide association analysis of *A. thaliana* Hap-map populations grown in Zn contaminated and normal soil conditions.

5.1. Introduction

The causal relationship between genetic polymorphism within a species and the phenotypic differences observed between individuals is of fundamental biological interest (Korte and Farlow, 2013). The genome-wide association (GWA) mapping is a powerful technique to address the molecular basis of genotype to phenotype relationships and to map regulators of biological processes. Thus, allowing investigation of the genetics underlying natural phenotypic variation (Francisco et al., 2016; Kooke et al., 2016).

A. thaliana, due to its small size, highly selfing nature, small genome size, short generation time, and wide geographic distribution, becomes a perfect model plant organism to understand the natural variation at genetic and molecular levels. Causal SNPs (Single Nucleotide Polymorphisms) of the natural variation in *A. thaliana* may be identified using the GWA mapping.

GWA mapping was previously applyied to important economically species like *Zea mays* (Hao et al., 2011; Tian et al., 2011) and *Triticum vulgare* (Cockram et al., 2010; Long et al., 2013). The first extensive GWA study (GWAS) in *A. thaliana* was performed by Atwell (2010), to investigate the genetic architecture of 107 different traits involved in flowering time, plant development, element composition and resistance to pathogens. An interactive Web-based application was dissenyed to perform GWAS on *A. thaliana* populations (Seren et al., 2012). The principal obstacle to conduct *A. thaliana* studies is the complex population structure due to isolation by distance (Platt et al., 2010) observed in this species. This must unequivocally be taken into account in statistical analyses of any GWAS (Aranzana et al., 2005; Atwell et al., 2010). The statistical method that appears to be more effective for this purpose in *A. thaliana* is to implement a mixed model that fits a genetic relatedness matrix taking the population structure into account (Yu et al., 2006; Zhao et al., 2007). Using some statistical corrections (Kang et al., 2010; Zhang et al., 2010), the mapping is performed on-the-fly, scanning around 206,000 SNPs genome-wide in 1,386 demes. GWAPP (a web application for genome-wide association mapping in *Arabidopsis*) enables the user to view, select subsets, and choose the appropriate transformation before carrying out the GWAS. GWAPP can be accessed at

http://gwas.gmi.oeaw.ac.at; all code is publicly available and can be obtained at https://github.com/timeu/GWAPP.

Based on linkage disequilibrium (LD), a non-random association between alleles and phenotypes, GWA mapping identifies putatibe causal loci and evaluates the statistical significance of associations between SNPs and phenotypes across many genetically different plant populations. The term LD explains changes in genetic variation within a population over time. It relates to the concept of *chromosomal linkage*, where two markers on a chromosome remain physically joined on this chromosome through generations of a family. (Bush et al., 2012)

Here we applied Bioinformatics tools to further analyze the information obtained through the GWA analysis. This approach is useful to integrate all the GWA information creating a complex network. For example, STRING, a web resource and a biological database, has useful protein-protein interactions datas of 2,031 different organisms and the Gene Ontology interface, supported by the National Human Genome Research Institute. These resources were used to identify biological processes, molecular functions or cellular components associated with disturbed proteins genes. These tools provide a critical assessment and integration of protein–protein interactions, including direct (physical) as well as indirect (functional) associations.

The aim of this experiment was to identify loci linked to the natural adaptation of a big number of accessions (360) growing on two soils with different Zn content (Zn polluted and control soil). This chapter presents a protocol for GWA mapping in *Arabidopsis thaliana* using accessions with genotypic information from a large number of SNPs (Hapmap; Weigel and Mott, 2009) from the user-friendly Internet application GWAPP (https://gwas.gmi.oeaw.ac.at/; Seren et al., 2012). The accessions were grown in duplicate and the nutrient profile and the growth ratio were also measured.

5.2. Material and methods

5.2.1. Pot experiment

A pot experiment was performed using a Hapmap collection of 360 natural populations of *A. thaliana* to assess their natural adaptation to Zn contaminated soil. The collection of seeds was purchased from the Nottingham *A. thaliana* Stock Centre (NASC, Nottingham, UK). Seeds were sterilized by soaking in 70% (v/v) ethanol for 1 min, in bleach 30% (v/v) and 1 drop of

Tween-20 for 10 min, and finally rinsed 3 times in sterile MilliQ water. After that, seeds were vernalized at 4 ºC for 48 hours in the dark and then allowed to germinate on contrasting soils (Zn polluted and control soils).

The control soil was collected in Mallorca pH of 7.1 and low heavy metal content (Annex 1). For the pot experiment, this soil was mixed with perlite (2:1). The Zn polluted soil contained a portion of an ancient Zn mine soil mixed with the control soil and perlite (1:1:1). In a previous experiment, the *A. thaliana* seed collection was sowed in the Zn-mine soil just mixed with perlite (2:1); but and any of the populations was able to grow on this strongly polluted substrate. Both soils were prepared per duplicate on planting trays (50 x 30 cm) of 70-ml cells. Among 3-4 seeds were sown per population and acell. After 1 week, one or two seedlings were kept per aplanting try cell, and the others were removed. Plants were grown in a growth chamber with 100 mmol/m^2s of light intensity, 8 h day/16 h photoperiod, and 25 ºC /20 ºC day/night temperature.

The original purchased collection of 360 populations were sowed in both soils but the Zn polluted soil was toxic for the most part of them, therefore plants died along the experiment. For this reason, the final analysis and the measurements were conditioned by the survival factor. Plants were kept in the conditions above for 50 days being watered with deionized water 2 times per week. The diameter of the different populations was measured on 20-days old seedlings and it was repeated every 10 days. After the last measurement, the plants were collected and analyzed for shoot ionome.

5.2.2. Nutrient content analysis by ICP

The differences in nutrient composition among populations exposed to both soils (Zn polluted and control) were detected by ICP analys.

Plants from the two different soils were sampled by removing 2–3 leaves (1–5 mg of dry weight), washed with Mili-Q water and then placed into Pyrex digestion tubes. Dry material (0.1 g) was pre-digested overnight in H_2O_2 30% HNO_3 69% (v/v) (2:5) and then digested during 4 h at 110 ºC (HotBloc model 154-240, Environmental Express, Charleston, South Carolina, USA). After that, the final volume was adjusted to 25 ml with Milli-Q water and ion concentration was analyzed by inductively coupled plasma (ICP) mass spectrometry (PerkinElmer, Elan-6000). The elements analyzed (in ppm) were P, S, Mg, Zn, Fe, Mn, Cu, B, Ca, K, Na and Pb.

To compare the differences between treatments, differences in nutrient composition were calculated and inputted into the GWA analysis as phenotypic trait.

5.2.3. Growth measurements

The diameter of the different plants was measured 4 times along the experiment: the first one in 20-days old plant and then every ten days. The maximum rosette diameter of three plants per population was measured and the average of the maximum diameter was calculated per population. The increment of diameter was also calculated taking as t = 0 the first diameter measurement. At the end, data on 24 growth parameters was collected: maximum diameter and increment of maximum diameter in control soil, Zn soil and the difference between them at 4 different times. Plants with symptoms of toxicity were also analyzed until senescence.

5.2.4. GWAPP analysis

The interface used to run the GWAS was the GWAPP that consist of a web front end with a graphical user interface and a back end that handles the data and performs the mapping. Firstly, the phenotypic information (nutrient content and growth measurements) has been uploaded including the ID (identification code) for each population with the correct format for the online interface (.txt). Once the phenotype file was created, the results were visualized via the *Plots* tab, on an interactive Manhattan plot (a scatterplot with the negative logarithm P value for the SNP association plotted against each SNP chromosome base-paired positions), for all five chromosomes.

The applied statistical analysis was the Accelerated Mixed Model (AMM) that employs a parametric F-test to obtain P values (Zhang et al. (2010); Kang et al., 2008) (Fig 5.1).

The accumulation errors from multiple test, requires a cutoff to valid statistical evidence. Different methods are described, but False Discovery Rate (FDR), introduced by Benjamini and Hochberg (1995), is less stringent and tolerates more false positives. FDR method first ranks all p-values from the smallest to the largest, and then adjusts each p-value.

LD structure can be also detected by GWAPP. It calculates genome-wide correlation r^2 values between the selected SNP and all other displayed SNPs, colouring them in the Manhattan plot. We used two types of phenotype traits to perform the association with the genotype: Ionomic analysis (P, S, Mg, Zn, Fe, Mn, Cu, B, Ca, K and Na) and growth, such as the maxium rosette diameter.

For analysis of ionomic variables two scenarios were analyzed: ion leaf concentration of plants grown in Zn polluted soil (Z) and difference on ion leaf concentration between Zn and control (ZND), as the relative concentration between plants grown in Zn polluted soils and control soil per unit of leaf concentration in control soil. It was calculated using follow equation:

$$ZND = ((Z - C) / C) * 100$$

where (Z) is leaf concentration in Zn soil and (C) is the concentration in control soil.

For the analysis of the maximum rosette diameter, the data used was: “differential growth rate” (GRD). The GRD is obtained by calculating the increment of maximum diameter from measure 1 (t = 0) until measure 4 among plants grown in Zn polluted soil per unit of control soil. It was calculated using the following equation:

GR_14_Zn/GRD_14_N.

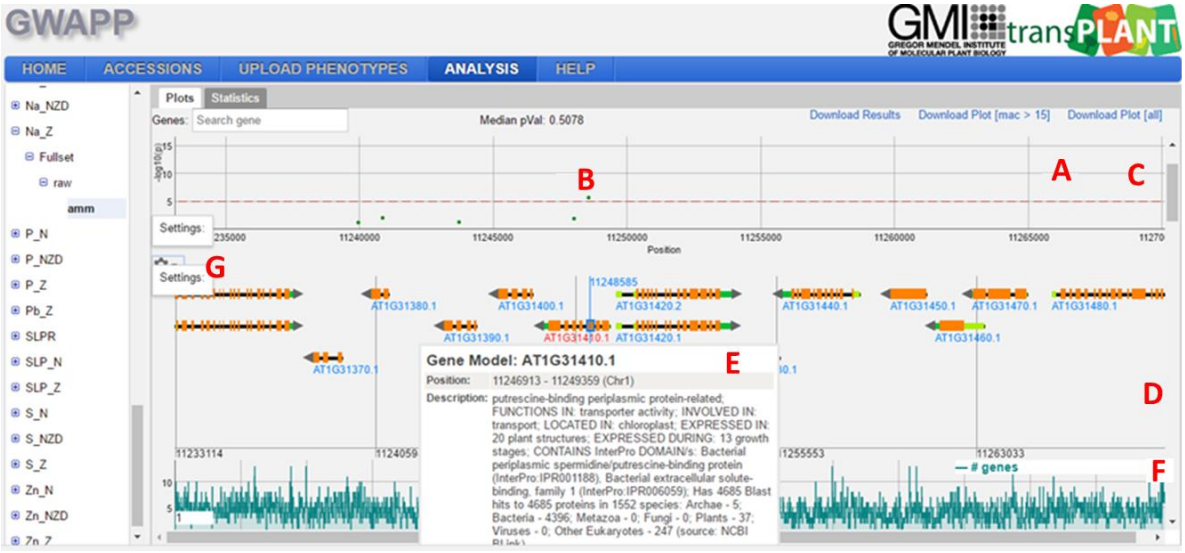

Figure 5.1: GWAPP results for the nutrient content of the analyzed 138 populations. Results are divided in three panels. The top panel (A) contains the Manhattan plot. The positions on the chromosome are on the x axis and the score on the y axis. The dots in the scatterplot represent the SNPs (B). A horizontal dashed line (C) shows the 5% FDR threshold. The second panel (D) shows the gene annotation where genes, gene features and gene names are displayed. Additional information can be also displayed in a pop-up moving the mouse over a gene(E), these genes are linked to TAIR page and cliking on them more specific information will be obtained. The third panel (F) displays various chromosome-wide statistics. The gear icon opens a pop-up (G) with the available statistics the user can choose from.

5.2.6. STRING analysis and Gene Ontology

The linkage between the GWAPP interface and The Arabidopsis Information Resource (TAIR) (Lamesch et al., 2011) let know which gene could be influenced by the identified SNPs. The function of the majority of the genes and their codification proteins is described in the TAIR page.

The putative disturbed proteins were introduced in the STRING database (http://string-db.org/) which gives a complete knowledge of all direct and indirect interactions between proteins (Franceschini et al., 2012; Szklarczyk et al., 2014). After that, the Gene Ontology (GO) interface was run to find out the biological process, molecular function or cellular compartment of the disturbed proteins.

5.3. Results and Discussion

5.3.1. Plant growth

Differences in the germination ratio was clearly observed between Zn polluted soil and control soil. The mine soil reduced the germination of plants and only 287 populations were able to germinate. Moreover, some germinated populations showed stress symptoms like leaf chlorosis or necrosis (Fig. 5.2) inducing plant mortality along the experiment. The growth of plants in the mine soil was also reduced. The heavy metal content (As, Cu, Pb, Zn, Cu, Co and Fe) of both soils was analyzed and all metals showed increased levels on the mine soil compared to control soil from Mallorca (Annex 1). Zn concentrations in the range of 150–300 mg/kg have been measured in polluted soils (De Vries et al. 2007; Warne et al. 2008). Related to Pb, the normal range in soils is 2-200 ppm. Compared to these concentrations, the mine soil used here was highly polluted by Zn and Pb while the control soil from Mallorca had background metal concentrations.

The main important differences between both soils weree the high Zn and Pb levels in the mine soil, most likely being the cause of the low germination rate and the altered phenotype. In fact, the phytotoxicity of Zn induces reduced growth and chlorosis in the younger leaves, among other symptoms (Ebbs and Kochian, 1997). Both Zn and Pb toxicity may have contributed to plant growth reduction. Lead toxicity is associated with reduced plant growth and an inhibition of seed germination due to its interference with important enzymes (Nagajyoti et al. 2010)..

At the end of the experiment (50 days later), the surviving populations decreased from the initial collection from 360 to 166. Lost populations were eliminated from the experiment due to missing data not being able to be upload to the GWAPP analysis. For this reason, the phenotypic variation related to growth was based on 287 populations and the variation related to nutrition based on 166.

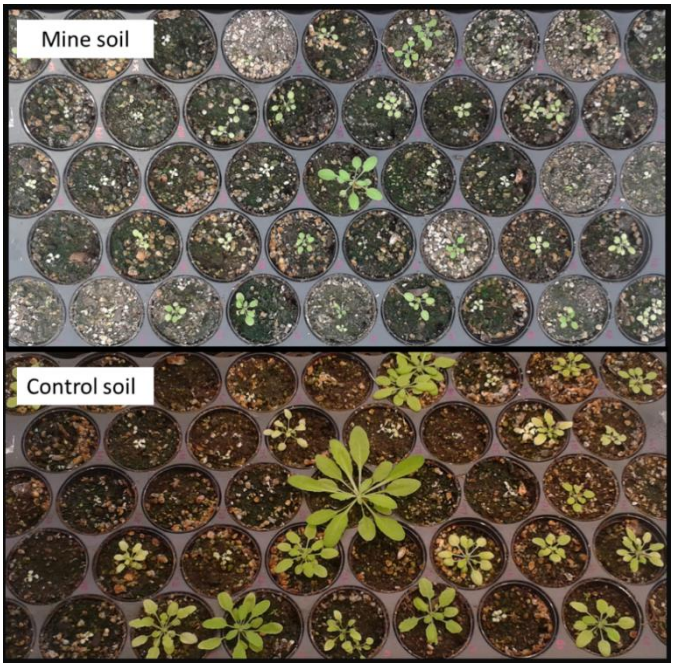

Figure 5.2: Plants growing on the mine soil (top) and control soil (bottom) at the end of the experiment (50 days).

5.3.2. GWAPP analysis

The increment in maximum rosette diameter, called the differential growth rate, was the parameter analyzed for plant growth. No significant SNPs were obtained for the growth parameter in the GWAPP analysis. However, the nutrient content showed significant SNPs (- log P values above 5 in the Manhattan plot): 7 different SNPs between soils and 46 different SNPs only in the Zn soil. The GWAPP analysis displayed differences in the ion concentration in the mine soil (Z), and the difference on the leaf element concentration (NZD) between the control soil (C) and the mine soil (Z). For the differences between leaf element concentration in normal (C) and mine soil (Z), significant SNP were obtained for the following elements: Fe, K and Zn (Tab. 5.1). The Zn phenotype was the nutrient with more significant SNP (4) and the highest P values.

Two od these SNPs correspond to a protein which belongs to the pentatricopeptide repeat (PPR) superfamily. The function of PPR proteins is not clear. In Arabidopsis these proteins may interact (often essentially) with mitochondria and other organelles (Lurin et al., 2004) and they are possibly involved in RNA editing (Kotera et al., 2005). The function of the two SNPs (3:8608168 and 5:13371560) associated to Zn are unknown.

The Fe phenotype is related to a ubiquitin-conjugating enzyme family protein by the SNP (2:13905684). The ubiquitin-conjugating enzymes are involved in the ubiquitination reaction that targets a protein for degradation via the proteasome. A second SNP (3:19122386) relates the Fe phenotype with a disease resistance protein. The possible connection between Fe and the biotic stress is revealed. Pathogens require efficient iron acquisition mechanisms to enable them to compete successfully for iron in the highly iron-restricted environment of the host's tissues (Cornelis and Andrews, 2010). The Fe plant content is crucial for a successful tissue colonization of pathogens.

The potassium phenotype is related to one significant SNP in a gene described as oxidoreductase/transition metal ion-binding protein. The plant sinergy of K and Zn is not very well documented but it was shown that it can increase the vegetative growth of the sweet potato after a combined fertilization (Abd El-Baky et al., 2010). Although Zn is not always considered a transition metal, some oxidoreductase presents a catalytic zinc-binding site (McCall et al., 2000) so the reported protein could be implicated in electron transport processes.

Table 5.1: List of SNPs with more than 5% of FDR threshold in relation to differences between the ICP analysis of the two analyzed soils and the gene described function.

Phenotype	SNP	Chromosome	-log P value	P value	related gene	Gene functional anotation
Fe	13905684	2	6.9	1,26E-07	AT2G32790.1	Ubiquitin-conjugating enzyme family protein
	19122386	3	5.73	1,86E-06	AT3G51560.1	Disease resistance protein (TIR-NBS-LRR class)
K	21279862	5	6.32	4,79E-07	AT5G52410.1	oxidoreductase/transition metal ion-binding protein
Zn	23984745	1	7.16	6,92E-08	AT1G64580.1	Pentatricopeptide repeat (PPR) superfamily protein
	23985939	1	7	1E-07	AT1G64580.1	Pentatricopeptide repeat (PPR) superfamily protein
	8608168	3	9.54	2,88E-10	no determinated	-
	13371560	5	6.28	5,25E-07	no determinated	-

The GWAPP analysis reported more putative altered genes when the HapMap collection was grown in the Zn polluted soil than for the comparaison between soils. For the leaf element concentration in Zn soil, significant SNPs were obtained for the following elements: Cu, Fe, K, Mn, Na, Pb and S (Tab. 5.2). The list of the associated genes may be potentially implicated in the adaptation of the *A. thaliana* plants in relation to Zn and Pb polluted soils.

Interestingly, two significant SNPs (2:13905684, 3:19122386) related to Fe phenotype were also revealed in the comparaison of both studied soils (see Tab. 5.1 and Tab. 5.2). Moreover, the SNP 2:13905684 was also found significant in the Mn analysis (Tab. 5.2). The SNP 2:13905684 is located in a gene AT2G32790.1 which is described as an ubiquitin-conjugating enzyme family protein. This family of proteins are likely described as RNA editors and protein degraders involved in transcriptional and post-transcriptional regulation, respectively (Lurin et al., 2004; Kotera et al., 2005). The SNP 3:19122386 is placed in the gene AT3G51560.1, described in TAIR as a disease resistance protein (TIR-NBS-LRR class) family. The majority of disease resistance genes in plants encode nucleotide-binding site leucine-rich repeat (NBS-LRR) proteins with the functionally distinct TIR-domain-containing. Their precise role in recognition is unknown; however, they are thought to monitor the status of plant proteins that are targeted by pathogen effectors (McHale, 2006). Interestingly, this SNP appears in the phenotype of rosette iron. Iron homeostasis is a key factor in plant's pathogen resistance (Leeman, 1996; Liu et al., 2007). It is well established that Zn toxity can promote Fe deficiency in plants (Fontes, 1998). and the observation of a SNP related to a disease resitance gene deserves further functional analyses of this gene.

The phenotype with the highest related number of SNPs (34) was leaf sodium. SNP 1:21762851 was associated to AT1G58602.2 and AT1G58602.1., genes also related to disease resistance. Moreover, it has been shown that plants transformed with this gene are yielding high biomass under high salinity (https://www.google.com/patents/US8822758).

A further significant SNP (1:21852497) in the Na phenotype was related to the gene AT1G59500.1. The protein acts as an IAA-amido synthase that conjugates Asp and other amino acids to auxin in vitro. These GH3 genes encode IAA-amido synthetases, which help to maintain auxin homeostasis by conjugating excess IAA to amino acids (Staswick et al., 2005).

Most significant SNPs were not related with any functional gene (no determined). Therefore, this preliminary work could be complemented in a future with more complete information about the no determined regions.

Table 5.2: List of SNPs with more than 5% of FDR threshold in relation to differences between the ICP analysis on the Zn soil and the gene described function. In red, coincident SNPs with Table 5.1.

Phenotype	SNP	Chromosome	-log P value	P value	Related gene	Gene functional anotation
Cu	25393040	1	5.3	5,01187E-06	AT1G67730.1	KCR1 - Beta-ketoacyl reductase 1; Beta-ketoacyl-coenzyme A reductase.
Fe	8521742	1	5.65	2,23872E-06	AT1G24090.1	RNase H family protein
	13905684	2	6.47	3,38844E-07	AT2G32790.1	Ubiquitin-conjugating enzyme family protein
	19122386	3	7.39	4,0738E-08	AT3G51560.1	Disease resistance protein (TIR-NBS-LRR class) family
K	9986092	1	5.74	1,8197E-06	AT1G28420.1	homeobox-1
	2258594	2	5.61	2,45471E-06	AT2G05910.1	LURP-one-like protein
	5497808	5	6.67	2,13796E-07	AT5G16730.1	Encodes a microtubule-associated protein. The mRNA is cell-to-cell mobile.
Mn	13905684	2	6.31	4,89779E-07	AT2G32790.1	Ubiquitin-conjugating enzyme family protein
Na	7429396	1	5.84	1,44544E-06	no determinated	-
	11248583	1	5.7	1,99526E-06	AT1G31410.1	putrescine-binding periplasmic protein-like protein
	21762851	1	5.97	1,07152E-06	AT1G58602.2, AT1G58602.1	LRR and NB-ARC domains-containing disease resistance
	21852497	1	5.57	2,69153E-06	AT1G59453.1	B-block-binding subunit of TFIIIC protein.

				1	AT1G59500.1	encodes an IAA-amido synthase that conjugates Asp and other amino acids to auxin in vitro.
	23725767	1	5.57	2,69153E-06	no determinated	-
	1845643	2	5.09	8,12831E-06	AT2G05120.2	Nucleoporin, Nup133/Nup155-like protein.
	6886238	2	5.46	3,46737E-06	no determinated	-
	5905281	3	5.82	1,51356E-06	no determinated	-
	9133148	3	5.17	6,76083E-06	AT3G25070.1	Encodes a member of the R protein complex and may represent a virulence target of type III pili effector proteins (virulence factors) from bacterial pathogens, which is 'guarded' by R protein complex (RPM1 and RPS2 proteins).
	9139731	3	5.83	1,47911E-06	no determinated	-
	14924619	3	6.89	1,28825E-07	no determinated	-
	709097	4	5.26	5,49541E-06	AT4G01660.1	Encodes an ABC1-like protein, member of the ATH subfamily; putative ABC transporter; isolated by functional complementation of a yeast abc1 mutant.
	1315280	4	5.15	7,07946E-06	no determinated	-

	5150464	4	5.58	2,63027E-06	AT4G08150.1	A member of class I knotted1-like homeobox gene family (together with KNAT2). Similar to the knotted1 (kn1) homeobox gene of maize.
	6388940	4	5.23	5,88844E-06	no determinated	-
	6786088	4	5.39	4,0738E-06	no determinated	-
	7229368	4	5.74	1,8197E-06	AT4G12060.1	Double Clp-N motif protein.
	7660588	4	5.11	7,76247E-06	AT4G13190.1	Protein kinase superfamily protein.
	9085582	4	5.31	4,89779E-06	no determinated	-
	10685620	4	5.03	9,33254E-06	no determinated	-
	13374153	4	5.99	1,02329E-06	AT4G26480.1	RNA-binding KH domain-containing protein.
	13378608	4	5.99	1,02329E-06	no determinated	-
	13387617	4	5.58	2,63027E-06	AT4G26510.1	One of the homologous genes predicted to encode proteins with UPRT domains (Uracil phosphoribosyl transferase)
				1	AT4G26510.2	
	13389440	4	5.02	9,54993E-06	AT4G26520.1	Aldolase superfamily protein.
	13420604	4	6.22	6,0256E-07	AT4G26600.1	S-adenosyl-L-methionine-dependent methyltransferases superfamily protein.

	13425225	4	5.69	2,04174E-06	AT4G26610.1	D6 protein kinase like 1.
	13427159	4	5.05	8,91251E-06	AT4G26610.1	D6 protein kinase like 1.
	13437460	4	5.91	1,23027E-06	AT4G26640.1, AT4G26640.2	member of WRKY Transcription Factor; Group I
	13451910	4	5	0,00001	AT4G26660.1	kinesin-like protein.
	1495555	5	5.12	7,58578E-06	no determinated	-
	6401486	5	5.25	5,62341E-06	no determinated	-
	6423197	5	5.11	7,76247E-06	AT5G19140.2	aluminum induced protein with YGL and LRDR motifs.
	26044222	5	5.04	9,12011E-06	no determinated	-
Pb	6767605	2	6.03	9,33254E-07	no determinated	-
	6774821	2	5.39	4,0738E-06	AT2G15530.1, AT2G15530.2, AT2G15530.3, AT2G15530.4	RING/U-box superfamily protein.
	20526113	3	5.85	1,41254E-06	no determinated	-
S	8608168	3	6.31	4,89779E-07	no determinated	-
	7496838	4	6.47	3,38844E-07	AT4G12740.1	HhH-GPD base excision DNA repair family protein.

5.3.3. Linkage disequilibrium (LD)

The linkage disequilibrium produced by a specific SNP over other gene regions was also calculated (Tab. 5.3). Table 5.3 shows the affected genes for this LD in the differences (NZD) between control soil (C) and Zn polluted soil (Z).

Table 5.3: Linkage disequilibrium results of the SNP with more than 5% FDR threshold analysis of the two used soils.

Phenotype	SNP	Chromosome	Region	Genes in LD	Gene Model Description
Fe	13905684	2	13888432-13905826	AT2G32740	galactosyltransferase 13
				AT2G32750	Exostosin family protein
				AT2G32760	UV radiation resistance-associated protein
				AT2G32770	purple acid phosphatase 13
				AT2G32780	ubiquitin-specific protease 1
				AT2G32785	Encodes a Rapid ALkalinization Factor (RALF) family protein
				AT2G32788	Encodes a Rapid ALkalinization Factor (RALF) family protein
				AT2G32790	Ubiquitin-conjugating enzyme family protein
	19122386	3	19122386-19128610	AT3G51560	Disease resistance protein (TIR-NBS-LRR class) family
				AT3G51570	Disease resistance protein (TIR-NBS-LRR class) family
				AT3G51580	transmembrane protein
K	21279862	5	21277428-21279862	AT5G52410	oxidoreductase/transition metal ion-binding protein
Zn	23984745	1	23966660-23987271	AT1G64540	F-box/FBD-like domains containing protein
	23985939	1		AT1G64550	Encodes a member of GCN subfamily. Predicted to be involved in stress-associated protein translation control. The mutant is affected in MAMP ((microbe-associated molecular patterns)-induced stomatal closure, but not other MAMP-induced responses in the leaves.

				AT1G64561	hypothetical protein
				AT1G64570	Homeodomain-like superfamily protein
				AT1G64580	Pentatricopeptide repeat (PPR) superfamily protein
				AT1G64583	Tetratricopeptide repeat (TPR)-like superfamily protein
	8608168	3	8608168	No determined	
	13371560	5	13364523-13371560	No determined	

In the Fe phenotype, AT3G51560 gene was involved and described as a disease resistance protein. When linkage disequilibrium was analyzed, region 3:19122386-3:19128610 was affected and other gene (AT3G51570) related with disease resistance was obtained. This result could be explained, also, for the implication of iron in pathogen and disease resistance (Leeman, 1996; David, 2007).

5.3.3. STRING analysis

The list of affected genes was analyzed using the STRING interface and the protein interaction map was obtained after the analysis. The protein network interaction of the differences between the Zn polluted and the control soils is presented in Figure 5.3 and 5.4 shows the protein interaction map for the Zn polluted soil.

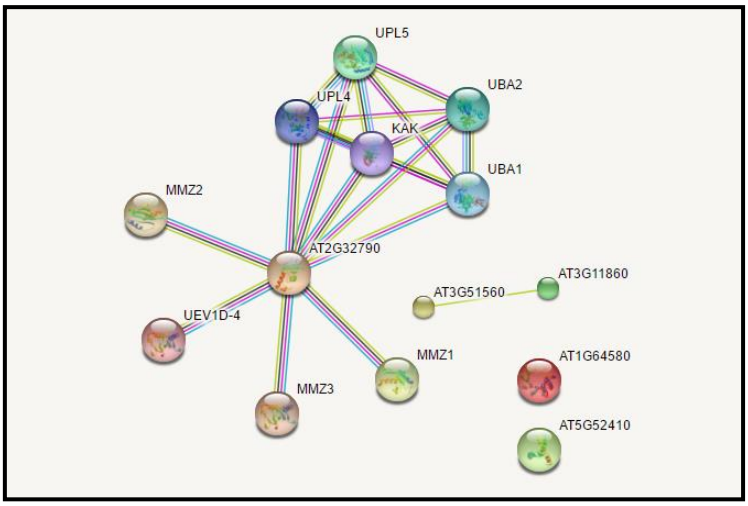

Figure 5.3: Protein interaction map obtained by STRING analysis. The significant genes from the ionome of Zn polluted soil and control soil were selected by GWAS analysis.

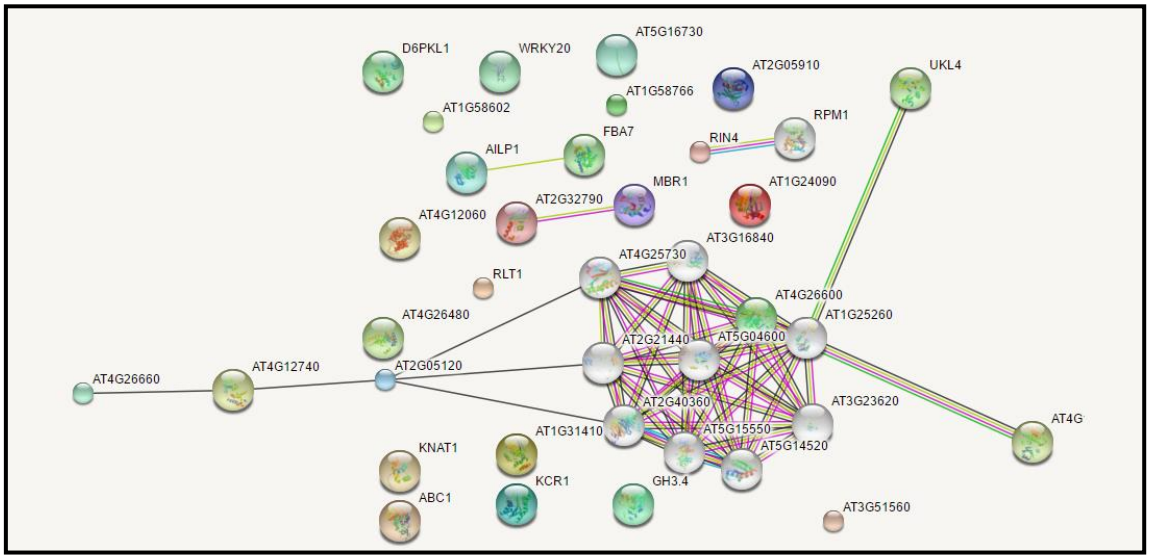

Figure 5.4: Protein interaction map obtained by STRING analysis. The significant genes from the ionome of the Zn polluted soil were selected by GWAS analysis.

With the previous information, the affected pathways in relation to biological processes (Tab. 5.4, 5.7), molecular functions (Tab.5.5, 5.8) and cellular components (Tab. 5.6) were also described.

Table 5.4: STRING statistical analysis results of principal biological process. The studied genes were selected by GWAs analysis from the ionome of the Zn polluted soil.

Biological Process (GO)			
#pathway ID	**pathway description**	**observed gene count**	**false discovery rate**
GO.0006412	translation	9	5.71e-05
GO.1901566	Organo-nitrogen compound biosynthetic process	10	0.00177
GO.1901564	Organo-nitrogen compound metabolic process	11	0.00394

Table 5.5: STRING statistical analysis results of principal molecular function. The studied genes were selected by GWAs analysis from the ionome of the Zn polluted soil.

Molecular Function (GO)			
#pathway ID	**pathway description**	**observed gene count**	**false discovery rate**
GO.0003735	structural constituent of ribosome	9	$2.59\ e^{-6}$
GO.0003723	RNA binding	10	$5.46\ e^{-5}$
GO.0019843	rRNA binding	5	0.000221
GO.0008097	5S rRNA binding	2	0.00145
GO.0003676	nucleic acid binding	13	0.0347

Table 5.6: STRING statistical analysis results of principal cellular component. The studied genes were selected by GWAs analysis from the ionome of the Zn polluted soil.

Cellular component (GO)			
#pathway ID	**pathway description**	**observed gene count**	**false discovery rate**
GO.0022625	cytosolic large ribosomal subunit	9	$1.37\ e^{-10}$
GO.0044391	ribosomal subunit	10	$1.2\ e^{-09}$

GO.0005840	ribosome	10	9.12 e^{-8}
GO.0022626	cytosolic ribosome	9	9.4 e^{-8}
GO.0043232	intracellular non-membrane-bounded organelle	12	1.01 e^{-5}
GO.0005730	nucleolus	7	4.01 e^{-5}
GO.0070013	intracellular organelle lumen	8	0.000856
GO.0044428	nuclear part	8	0.0012
GO.0031981	nuclear lumen	7	0.0015
GO.0032991	macromolecular complex	11	0.00392
GO.0019897	extrinsic component of plasma membrane	2	0.00844
GO.0005829	cytosol	9	0.0154
GO.0044446	intracellular organelle part	15	0.0231

Table 5.7: STRING statistical analysis results of principal biological process, selected genes of GWAs analysis from ICP results from differences between two used soils.

Biological Process (GO)			
#pathway ID	**pathway description**	**observed gene count**	**false discovery rate**
GO.0016567	protein ubiquitination	8	1.37 e^{-7}
GO.0070534	protein K63-linked ubiquitination	3	2.56 e^{-6}
GO.0006301	postreplication repair	3	1.23 e^{-5}
GO.0042787	protein ubiquitination involved in ubiquitin-dependent protein catabolic process	3	1.87 e^{-5}
GO.0006259	DNA metabolic process	4	0.00553
GO.0006511	ubiquitin-dependent protein catabolic process	3	0.0385
GO.0044257	cellular protein catabolic process	3	0.0479

Table 5.8: STRING statistical analysis results of principal molecular function, selected genes of GWAs analysis from ICP results from differences between two used soils.

Molecular Function (GO)			
#pathway ID	**pathway description**	**observed gene count**	**false discovery rate**
GO.0004842	ubiquitin-protein transferase activity	8	2.74 e^{-11}
GO.0016874	ligase activity	5	0.000619
GO.0061630	ubiquitin protein ligase activity	3	0.000619
GO.0008641	small protein activating enzyme activity	2	0.00477

In the presented tables (Tab. 5.1 to 5.8), different SNPs and the associated genes could be explained in different metabolic function envolving biological process and molecular functions. All these results show a preliminar bioinformatic study to understand the genetic implications of the natural variation of the Hapmap population under Zn toxicity.

During the last 10 years, the technology of the high-density SNP arrays and DNA re-sequencing increased the genotypic space for a large number of organisms including *A. thaliana*. The principal biological interest is to elucidate the causal relationship between genetic polymorphism within a species and the phenotypic differences observed between individuals. The genetic differences which are currently screened can be obtained from both, mutagenesis analyses and natural population samples (Korte and Farlow, 2013). *A. thaliana* is considered an ideal organism, mainly for its self-fertilization and 1,300 distinct accessions have been genotyped for 250,000 SNPs (Horton et al., 2012). For these reasons, we consider this screening as a preliminary study for further projects and other analyses, which may include:

- Study performance on mine soil of mutants for the interesting genes related with the phenotypic traits.
- Sequencing of the SNPs of our contrasting demes (see section 1) to compare the significant differences in relation to soil adaptation of the different well-characterized *A. thaliana* natural populations.

- Repeat the analyses either or both increasing the *A. thaliana* natural populations to obtain more significant SNPs and use a lower proportion of the mine soil in the substrate to reduce plant mortality.
- Analyze SNP-SNP interactions which may have an accumulative effect on a phenotypic trait.
- Analyze the SNPs located in intergenic regions to know if they are in regulatory-gene position (promotors, enhancers, silencers). Then, analyze their effects in the gene expression patterns and the function of the differentially expressed genes obtained.
- Perform GWA on populations growing on a deficiency soil or Zn-deficient nutrient solution to get a complete analysis of genetic variance under extreme Zn conditions.

5.4. Conclusion

- Mine soil with high Zn and Pb content reduces the growth and increases the mortality of all accessions of the Hapmap collection in comparison to the control commercial soil. For this reason, we conclude that any natural populations of this world-wide collection behave as a pseudo-metallophyte well-adapted to the mine-soil-containing substrate.
- Significant differences in survival and growth on mine soil among the populations indicate large differences in metal tolerance among the *A. thaliana* populations
- GWA did not reveal any significant SNP for rosette diameter, indicating this is a quantitative trait controlled by multiple genes.
- Differences in leaf ionome were not associated to major SNPs related to ion transporters.
- The mortality of metal sensitive populations may be responsible for the failure to detect SNPs related to ion transport because the lack of rosette Zn data from the sensitive populations.
- Differences in leaf ionome were associated to major SNPs related to pathogen defense related genes.
- Further analysis should address the role of Fe and Zn homeostasis on these defense related genes.

- GWA revealed two major SNPs related to leaf Pb. These should be further characterized.

6. Concluding remarks and outlook

This study aimed to charaterize soil Zn as a factor of natural selection in *Arabidopsis thaliana*, as well as in soil and rhizopshere bacteria with the purpose to get useful information for future application in both sustainable crop production on soils with low Zn availablity and remediation of Zn polluted mine soils. The thesis was divided into three different chapters each reporting and discussing specific results concerning: response of natural populations of *A. thaliana* to differences in substrate Zn availability (section 3), characterization of soil and rhizosphere bacteria able to promote plant growth and to mobilize Zn, Fe and P (section 4), and genome wide association analysis on 360 natural populations of an *A. thaliana* world-wide collection for the identification of major SNPs related to rosette growth and ionome on soil contaminated with Zn and Pb by mining activity (section 5).

Taking together the results from the different environmental analyses and experiments, both under field and lab conditions, it gets evident that *A. thaliana* is unable to colonize neither metal-rich mine soils nor carbonate-rich unpolluted soils. However, natural populations of *A. thaliana* in NE Catalonia occur on soils with different pH values, carbonate contents, and Zn availability. *Arabidopsis thaliana* demes have locally adapted to these different soil conditions and when exposed to extreme conditions the relative tolerance of the demes was strictly dependent on the Zn concentration and carbonate level in the soil of origin.

Real time qPCR analysis revealed distinctively higher expression of different genes involved in Zn transport in LLAM, the *A. thaliana* deme from a site with relatively high soil Zn and carbonate levels than in two other demes spontaneously growing on soil with lower Zn and carbonate. This result demonstrates that relatively small variations in soil Zn can act as a driving factors for selection of traits that allow better Zn homeostasis under both Zn deficient or Zn toxic conditions. This deme was also more tolerant to carbonate. This was in accordance with the somewhat higher carbonate concentration in its soil of origin. The natural adaptation to carbonate was an inheritable trait as revealed by crossing more tolerant LLAM with the highly carbonate sensitive deme T6. The resulting F1 generation showed intermediate characteristics in relation to rosette diameter and number of siliques when grown along with the parentals on the highly carbonated soil from Les Planes d'Hostoles (LPH).

Exploration of a considerably larger genetic background from 360 *A. thaliana* populations from around the world revealed large differences in tolerance to high Zn and Pb concentrations in a

soil polluted by mining activity with huge differences in survival, rosette growth and leaf ionome. GWA approach however did not reveal major SNPs related to metal ion transporters that may be mainly responsible for differences in metal tolerance. The high mortality of metal sensitive populations and the consequent lack of leaf ionomic data from non-adapted genotypes is most probably the reason for this failure. Future work shoud repeat this approach using substrates with lower metal burdens. An intersting result was the observation that ionomic variations in the leaves of the metal-tolerant survivers were related to several SNPs associated with genes coding for pathogen resistance. This is in line with the important role of Zn and Fe homeostasis in plant defense against pathogen infection. These genes deserve detailled analysis in the future.

Our results further demostrate that soil Zn is not only a driver for natural selection in *A. thaliana* plants, but also for soil and rhizosphere bacteria. As we aimed to isolate Zn tolerant bacterial strains able to mobilize Zn, our first selection filter was ability to grow on a high, potentially toxic Zn concentration (2.5mM Zn) followed by selection of strains able to mobilize Zn from a sparingly soluble source. As expected most bacteria tolerant to excess Zn were found in the Zn polluted mine soil. In *Pseudomonas fluorescens*, *P. antarctica* and *Serratia marcescens* this high Zn tolerance was not due to external precipitation. On the contrary, these bacteria efficiently mobilized Zn from sparingly soluble ZnO. Only *S. liquefasciens* and *Bacillus thuringensis* may ow their ability to grow on medium with excess Zn to exclusion, as suggested by theit inability to mobilize Zn from ZnO. Taking into account these properties, along with the results on Cd tolerance, IAA production, and ability to mobilize phosphate the best candidates for future application in phytoextraction technologies could be: *P. fluorescens* strain uab9 with excellent Zn tolerance and mobilization, but the handicap of lack of Cd tolerance, *P. antarctica* strain uab7 combining Zn tolerance with excellent P mobilization, Cd tolerance and IAA production, and *S. marcescens* strain 10 with Zn and Cd tolerance combined with highest IAA production a crucial factor for root development.

As expeted, bacteria with high tolerance to excess Zn were not found in the unpolluted soils at SCF, LPH, or the natural habitats of the *A. thaliana demes*, with one, highly interesting exception, CALA, the deme with the highest rosette Zn concetrations under Zn deficient conditions. The rhizoplane of *A. thaliana* deme CALA hosted two diffferent bacterial species with high Zn tolerance: *Pseudomonas rhodesiae* (strain uab 4/5) and *Serratia marcescens* (uab1 strain). Both were high siderophore producers, able to solubilize Zn and P, as well as to produce IAA. Moreover, *S. marcescens* was Cd tolerant despite the CALA soil Cd concentration was low. Both bacteria seem excellent candidates for plant growth promotion and enhancement of nutrient availability in crop plants in carbonated soils with low availability of Fe and Zn.

Outlook

This study confirms our working hypothesis regarding Zn as a driver of natural selection in both *A. thaliana* en bacteria. However, within the time frame of this thesis several open questions remain pending on future experiments.

- Efficiency assessment and practical use of the selected bacterial strains for promoting Zn phytoextraction by metallophytes (e.g. hyperaccumulators like *A. halleri* and *N. caerulescens* or higher biomass producing crops like *Brassica juncea*) under greenhouse and field conditions.
- Efficiency assessment and practical use of the selected bacterial strains for promoting nutrient acquisition and plant growth on soils with low Zn availability under greenhouse and field conditions.
- Further characterization of the genetic traits underlying Zn homeostasis in *A. thaliana* using the SNPs identified here as well as further GWAs approaches with less toxic Zn concentations to avoid massive mortality of sensitive genotypes.

7. Bibliography

Aboudrar, W., Schwartz, C., Benizri, E., Morel, J. L., & Boularbah, A. (2007). Soil microbial diversity as affected by the rhizosphere of the hyperaccumulator Thlaspi caerulescens under natural conditions. *International journal of phytoremediation*, *9*(1), 41-52.

Adhya, T. K., Kumar, N., Reddy, G., Podile, A. R., Bee, H., & Samantaray, B. (2015). Microbial mobilization of soil phosphorus and sustainable P management in agricultural soils. *Current Science*, *108*(7), 1280-1287.

Ahmad, F., Ahmad, I., & Khan, M. S. (2008). Screening of free-living rhizospheric bacteria for their multiple plant growth promoting activities. *Microbiological research*, *163*(2), 173-181.

Alexander, D. B., & Zuberer, D. A. (1991). Use of chrome azurol S reagents to evaluate siderophore production by rhizosphere bacteria. *Biology and Fertility of soils*, *12*(1), 39-45.

Alhendawi, R. A., Römheld, V., Kirkby, E. A., & Marschner, H. (1997). Influence of increasing bicarbonate concentrations on plant growth, organic acid accumulation in roots and iron uptake by barley, sorghum, and maize. *Journal of Plant Nutrition*, *20*(12), 1731-1753.

Alloway, B. J. (2004). Zinc in soils and crop nutrition. Second edition, *IZA and IFA publisher*.

Alloway, B. J. (2009). Soil factors associated with zinc deficiency in crops and humans. *Environmental Geochemistry and Health*, *31*(5), 537-548.

Almås, Å. R., Bakken, L. R., & Mulder, J. (2004). Changes in tolerance of soil microbial communities in Zn and Cd contaminated soils. *Soil Biology and Biochemistry*, *36*(5), 805-813.

Alonso-Blanco, C. and Koornneef, M. (2000) Naturally occurring variation in Arabidopsis: an underexploited resource for plant genetics. Trends Plant Sci. 5, 22–29.

Al-Shehbaz, I. A., & O'Kane Jr, S. L. (2002). Taxonomy and phylogeny of Arabidopsis (Brassicaceae). *The Arabidopsis Book*, e0001.

Altschul, S. F., Madden, T. L., Schäffer, A. A., Zhang, J., Zhang, Z., Miller, W., & Lipman, D. J. (1997). Gapped BLAST and PSI-BLAST: a new generation of protein database search programs. *Nucleic acids research*, *25*(17), 3389-3402.

Andreini, C., Banci, L., Bertini, I., & Rosato, A. (2006). Zinc through the three domains of life. *Journal of proteome research*, *5*(11), 3173-3178.

Andrews, S. C., Robinson, A. K., & Rodríguez-Quiñones, F. (2003). Bacterial iron homeostasis. *FEMS microbiology reviews*, *27*(2-3), 215-237.

Aranzana, M. J., Kim, S., Zhao, K., Bakker, E., Horton, M., Jakob, K., ... & Toomajian, C. (2005). Genome-wide association mapping in Arabidopsis identifies previously known flowering time and pathogen resistance genes. *PLoS Genet*, *1*(5), e60.

Archana, G., Buch, A., & Kumar, G. N. (2012). Pivotal role of organic acid secretion by rhizobacteria in plant growth promotion. In *Microorganisms in Sustainable Agriculture and Biotechnology* (pp. 35-53). Springer Netherlands.

Arrivault, S., Senger, T., & Krämer, U. (2006). The Arabidopsis metal tolerance protein AtMTP3 maintains metal homeostasis by mediating Zn exclusion from the shoot under Fe deficiency and Zn oversupply. *The Plant Journal*, *46*(5), 861-879.

Artursson, V., Finlay, R. D., & Jansson, J. K. (2006). Interactions between arbuscular mycorrhizal fungi and bacteria and their potential for stimulating plant growth. *Environmental microbiology*, *8*(1), 1-10.

Arunakumara, K. K. I. U., Walpola, B. C., & Yoon, M. H. (2015). Bioaugmentation-assisted phytoextraction of Co, Pb and Zn: an assessment with a phosphate-solubilizing bacterium isolated from metal-contaminated mines of Boryeong Area in South Korea/Phytoextraction de Co, PB et Zn par bioaugmentation assistée: une évaluation avec une bactérie solubilisant le phosphate isolée de mines contaminées par les métaux dans la région de Boryeong en Corée du Sud. *Biotechnologie, Agronomie, Société et Environnement*, *19*(2), 143.

Asimit, J., & Zeggini, E. (2010). Rare variant association analysis methods for complex traits. *Annual review of genetics*, *44*, 293-308.

Assunçao, A. G., Persson, D. P., Husted, S., Schjørring, J. K., Alexander, R. D., & Aarts, M. G. (2013). Model of how plants sense zinc deficiency. *Metallomics*, *5*(9), 1110-1116.

Atwell, S., Huang, Y. S., Vilhjálmsson, B. J., Willems, G., Horton, M., Li, Y., ... & Jiang, R. (2010). Genome-wide association study of 107 phenotypes in Arabidopsis thaliana inbred lines. *Nature*, *465*(7298), 627-631.

Atwell, S., Huang, Y. S., Vilhjálmsson, B. J., Willems, G., Horton, M., Li, Y., ... & Jiang, R. (2010). Genome-wide association study of 107 phenotypes in Arabidopsis thaliana inbred lines. *Nature*, *465*(7298), 627-631.

Babu-Khan, S., Yeo, T. C., Martin, W. L., Duron, M. R., Rogers, R. D., & Goldstein, A. H. (1995). Cloning of a mineral phosphate-solubilizing gene from Pseudomonas cepacia. *Applied and environmental microbiology*, *61*(3), 972-978.

Badri, D. V., Weir, T. L., van der Lelie, D., & Vivanco, J. M. (2009). Rhizosphere chemical dialogues: plant–microbe interactions. *Current opinion in biotechnology*, *20*(6), 642-650.

Bais, H. P., Weir, T. L., Perry, L. G., Gilroy, S., & Vivanco, J. M. (2006). The role of root exudates in rhizosphere interactions with plants and other organisms. *Annu. Rev. Plant Biol.*, *57*, 233-266.

Barak, P., & Helmke, P. A. (1993). The chemistry of zinc. In *Zinc in soils and plants* (pp. 1-13). Springer Netherlands.

Barillot, C. D., Sarde, C. O., Bert, V., Tarnaud, E., & Cochet, N. (2013). A standardized method for the sampling of rhizosphere and rhizoplan soil bacteria associated to a herbaceous root system. *Annals of microbiology*, *63*(2), 471-476.

Baxter, I., Brazelton, J. N., Yu, D., Huang, Y. S., Lahner, B., Yakubova, E., ... & Vitek, O. (2010). A coastal cline in sodium accumulation in Arabidopsis thaliana is driven by natural variation of the sodium transporter AtHKT1; 1. *PLoS genetics*, *6*(11), e1001193.

Becher, M., Talke, I. N., Krall, L., & Krämer, U. (2004). Cross-species microarray transcript profiling reveals high constitutive expression of metal homeostasis genes in shoots of the zinc hyperaccumulator Arabidopsis halleri. *The Plant Journal*, *37*(2), 251-268.

Beck, J. B., Schmuths, H., & Schaal, B. A. (2008). Native range genetic variation in Arabidopsis thaliana is strongly geographically structured and reflects Pleistocene glacial dynamics. *Molecular Ecology*, *17*(3), 902-915.

Benjamini, Y., & Hochberg, Y. (1995). Controlling the false discovery rate: a practical and powerful approach to multiple testing. *Journal of the royal statistical society. Series B (Methodological)*, 289-300.

Bergman, P., & Glimelius, K. (1993). Electroporation of rapeseed protoplasts–transient and stable transformation. *Physiologia Plantarum*, *88*(4), 604-611.

Bergmann, W. (1988). *Ernahrungsstorungen bei Kulturpflanzen*. Fischer.

Bert, P. F., Bordenave, L., Donnart, M., Hévin, C., Ollat, N., & Decroocq, S. (2013). Mapping genetic loci for tolerance to lime-induced iron deficiency chlorosis in grapevine rootstocks (Vitis sp.). *Theoretical and applied genetics*, *126*(2), 451-473.

Black, C. A., Evans, D. D., & Dinauer, R. C. (1965). *Methods of soil analysis* (Vol. 9, pp. 653-708). Madison, WI: American Society of Agronomy.

Blanck, H. (2002). A critical review of procedures and approaches used for assessing pollution-induced community tolerance (PICT) in biotic communities. *Human and ecological risk assessment*, *8*(5), 1003-1034.

Blanck, H., Wängberg, S. Å., & Molander, S. (1988). Pollution-induced community tolerance—a new ecotoxicological tool. In *Functional testing of aquatic biota for estimating hazards of chemicals*. ASTM International.

Brachi, B., Faure, N., Horton, M., Flahauw, E., Vazquez, A., Nordborg, M., Bergelson, J., Cugue n, J., Roux, F. (2010) Linkage and association mapping of Arabidopsis thaliana flowering time in nature. PLoS Genetics. 6

Brady, N.C. and R.R. Weil (1999) The Nature and Properties of Soils. 12th Edition. Prentice Hall , Upper Saddle River, New Jersey.

Bric, J. M., Bostock, R. M., & Silverstone, S. E. (1991). Rapid in situ assay for indoleacetic acid production by bacteria immobilized on a nitrocellulose membrane. *Applied and environmental Microbiology*, *57*(2), 535-538.

Broadley, M. R., White, P. J., Hammond, J. P., Zelko, I., & Lux, A. (2007). Zinc in plants. *New Phytologist*, *173*(4), 677-702.

Brümmer, G., Tiller, K. G., Herms, U., & Clayton, P. M. (1983). Adsorption—desorption and/or precipitation—dissolution processes of zinc in soils. *Geoderma*, *31*(4), 337-354.

Burges, A., Epelde, L., Blanco, F., Becerril, J. M., & Garbisu, C. (2017). Ecosystem services and plant physiological status during endophyte-assisted phytoremediation of metal contaminated soil. *Science of The Total Environment*, *584*, 329-338.

Bush, W. S., & Moore, J. H. (2012). Genome-wide association studies. *PLoS computational biology*, *8*(12), e1002822.

Busoms, S., Teres, J., Huang, X. Y., Bomblies, K., Danku, J., Douglas, A., Weigel, D., Poschenrieder., Salt, D. E. (2015). Salinity is an agent of divergent selection driving local adaptation of Arabidopsis to coastal habitats. *Plant physiology*, *168*(3), 915-929.

Cakmak, I. (2008). Enrichment of cereal grains with zinc: agronomic or genetic biofortification? *Plant and soil*, *302*(1-2), 1-17.

Chaney, R. L. (1993). Zinc phytotoxicity. *Developments in Plant and Soil Sciences*, *55*, 135-135.

Chasapis, C. T., Loutsidou, A. C., Spiliopoulou, C. A., & Stefanidou, M. E. (2012). Zinc and human health: an update. *Archives of toxicology*, *86*(4), 521-534.

Chen, H., & Cutright, T. J. (2003). Preliminary evaluation of microbially mediated precipitation of cadmium, chromium, and nickel by rhizosphere consortium. *Journal of environmental engineering*, *129*(1), 4-9.

Chen, J., He, F., Zhang, X., Sun, X., Zheng, J., & Zheng, J. (2014). Heavy metal pollution decreases microbial abundance, diversity and activity within particle-size fractions of a paddy soil. *FEMS microbiology ecology*, *87*(1), 164-181.

Chen, Y. P., Rekha, P. D., Arun, A. B., Shen, F. T., Lai, W. A., & Young, C. C. (2006). Phosphate solubilizing bacteria from subtropical soil and their tricalcium phosphate solubilizing abilities. *Applied soil ecology*, *34*(1), 33-41.

Chen, Y., & Barak, P. (1982). Iron nutrition of plants in calcareous soils. *Advances in agronomy*, *35*, 217-240.

Classen, A. T., Sundqvist, M. K., Henning, J. A., Newman, G. S., Moore, J. A., Cregger, M. A., ... & Patterson, C. M. (2015). Direct and indirect effects of climate change on soil microbial and soil microbial-plant interactions: What lies ahead?. *Ecosphere*, *6*(8), 1-21.

Clemens, S. (2001). Molecular mechanisms of plant metal tolerance and homeostasis. *Planta*, *212*(4), 475-486.

Cleyet-Marel, J. C., & Hinsinger, P. (2000). Soil as a living environment, a medium to be discovered and put to good use. *OCL-Oléagineux, Corps Gras, Lipides*, *7*(6), 490-493.

Cockram, J., White, J., Zuluaga, D. L., Smith, D., Comadran, J., Macaulay, M., ... & Tapsell, C. (2010). Genome-wide association mapping to candidate polymorphism resolution in the unsequenced barley genome. *Proceedings of the National Academy of Sciences*, *107*(50), 21611-21616.

Conyers, M. K. and Davey, B. G. (1988) Observations on some routine methods for soil pH determination. Soil Science 145, 29-36.

Cornelis, P., & Andrews, S. C. (Eds.). (2010). Iron uptake and homeostasis in microorganisms. *Horizon Scientific Press*.

Croes, S., Weyens, N., Janssen, J., Vercampt, H., Colpaert, J. V., Carleer, R., & Vangronsveld, J. (2013). Bacterial communities associated with Brassica napus L. grown on trace element-contaminated and non-contaminated fields: a genotypic and phenotypic comparison. *Microbial biotechnology*, *6*(4), 371-384.

da Costa, P. B., Granada, C. E., Ambrosini, A., Moreira, F., de Souza, R., dos Passos, J. F. M., Arruda, L., Passaglia, L. M. (2014). A model to explain plant growth promotion traits: a multivariate analysis of 2,211 bacterial isolates. *PLoS One*, *9*(12), e116020.

Datta, M., Banik, S., & Gupta, R. K. (1982). Studies on the efficacy of a phytohormone producing phosphate solubilizing Bacillus firmus in augmenting paddy yield in acid soils of Nagaland. *Plant and Soil*, *69*(3), 365-373.

De Deyn, G. B., Cornelissen, J. H., & Bardgett, R. D. (2008). Plant functional traits and soil carbon sequestration in contrasting biomes. *Ecology letters*, *11*(5), 516-531.

de Ridder-Duine, A. S., Kowalchuk, G. A., Gunnewiek, P. J. K., Smant, W., van Veen, J. A., & de Boer, W. (2005). Rhizosphere bacterial community composition in natural stands of Carex arenaria (sand sedge) is determined by bulk soil community composition. *Soil Biology and Biochemistry*, *37*(2), 349-357.

de Souza, R., Beneduzi, A., Ambrosini, A., Da Costa, P. B., Meyer, J., Vargas, L. K., Schoenfeld, R., Passaglia, L. M. (2013). The effect of plant growth-promoting rhizobacteria on the growth of rice (Oryza sativa L.) cropped in southern Brazilian fields. *Plant and soil*, *366*(1-2), 585-603.

de Villemereuil, P., Gaggiotti, O. E., Mouterde, M., & Till-Bottraud, I. (2016). Common garden experiments in the genomic era: new perspectives and opportunities. *Heredity*, *116*(3), 249.

De Vries, W., Lofts, S., Tipping, E., Meili, M., Groenenberg, J. E., & Schütze, G. (2007). Impact of soil properties on critical concentrations of cadmium, lead, copper, zinc, and mercury in soil and soil solution in view of ecotoxicological effects. In *Reviews of Environmental Contamination and Toxicology* (pp. 47-89). Springer New York.

Dell'Amico, E., Cavalca, L., & Andreoni, V. (2005). Analysis of rhizobacterial communities in perennial Graminaceae from polluted water meadow soil, and screening of metal-resistant, potentially plant growth-promoting bacteria. *FEMS Microbiology Ecology*, *52*(2), 153-162.

Dereeper, A., Guignon, V., Blanc, G., Audic, S., Buffet, S., Chevenet, F., ... & Claverie, J. M. (2008). Phylogeny. fr: robust phylogenetic analysis for the non-specialist. *Nucleic acids research*, *36*(suppl 2), W465-W469.

Desbrosses-Fonrouge, A. G., Voigt, K., Schröder, A., Arrivault, S., Thomine, S., & Krämer, U. (2005). Arabidopsis thaliana MTP1 is a Zn transporter in the vacuolar membrane which mediates Zn detoxification and drives leaf Zn accumulation. *FEBS letters*, *579*(19), 4165-4174.

Di Simine, C. D., Sayer, J. A., & Gadd, G. M. (1998). Solubilization of zinc phosphate by a strain of Pseudomonas fluorescens isolated from a forest soil. *Biology and Fertility of Soils*, *28*(1), 87-94.

Diels, L., Dong, Q., van der Lelie, D., Baeyens, W., & Mergeay, M. (1995). Theczc operon of Alcaligenes eutrophus CH34: from resistance mechanism to the removal of heavy metals. *Journal of Industrial Microbiology & Biotechnology*, *14*(2), 142-153.

Dimkpa, C. O., Merten, D., Svatoš, A., Büchel, G., & Kothe, E. (2009b). Siderophores mediate reduced and increased uptake of cadmium by Streptomyces tendae F4 and sunflower (Helianthus annuus), respectively. *Journal of applied microbiology*, *107*(5), 1687-1696.

Dorman, M., Sapir, Y., & Volis, S. (2009). Local adaptation in four Iris species tested in a common-garden experiment. *Biological journal of the Linnean Society*, *98*(2), 267-277.

Dräger, D. B., Desbrosses-Fonrouge, A. G., Krach, C., Chardonnens, A. N., Meyer, R. C., Saumitou-Laprade, P., & Krämer, U. (2004). Two genes encoding Arabidopsis halleri MTP1 metal transport proteins co-segregate with zinc tolerance and account for high MTP1 transcript levels. *The Plant Journal*, *39*(3), 425-439.

Drissi, S., Houssa, A. A., Bamouh, A., Bouaziz, A., Benbella, M. (2016). Zinc migration in the Sandy soil and its impacto n the bioavailability of some nutrients in the root environment. *Journal of soil science and agroclimatology*. Vol.13 No.1

Drosinos, E. H., & Board, R. G. (1994). Metabolic activities of pseudomonads in batch cultures in extract of minced lamb. *Journal of Applied Microbiology*, *77*(6), 613-620.

Duffner, A., Weng, L., Hoffland, E., & van der Zee, S. E. (2014). Multi-surface modeling to predict free zinc ion concentrations in low-zinc soils. *Environmental science & technology*, *48*(10), 5700-5708.

Ebbs, S. D., & Kochian, L. V. (1997). Toxicity of zinc and copper to Brassica species: implications for phytoremediation. *Journal of Environmental Quality*, *26*(3), 776-781.

El-Baky, A., Ahmed, A. A., El-Nemr, M. A., & Zaki, M. F. (2010). Effect of potassium fertilizer and foliar zinc application on yield and quality of sweet potato. Research Journal of Agriculture & Biological Sciences, 6(4), 386-394.

Epstein E, Bloom AJ (2004) Mineral Nutrition of Plants: Principles and Perspectives. 2nd edition; *Sinauer Publisher*.

Erturk, Y., Ercisli, S., Haznedar, A., & Cakmakci, R. (2010). Effects of plant growth promoting rhizobacteria (PGPR) on rooting and root growth of kiwifruit (Actinidia deliciosa) stem cuttings. *Biological research*, *43*(1), 91-98.

Etesami, H., Alikhani, H. A., & Hosseini, H. M. (2015). Indole-3-acetic acid (IAA) production trait, a useful screening to select endophytic and rhizosphere competent bacteria for rice growth promoting agents. *MethodsX*, *2*, 72-78.

Fasim, F., Ahmed, N., Parsons, R., & Gadd, G. M. (2002). Solubilization of zinc salts by a bacterium isolated from the air environment of a tannery. *FEMS Microbiology Letters*, *213*(1), 1-6.

Fesel, P. H., & Zuccaro, A. (2016). Dissecting endophytic lifestyle along the parasitism/mutualism continuum in Arabidopsis. *Current opinion in microbiology*, *32*, 103-112.

Fourcroy, P., Sisó-Terraza, P., Sudre, D., Savirón, M., Reyt, G., Gaymard, F., ... & Briat, J. F. (2014). Involvement of the ABCG37 transporter in secretion of scopoletin and derivatives by Arabidopsis roots in response to iron deficiency. *New Phytologist*, *201*(1), 155-167.

Franceschini, A., Szklarczyk, D., Frankild, S., Kuhn, M., Simonovic, M., Roth, A., Lin, J., Minguez, P., Bork, P., von Mering, C., Jensen, L. J. (2012). STRING v9. 1: protein-protein interaction networks, with increased coverage and integration. *Nucleic acids research*, *41*(D1), D808-D815.

Francisco, M., Joseph, B., Caligagan, H., Li, B., Corwin, J. A., Lin, C., ... & Kliebenstein, D. J. (2016). Genome wide association mapping in Arabidopsis thaliana identifies novel genes involved in linking allyl glucosinolate to altered biomass and defense. *Frontiers in plant science*, *7*.

François, O., Blum, M. G., Jakobsson, M., & Rosenberg, N. A. (2008). Demographic history of European populations of Arabidopsis thaliana. *PLoS genetics*, *4*(5), e1000075.

Gadd, GM (1996). Roles of microorganisms in the environmental fate of radionuclides. Endeavour 20:150–156.

Garland, J. L., & Mills, A. L. (1991). Classification and characterization of heterotrophic microbial communities on the basis of patterns of community-level sole-carbon-source utilization. *Applied and environmental microbiology*, *57*(8), 2351-2359.

Geber, M. A., & Griffen, L. R. (2003). Inheritance and natural selection on functional traits. *International Journal of Plant Sciences*, *164*(S3), S21-S42.

Gibson, G. (2012). Rare and common variants: twenty arguments. *Nature Reviews Genetics*, *13*(2), 135-145.

Giller, K. E., Witter, E., & Mcgrath, S. P. (1998). Toxicity of heavy metals to microorganisms and microbial processes in agricultural soils: a review. *Soil Biology and Biochemistry*, *30*(10), 1389-1414.

Glass ADM (1989) Plant Nutrition: An Introduction to Current Concepts. *Jones and Bartlett Publishers*, Boston, 234 p.

Glick, B. R. (1995). The enhancement of plant growth by free-living bacteria. *Canadian Journal of Microbiology*, *41*(2), 109-117.

Glick, B. R. (2012). Plant growth-promoting bacteria: mechanisms and applications. *Scientifica*, *2012*.

Goldstein, A. H. (1986). Bacterial solubilization of mineral phosphates: historical perspective and future prospects. *American Journal of Alternative Agriculture*, *1*(2), 51-57.

Goldstein, A. H., Rogers, R. D., & Mead, G. (1993). Mining by microbe. *Nature Biotechnology*, *11*(11), 1250-1254.

Gong, J., Forster, R. J., Yu, H., Chambers, J. R., Sabour, P. M., Wheatcroft, R., & Chen, S. (2002). Diversity and phylogenetic analysis of bacteria in the mucosa of chicken ceca and comparison with bacteria in the cecal lumen. *FEMS microbiology letters*, *208*(1), 1-7.

Gontia-Mishra, I., Sapre, S., & Tiwari, S. (2017). Zinc solubilizing bacteria from the rhizosphere of rice as prospective modulator of zinc biofortification in rice. *Rhizosphere*, *3*, 185-190.

Goteti, P. K., Emmanuel, L. D. A., Desai, S., & Shaik, M. H. A. (2013). Prospective zinc solubilising bacteria for enhanced nutrient uptake and growth promotion in maize (Zea mays L.). *International journal of microbiology*, *2013*.

Gravot, A., Lieutaud, A., Verret, F., Auroy, P., Vavasseur, A., & Richaud, P. (2004). AtHMA3, a plant P1B-ATPase, functions as a Cd/Pb transporter in yeast. *FEBS letters*, *561*(1-3), 22-28.

Grotz, N., Fox, T., Connolly, E., Park, W., Guerinot, M. L., & Eide, D. (1998). Identification of a family of zinc transporter genes from Arabidopsis that respond to zinc deficiency. *Proceedings of the National Academy of Sciences*, *95*(12), 7220-7224.

Grover, M., Ali, S. Z., Sandhya, V., Rasul, A., & Venkateswarlu, B. (2011). Role of microorganisms in adaptation of agriculture crops to abiotic stresses. *World Journal of Microbiology and Biotechnology*, *27*(5), 1231-1240.

Guo, H., Nasir, M., Lv, J., Dai, Y., & Gao, J. (2017). Understanding the variation of microbial community in heavy metals contaminated soil using high throughput sequencing. *Ecotoxicology and Environmental Safety*, *144*, 300-306.

Gupta, P., & Diwan, B. (2017). Bacterial Exopolysaccharide mediated heavy metal removal: a review on biosynthesis, mechanism and remediation strategies. *Biotechnology Reports*, *13*, 58-71.

Gustin, J. L., Loureiro, M. E., Kim, D., Na, G., Tikhonova, M., & Salt, D. E. (2009). MTP1-dependent Zn sequestration into shoot vacuoles suggests dual roles in Zn tolerance and accumulation in Zn-hyperaccumulating plants. *The Plant Journal*, *57*(6), 1116-1127.

Hacisalihoglu, G., & Kochian, L. V. (2003). How do some plants tolerate low levels of soil zinc? Mechanisms of zinc efficiency in crop plants. *New phytologist*, *159*(2), 341-350.

Hall, T. A. (1999, January). BioEdit: a user-friendly biological sequence alignment editor and analysis program for Windows 95/98/NT. In *Nucleic acids symposium series* (Vol. 41, No. 41, pp. 95-98). [London]: Information Retrieval Ltd., c1979-c2000.

Hao, Z., Li, X., Xie, C., Weng, J., Li, M., Zhang, D., ... & Zhang, S. (2011). Identification of functional genetic variations underlying drought tolerance in maize using SNP markers. *Journal of integrative plant biology*, *53*(8), 641-652.

He, Z. L., Yang, X. E., & Stoffella, P. J. (2005). Trace elements in agroecosystems and impacts on the environment. *Journal of Trace elements in Medicine and Biology*, *19*(2), 125-140.

Helal, H. M., & Sauerbeck, D. (1986). Effect of plant roots on carbon metabolism of soil microbial biomass. *Journal of plant nutrition and soil science*, *149*(2), 181-188.

Hiltner, L. (1994). Über neuere Erfahrungen und Probleme auf dem Debiete der Bo denbakteriologie und unter Besonderer Berucksichtigung der Grundund und Brache. *Zbl. Bakteriol*, *2*, 14-25.

Hinsinger, P. (2001). Bioavailability of trace elements as related to root-induced chemical changes in the rhizosphere. *Trace elements in the rhizosphere*, 25-41.

Hirschhorn, J. N., & Daly, M. J. (2005). Genome-wide association studies for common diseases and complex traits. *Nature Reviews Genetics*, *6*(2), 95-108.

Hoagland, D. R., & Arnon, D. I. (1950). The water-culture method for growing plants without soil. *Circular. California Agricultural Experiment Station*, *347*(2nd edit).

Hoffmann, M. H. (2002), Biogeography of *Arabidopsis thaliana* (L.) Heynh. (Brassicaceae). Journal of Biogeography, 29: 125–134.

Horton, M. W., Hancock, A. M., Huang, Y. S., Toomajian, C., Atwell, S., Auton, A., ... & Nordborg, M. (2012). Genome-wide patterns of genetic variation in worldwide Arabidopsis thaliana accessions from the RegMap panel. *Nature genetics*, *44*(2), 212-216.

Hotz, C., & Brown, K. H. (2004). *Assessment of the risk of zinc deficiency in populations and options for its control*. International nutrition foundation: for UNU.

Hughes, M. N., & Poole, R. K. (1991). Metal speciation and microbial growth—the hard (and soft) facts. *Microbiology*, *137*(4), 725-734.

Husen, E. (2016). Screening of soil bacteria for plant growth promotion activities in vitro. *Indonesian Journal of Agricultural Science*, *4*(1), 27-31.

Illmer, P., & Schinner, F. (1992). Solubilization of inorganic phosphates by microorganisms isolated from forest soils. *Soil Biology and Biochemistry*, *24*(4), 389-395.

Inan, G., Zhang, Q., Li, P., Wang, Z., Cao, Z., Zhang, H., ... & Shi, H. (2004). Salt cress. A halophyte and cryophyte Arabidopsis relative model system and its applicability to molecular genetic analyses of growth and development of extremophiles. *Plant physiology*, *135*(3), 1718-1737.

Jensen, M. T., Cox, R. P., & Jensen, B. B. (1995). 3-Methylindole (skatole) and indole production by mixed populations of pig fecal bacteria. *Applied and Environmental Microbiology*, *61*(8), 3180-3184.

Jones, D. L. (1998). Organic acids in the rhizosphere–a critical review. *Plant and soil*, *205*(1), 25-44.

Jones, D. L., Hodge, A., & Kuzyakov, Y. (2004). Plant and mycorrhizal regulation of rhizodeposition. *New Phytologist*, *163*(3), 459-480.

Jones, D.L. and Darrah, P.R. (1994) Role of root derived organic acids in the mobilization of nutrients from the rhizosphere. *Plant Soil.* **166**, 247–257.

Kang, H. M., Sul, J. H., Service, S. K., Zaitlen, N. A., Kong, S. Y., Freimer, N. B., ... & Eskin, E. (2010). Variance component model to account for sample structure in genome-wide association studies. *Nature genetics*, 42(4), 348-354.

Kang, H. M., Zaitlen, N. A., Wade, C. M., Kirby, A., Heckerman, D., Daly, M. J., & Eskin, E. (2008). Efficient control of population structure in model organism association mapping. *Genetics*, 178(3), 1709-1723.

Katznelson, H., Peterson, E. A., & Rouatt, J. W. (1962). Phosphate-dissolving microorganisms on seed and in the root zone of plants. *Canadian Journal of Botany*, *40*(9), 1181-1186.

Kawachi, M., Kobae, Y., Mimura, T., & Maeshima, M. (2008). Deletion of a histidine-rich loop of AtMTP1, a vacuolar Zn2+/H+ antiporter of Arabidopsis thaliana, stimulates the transport activity. *Journal of Biological Chemistry*, *283*(13), 8374-8383.

Kawecki, T. J., & Ebert, D. (2004). Conceptual issues in local adaptation. *Ecology letters*, *7*(12), 1225-1241.

Khalid, A., Arshad, M., & Zahir, Z. A. (2004). Screening plant growth-promoting rhizobacteria for improving growth and yield of wheat. *Journal of Applied Microbiology*, *96*(3), 473-480.

Khan, A. R., Park, G. S., Asaf, S., Hong, S. J., Jung, B. K., & Shin, J. H. (2017). Complete genome analysis of Serratia marcescens RSC-14: A plant growth-promoting bacterium that alleviates cadmium stress in host plants. *PloS one*, *12*(2), e0171534.

Khan, M. S., Zaidi, A., Wani, P. A., & Oves, M. (2009). Role of plant growth promoting rhizobacteria in the remediation of metal contaminated soils. *Environmental chemistry letters*, *7*(1), 1-19.

Kidd, P., Barceló, J., Bernal, M. P., Navari-Izzo, F., Poschenrieder, C., Shilev, S., Clemente, R., Monterroso, C. (2009). Trace element behaviour at the root–soil interface: implications in phytoremediation. *Environmental and Experimental Botany*, *67*(1), 243-259.

Kiekens, L (1995) Zinc, in Alloway, B.J. (ed.) Heavy Metals in Soils (2nd edn.). *Blackie Academic and Professiona*l, London, pp 284-305.

Kisko, M., Bouain, N., Rouached, A., Choudhary, S. P., & Rouached, H. (2015). Molecular mechanisms of phosphate and zinc signalling crosstalk in plants: phosphate and zinc loading into root xylem in Arabidopsis. *Environmental and Experimental Botany*, *114*, 57-64.

Kloepper, J. W., Lifshitz, R., & Schroth, M. N. (1988). Pseudomonas inoculants to benefit plant production. *ISI ATLAS SCI: ANIM. PLANT SCI.*, *1*(1), 60-64.

Kobae, Y., Uemura, T., Sato, M. H., Ohnishi, M., Mimura, T., Nakagawa, T., & Maeshima, M. (2004). Zinc transporter of Arabidopsis thaliana AtMTP1 is localized to vacuolar membranes and implicated in zinc homeostasis. *Plant and Cell Physiology*, *45*(12), 1749-1758.

Kobayashi, T., & Nishizawa, N. K. (2012). Iron uptake, translocation, and regulation in higher plants. *Annual review of plant biology*, *63*, 131-152.

Kolbas, A., Kidd, P., Guinberteau, J., Jaunatre, R., Herzig, R., & Mench, M. (2015). Endophytic bacteria take the challenge to improve Cu phytoextraction by sunflower. *Environmental Science and Pollution Research*, *22*(7), 5370-5382.

Kooke, R., Kruijer, W., Bours, R., Becker, F. F., Kuhn, A., Buntjer, J., ... & Keurentjes, J. J. (2016). Genome-wide association mapping and genomic prediction elucidate the genetic architecture of morphological traits in Arabidopsis thaliana. *Plant Physiology*, pp-00997.

Koornneef, M., & Meinke, D. (2010). The development of Arabidopsis as a model plant. *The Plant Journal*, *61*(6), 909-921.

Koornneef, M., Alonso-Blanco, C., & Vreugdenhil, D. (2004). Naturally occurring genetic variation in Arabidopsis thaliana. *Annu. Rev. Plant Biol.*, *55*, 141-172.

Korte, A., & Farlow, A. (2013). The advantages and limitations of trait analysis with GWAS: a review. *Plant methods*, *9*(1), 29.

Kotera, E., Tasaka, M., & Shikanai, T. (2005). A pentatricopeptide repeat protein is essential for RNA editing in chloroplasts. *Nature*, *433*(7023), 326.

Kraemer, S. M. (2004). Iron oxide dissolution and solubility in the presence of siderophores. *Aquatic sciences*, *66*(1), 3-18.

Krämer, U. (2015). The Natural History of Model Organisms: Planting molecular functions in an ecological context with Arabidopsis thaliana. *Elife*, *4*, e06100.

Krewulak, K. D., & Vogel, H. J. (2008). Structural biology of bacterial iron uptake. *Biochimica et Biophysica Acta (BBA)-Biomembranes*, *1778*(9), 1781-1804.

Kucey, R. M. N., Janzen, H. H., & Leggett, M. E. (1989). Microbially mediated increases in plant-available phosphorus. *Advances in agronomy*, *42*, 199-228.

Lamesch, P., Berardini, T. Z., Li, D., Swarbreck, D., Wilks, C., Sasidharan, R., ... & Karthikeyan, A. S. (2011). The Arabidopsis Information Resource (TAIR): improved gene annotation and new tools. *Nucleic acids research*, *40*(D1), D1202-D1210.

Lemanceau, P., Bauer, P., Kraemer, S., & Briat, J. F. (2009). Iron dynamics in the rhizosphere as a case study for analyzing interactions between soils, plants and microbes. *Plant and Soil*, *321*(1-2), 513-535.

Leveau, J. H., & Lindow, S. E. (2005). Utilization of the plant hormone indole-3-acetic acid for growth by Pseudomonas putida strain 1290. *Applied and Environmental Microbiology*, *71*(5), 2365-2371.

Leyval, C. and Barthelin, J. (1989) Interactions between *Laccaria laccata, Agrobacterium radiobacter*and beech roots: influence on P, K, Mg and Fe mobilization from mineral and plant growth. *Plant Soil.* 17, 103–110.

Lindsay, W. L. (1979). Chemical Equilibria in Soils John Wiley and Sons New York Google Scholar.

Liu, G., Greenshields, D. L., Sammynaiken, R., Hirji, R. N., Selvaraj, G., & Wei, Y. (2007). Targeted alterations in iron homeostasis underlie plant defense responses. *J Cell Sci*, *120*(4), 596-605.

Livak, K. J., & Schmittgen, T. D. (2001). Analysis of relative gene expression data using real-time quantitative PCR and the 2− ΔΔCT method. *methods*, *25*(4), 402-408.

Loeppert, R. H., & Suarez, D. L. (1996). Carbonate and gypsum.

Loeppert, R. H., Hallmark, C. T., & Koshy, M. M. (1984). Routine procedure for rapid determination of soil carbonates. *Soil Science Society of America Journal*, *48*(5), 1030-1033.

Long, N. V., Dolstra, O., Malosetti, M., Kilian, B., Graner, A., Visser, R. G., & van der Linden, C. G. (2013). Association mapping of salt tolerance in barley (Hordeum vulgare L.). *Theoretical and applied genetics*, *126*(9), 2335-2351.

Long, N. V., Dolstra, O., Malosetti, M., Kilian, B., Graner, A., Visser, R. G., & van der Linden, C. G. (2013). Association mapping of salt tolerance in barley (Hordeum vulgare L.). *Theoretical and applied genetics*, *126*(9), 2335-2351.

Lugtenberg, B., & Kamilova, F. (2009). Plant-growth-promoting rhizobacteria. *Annual review of microbiology*, *63*, 541-556.

Lundberg, D. S., Lebeis, S. L., Paredes, S. H., Yourstone, S., Gehring, J., Malfatti, S., Tremblay, J., Engelbrektson, A., Kunin, V., del Rio, T. G., Edgar, R. C. (2012). Defining the core Arabidopsis thaliana root microbiome. *Nature*, *488*(7409), 86.

Lurin, C., Andrés, C., Aubourg, S., Bellaoui, M., Bitton, F., Bruyère, C., ... & Lecharny, A. (2004). Genome-wide analysis of Arabidopsis pentatricopeptide repeat proteins reveals their essential role in organelle biogenesis. *The Plant Cell*, *16*(8), 2089-2103.

Mahanty, T., Bhattacharjee, S., Goswami, M., Bhattacharyya, P., Das, B., Ghosh, A., & Tribedi, P. (2017). Biofertilizers: a potential approach for sustainable agriculture development. *Environmental Science and Pollution Research*, 1-21.

Malaikozhundan, B., Vaseeharan, B., Vijayakumar, S., & Thangaraj, M. P. (2017). Bacillus thuringiensis coated zinc oxide nanoparticle and its biopesticidal effects on the pulse beetle, Callosobruchus maculatus. *Journal of Photochemistry and Photobiology B: Biology*, *174*, 306-314.

Maloney, P. E., Van Bruggen, A. H. C., & Hu, S. (1997). Bacterial community structure in relation to the carbon environments in lettuce and tomato rhizospheres and in bulk soil. *Microbial Ecology*, *34*(2), 109-117.

Marschner H. (1995) Mineral Nutrition of Higher Plants. London: Academic. 2nd ed

Marschner, H. (2011). *Marschner's mineral nutrition of higher plants*. Academic press.

Marschner, H. (2012). Marschner's mineral nutrition of higher plants. Vol. 89.

Marschner, P., Crowley, D., & Rengel, Z. (2010, August). Interactions between rhizosphere microorganisms and plants governing iron and phosphorus availability. In *19th World congress of soil science, soil solutions for a changing world, Brisbane, Australia*.

Marschner, P., Crowley, D., & Rengel, Z. (2011). Rhizosphere interactions between microorganisms and plants govern iron and phosphorus acquisition along the root axis–model and research methods. *Soil Biology and Biochemistry*, *43*(5), 883-894.

Marschner, P., Fu, Q., & Rengel, Z. (2003). Manganese availability and microbial populations in the rhizosphere of wheat genotypes differing in tolerance to Mn deficiency. *Journal of Plant Nutrition and Soil Science*, *166*(6), 712-718.

Martos, S., Gallego, B., Cabot, C., Llugany, M., Barceló, J., & Poschenrieder, C. (2016). Zinc triggers signaling mechanisms and defense responses promoting resistance to Alternaria brassicicola in Arabidopsis thaliana. *Plant Science*, *249*, 13-24.

McCall KA, Huang CC, Fierke CA (2000). Function and Mechanism of Zinc Metalloenzymes. *Journal Nutrition* 130: 1437S-1446S

McConnell, I. L., Eaton-Rye, J. J., & van Rensen, J. J. (2012). Regulation of photosystem II electron transport by bicarbonate. In *Photosynthesis* (pp. 475-500). Springer Netherlands.
McCray JM, Matocha JE. (1992) Effects of soil water levels on solution bicarbonate, chlorosis a nd growth of sorghum. *Journal of Plant Nutrition*, 15:1877–1890.

McGrath, S. P., Chaudri, A. M., & Giller, K. E. (1995). Long-term effects of metals in sewage sludge on soils, microorganisms and plants. *Journal of Industrial Microbiology & Biotechnology*, *14*(2), 94-104.

McHale, L., Tan, X., Koehl, P., & Michelmore, R. W. (2006). Plant NBS-LRR proteins: adaptable guards. *Genome biology*, *7*(4), 212.

Meyer, J. A., & Abdallah, M. A. (1978). The fluorescent pigment of Pseudomonas fluorescens: biosynthesis, purification and physicochemical properties. *Microbiology*, *107*(2), 319-328.

Milner, M. J., Seamon, J., Craft, E., & Kochian, L. V. (2013). Transport properties of members of the ZIP family in plants and their role in Zn and Mn homeostasis. *Journal of Experimental Botany*, *64*(1), 369-381.

Mitchell-Olds, T. and Schmitt, J. (2006) Genetic mechanisms and evolutionary significance of natural variation in Arabidopsis. Nature 441, 947–952.

Mohsenian, Y., & Roosta, H. R. (2015). Effects of grafting on alkali stress in tomato plants: datura rootstock improve alkalinity tolerance of tomato plants. *Journal of plant nutrition*, *38*(1), 51-72.

Morel, M., Crouzet, J., Gravot, A., Auroy, P., Leonhardt, N., Vavasseur, A., & Richaud, P. (2009). AtHMA3, a P1B-ATPase allowing Cd/Zn/Co/Pb vacuolar storage in Arabidopsis. *Plant physiology*, *149*(2), 894-904.

Morgulis, A., Coulouris, G., Raytselis, Y., Madden, T. L., Agarwala, R., & Schäffer, A. A. (2008). Database indexing for production MegaBLAST searches. *Bioinformatics*, *24*(16), 1757-1764.

Nagajyoti, P. C., Lee, K. D., & Sreekanth, T. V. M. (2010). Heavy metals, occurrence and toxicity for plants: a review. *Environmental Chemistry Letters*, *8*(3), 199-216.

Neilands, J. B. (1995). Siderophores: structure and function of microbial iron transport compounds. *Journal of Biological Chemistry*, *270*(45), 26723-26726.

Nguyen, C., Yan, W., Le Tacon, F., & Lapeyrie, F. (1992). Genetic variability of phosphate solubilizing activity by monocaryotic and dicaryotic mycelia of the ectomycorrhizal fungus Laccaria bicolor (Maire) PD Orton. *Plant and Soil*, *143*(2), 193-199.

Olsen, L. I., & Palmgren, M. G. (2014). Many rivers to cross: the journey of zinc from soil to seed. *Frontiers in plant science*, *5*.

Panke-Buisse, K., Lee, S., & Kao-Kniffin, J. (2017). Cultivated sub-populations of soil microbiomes retain early flowering plant trait. *Microbial ecology*, *73*(2), 394-403.

Papadopoulos, P., & Rowell, D. L. (1988). The reactions of cadmium with calcite surfaces. *Journal of Soil Science*, *43*, 23-36.

Peech, M. (1965). Hydrogen-ion activity. *Methods of soil analysis. Part 2. Chemical and microbiological properties*, (methodsofsoilanb), 914-926.

Pii, Y., Mimmo, T., Tomasi, N., Terzano, R., Cesco, S., & Crecchio, C. (2015). Microbial interactions in the rhizosphere: beneficial influences of plant growth-promoting rhizobacteria on nutrient acquisition process. A review. *Biology and fertility of soils*, *51*(4), 403-415.

Pikovskaya, R.I. (1948) Mobilization of phosphorus in soil in connection with the vital activity of some microbial species. *Mikrobiologiya* 17, 362–370.

Platt, A., Vilhjálmsson, B. J., & Nordborg, M. (2010). Conditions under which genome-wide association studies will be positively misleading. *Genetics*, *186*(3), 1045-1052.

Poorter, H., Fiorani, F., Stitt, M., Schurr, U., Finck, A., Gibon, Y., ... & Pons, T. L. (2012). The art of growing plants for experimental purposes: a practical guide for the plant biologist. *Functional Plant Biology*, *39*(11), 821-838.

Pro, W. (2004). WinRHIZO Pro 2004a Software: Root Analysis. *Regent Instruments Inc., Quebec, Canada*.

Rajkumar, M., Ae, N., Prasad, M. N. V., & Freitas, H. (2010). Potential of siderophore-producing bacteria for improving heavy metal phytoextraction. *Trends in biotechnology*, *28*(3), 142-149.

Ramachandran, S., Fontanille, P., Pandey, A., & Larroche, C. (2006). Gluconic acid: properties, applications and microbial production. *Food Technology and Biotechnology*, *44*(2), 185-195.

Rehman, H. U., Aziz, T., Farooq, M., Wakeel, A., & Rengel, Z. (2012). Zinc nutrition in rice production systems: a review. *Plant and soil*, *361*(1-2), 203-226.

Rengel, Z. (2015). Availability of Mn, Zn and Fe in the rhizosphere. *Journal of soil science and plant nutrition*, *15*(2), 397-409.

Rengel, Z., & Marschner, P. (2005). Nutrient availability and management in the rhizosphere: exploiting genotypic differences. *New Phytologist*, *168*(2), 305-312.

Reynolds, W. D., & Topp, G. C. (2008). Soil water analyses: Principles and parameters. Soil sampling and methods of analysis. 2nd ed. *CRC Press, Boca Raton*, FL, 913-939.

Ricachenevsky, F. K., Menguer, P. K., Sperotto, R. A., & Fett, J. P. (2015). Got to hide your Zn away: molecular control of Zn accumulation and biotechnological applications. *Plant Science*, *236*, 1-17.

Richardson, A. E., & Simpson, R. J. (2011). Soil microorganisms mediating phosphorus availability update on microbial phosphorus. *Plant physiology*, *156*(3), 989-996.

Rodríguez, H., & Fraga, R. (1999). Phosphate solubilizing bacteria and their role in plant growth promotion. *Biotechnology advances*, *17*(4), 319-339.

Rodríguez, H., Fraga, R., Gonzalez, T., & Bashan, Y. (2006). Genetics of phosphate solubilization and its potential applications for improving plant growth-promoting bacteria. *Plant and soil*, *287*(1), 15-21.

Rodriguez, H., Vessely, S., Shah, S., & Glick, B. R. (2008). Effect of a nickel-tolerant ACC deaminase-producing Pseudomonas strain on growth of nontransformed and transgenic canola plants. *Current microbiology*, *57*(2), 170-174.

Román-Ponce, B., Reza-Vazquez, D. M., Guitierrez-Paredes, S., Maria de Jesis, D. E., Maldonado-Hernandez, J., Bahena-Osorio, Y., … & Vasquez-Murrieta, M. S. (2017). Plant growth-promoting traits in rhizobacteria of heavy metal-resistant plants and their effects on Brassica nigra seed germination. *Pedosphere*, *27*(3), 511-526.

Roosens, N. H., Willems, G., & Saumitou-Laprade, P. (2008). Using Arabidopsis to explore zinc tolerance and hyperaccumulation. *Trends in plant science*, *13*(5), 208-215.

Ruano, A., Barcelo, J., & Poschenrieder, C. (1987). Zinc toxicity-induced variation of mineral element composition in hydroponically grown bush bean plants. *Journal of plant nutrition*, *10*(4), 373-384.

Ruano, A., Poschenrieder, C. H., & Barcelo, J. (1988). Growth and biomass partitioning in zinc-toxic bush beans. *Journal of plant nutrition*, *11*(5), 577-588.

Salt, D. E., Baxter, I., & Lahner, B. (2008). Ionomics and the study of the plant ionome. *Annu. Rev. Plant Biol.*, *59*, 709-733.

Saravanan, V. S., Madhaiyan, M., & Thangaraju, M. (2007). Solubilization of zinc compounds by the diazotrophic, plant growth promoting bacterium Gluconacetobacter diazotrophicus. *Chemosphere*, *66*(9), 1794-1798.

Saravanan, V. S., Subramoniam, S. R., & Raj, S. A. (2004). Assessing in vitro solubilization potential of different zinc solubilizing bacterial (zsb) isolates. *Brazilian Journal of Microbiology*, *35*(1-2), 121-125.

Sarwar, M., & Kremer, R. J. (1995). Determination of bacterially derived auxins using a microplate method. *Letters in applied microbiology*, *20*(5), 282-285.

Schmid, N. B., Giehl, R. F., Döll, S., Mock, H. P., Strehmel, N., Scheel, D., ... & von Wirén, N. (2014). Feruloyl-CoA 6′-hydroxylase1-dependent coumarins mediate iron acquisition from alkaline substrates in Arabidopsis. *Plant Physiology*, *164*(1), 160-172.

Schwyn, B., & Neilands, J. B. (1987). Universal chemical assay for the detection and determination of siderophores. *Analytical biochemistry*, *160*(1), 47-56.

Seren, Ü., Vilhjálmsson, B. J., Horton, M. W., Meng, D., Forai, P., Huang, Y. S., Nordborg, M. (2012). GWAPP: a web application for genome-wide association mapping in Arabidopsis. *The Plant Cell*, *24*(12), 4793-4805.

Sessitsch, A., Kuffner, M., Kidd, P., Vangronsveld, J., Wenzel, W. W., Fallmann, K., & Puschenreiter, M. (2013). The role of plant-associated bacteria in the mobilization and phytoextraction of trace elements in contaminated soils. *Soil Biology and Biochemistry*, *60*, 182-194.

Shao, L., Shu, Z., Peng, C. L., Lin, Z. F., Yang, C. W., & Gu, Q. (2008). Enhanced sensitivity of Arabidopsis anthocyanin mutants to photooxidation: a study with fluorescence imaging. *Functional plant biology*, *35*(8), 714-724.

Sharbel, T. F., Haubold, B., & Mitchell-Olds, T. (2000). Genetic isolation by distance in Arabidopsis thaliana: biogeography and postglacial colonization of Europe. *Molecular Ecology*, *9*(12), 2109-2118.

Sharma, S. B., Sayyed, R. Z., Trivedi, M. H., & Gobi, T. A. (2013). Phosphate solubilizing microbes: sustainable approach for managing phosphorus deficiency in agricultural soils. *SpringerPlus*, *2*(1), 587.

Sheoran, V., Sheoran, A. S., & Poonia, P. (2010). Soil reclamation of abandoned mine land by revegetation: a review. *International Journal of Soil, Sediment and Water*, *3*(2), 13.

Shindo, C., Bernasconi, G., & Hardtke, C. S. (2007). Natural genetic variation in Arabidopsis: tools, traits and prospects for evolutionary ecology. *Annals of Botany*, *99*(6), 1043-1054.

Sims, J. T. (1985). A comparison of Mehlich I and Mehlich III extractants as predictors of manganese, copper and zinc availability in four Delaware soils 1. *Communications in Soil Science & Plant Analysis*, *16*(10), 1039-1052.

Sinclair, S. A., & Krämer, U. (2012). The zinc homeostasis network of land plants. *Biochimica et Biophysica Acta (BBA)-Molecular Cell Research*, *1823*(9), 1553-1567.

Singh, B., Natesan, S. K. A., Singh, B. K., & Usha, K. (2005). Improving zinc efficiency of cereals under zinc deficiency. *Current Science*, *88*(1), 36-44.

Smalla, K., Wieland, G., Buchner, A., Zock, A., Parzy, J., Kaiser, S., ... & Berg, G. (2001). Bulk and rhizosphere soil bacterial communities studied by denaturing gradient gel electrophoresis: plant-dependent enrichment and seasonal shifts revealed. *Applied and environmental microbiology*, *67*(10), 4742-4751.

Soltanpour, P. A., & Schwab, A. P. (1977). A new soil test for simultaneous extraction of macro- and micro-nutrients in alkaline soils 1. *Communications in Soil Science & Plant Analysis*, *8*(3), 195-207.

Souza, R. D., Ambrosini, A., & Passaglia, L. M. (2015). Plant growth-promoting bacteria as inoculants in agricultural soils. *Genetics and molecular biology*, *38*(4), 401-419.

Spaepen, S., Vanderleyden, J. and Remans, R. (2007), Indole-3-acetic acid in microbial and microorganism-plant signaling. FEMS Microbiology Reviews, 31: 425–448.

Staswick, P. E., Serban, B., Rowe, M., Tiryaki, I., Maldonado, M. T., Maldonado, M. C., & Suza, W. (2005). Characterization of an Arabidopsis enzyme family that conjugates amino acids to indole-3-acetic acid. *The Plant Cell*, *17*(2), 616-627.

Steenhoudt, O., & Vanderleyden, J. (2000). Azospirillum, a free-living nitrogen-fixing bacterium closely associated with grasses: genetic, biochemical and ecological aspects. *FEMS microbiology reviews*, *24*(4), 487-506.

Szklarczyk, D., Franceschini, A., Wyder, S., Forslund, K., Heller, D., Huerta-Cepas, J., ... & Kuhn, M. (2014). STRING v10: protein–protein interaction networks, integrated over the tree of life. *Nucleic acids research*, *43*(D1), D447-D452.

Taji, T., Komatsu, K., Katori, T., Kawasaki, Y., Sakata, Y., Tanaka, S., ... & Shinozaki, K. (2010). Comparative genomic analysis of 1047 completely sequenced cDNAs from an Arabidopsis-related model halophyte, Thellungiella halophila. *BMC plant biology*, *10*(1), 261.

Tanaka, K., Shinji, T., & Uchiki, H. (2014). Photoluminescence from Cu 2 ZnSnS 4 thin films with different compositions fabricated by a sputtering-sulfurization method. *Solar Energy Materials and Solar Cells*, *126*, 143-148.

Teres, J. (2017). Characterization of natural populations of Arabidopsis thaliana differing in tolerance to carbonate soil. (Doctoral Thesis). Universitat Autònoma Barcelona.

Tian, F., Bradbury, P. J., Brown, P. J., Hung, H., Sun, Q., Flint-Garcia, S., ... & Buckler, E. S. (2011). Genome-wide association study of leaf architecture in the maize nested association mapping population. *Nature genetics*, *43*(2), 159-162.

Trevors, J. T. (1998). Bacterial biodiversity in soil with an emphasis on chemically-contaminated soils. *Water, Air, & Soil Pollution*, *101*(1), 45-67.

Ueno, D., Milner, M. J., Yamaji, N., Yokosho, K., Koyama, E., Clemencia Zambrano, M., ... & Ma, J. F. (2011). Elevated expression of TcHMA3 plays a key role in the extreme Cd tolerance in a Cd-hyperaccumulating ecotype of Thlaspi caerulescens. *The Plant Journal*, *66*(5), 852-862.

Uroz, S., Calvaruso, C., Turpault, M. P., & Frey-Klett, P. (2009). Mineral weathering by bacteria: ecology, actors and mechanisms. *Trends in microbiology*, *17*(8), 378-387.

Valdez-Aguilar, L. A., & Reed, D. W. (2007). Response of selected greenhouse ornamental plants to alkalinity in irrigation water. *Journal of plant nutrition*, *30*(3), 441-452.

Valentinuzzi, F., Cesco, S., Tomasi, N., & Mimmo, T. (2015). Influence of different trap solutions on the determination of root exudates in Lupinus albus L. *Biology and fertility of soils*, *51*(6), 757-765.

van de Mortel, J. E., Villanueva, L. A., Schat, H., Kwekkeboom, J., Coughlan, S., Moerland, P. D., ... & Aarts, M. G. (2006). Large expression differences in genes for iron and zinc homeostasis, stress response, and lignin biosynthesis distinguish roots of Arabidopsis thaliana and the related metal hyperaccumulator Thlaspi caerulescens. *Plant Physiology*, *142*(3), 1127-1147.

van Wijk, S. J., & Timmers, H. M. (2010). The family of ubiquitin-conjugating enzymes (E2s): deciding between life and death of proteins. *The FASEB Journal*, *24*(4), 981-993.

Vangronsveld, J., Herzig, R., Weyens, N., Boulet, J., Adriaensen, K., Ruttens, A., Thewys, T., Vassilev, A., Meers, E., Nehnevajova, E., van der Lelie, D. (2009). Phytoremediation of contaminated soils and groundwater: lessons from the field. *Environmental Science and Pollution Research*, *16*(7), 765-794.

Vega, F. A., Covelo, E. F., & Andrade, M. L. (2005). Limiting factors for reforestation of mine spoils from Galicia (Spain). *Land degradation & development*, *16*(1), 27-36.

Vega, F. A., Covelo, E. F., & Andrade, M. L. (2006). Competitive sorption and desorption of heavy metals in mine soils: influence of mine soil characteristics. *Journal of Colloid and Interface Science*, *298*(2), 582-592.

Vessey, J. K. (2003). Plant growth promoting rhizobacteria as biofertilizers. *Plant and soil*, *255*(2), 571-586.

Warne, M. S. J., Heemsbergen, D., Stevens, D., McLaughlin, M., Cozens, G., Whatmuff, M., ... & Pritchard, D. (2008). Modeling the toxicity of copper and zinc salts to wheat in 14 soils. *Environmental Toxicology and Chemistry*, *27*(4), 786-792.

Weigel, D., & Mott, R. (2009). The 1001 genomes project for Arabidopsis thaliana. *Genome biology*, *10*(5), 107.

White P. J., Broadley M. R. (2009). Biofortification of crops with seven mineral elements often lacking in human diets - iron, zinc, copper, calcium, magnesium, selenium and iodine. New Phytol. 182 49–84

White, C., Sayer, J. A., & Gadd, G. M. (1997). Microbial solubilization and immobilization of toxic metals: key biogeochemical processes for treatment of contamination. *FEMS microbiology reviews*, *20*(3-4), 503-516.

White, D. C., Davis, W. M., Nickels, J. S., King, J. D., & Bobbie, R. J. (1979). Determination of the sedimentary microbial biomass by extractible lipid phosphate. *Oecologia*, *40*(1), 51-62.

White, P. J., & Broadley, M. R. (2011). Physiological limits to zinc biofortification of edible crops. *Frontiers in plant science*, *2*.

Whiting, P. H., Midgley, M., & Dawes, E. A. (1976). The role of glucose limitation in the regulation of the transport of glucose, gluconate and 2-oxogluconate, and of glucose metabolism in Pseudomonas aeruginosa. *Microbiology*, *92*(2), 304-310.

Williams, SG; Greenwood, JA; Jones, CW (1996). Physiological and biochemical changes accompanying the loss of mucoidy by Pseudomonas aeruginosa. Microbiology 142: 881–888.

Xie, Y., Fan, J., Zhu, W., Amombo, E., Lou, Y., Chen, L., & Fu, J. (2016). Effect of heavy metals pollution on soil microbial diversity and bermudagrass genetic variation. *Frontiers in plant science*, *7*.

Xu, X., Zhang, Z., Hu, S., Ruan, Z., Jiang, J., Chen, C., & Shen, Z. (2017). Response of soil bacterial communities to lead and zinc pollution revealed by Illumina MiSeq sequencing investigation. *Environmental Science and Pollution Research*, *24*(1), 666-675.

Yadav, K.S. and Dadarwal, K.R. (1997) Phosphate solubilization and mobilization through soil microorganisms. In: Biotechnological Approaches in Soil Microorganisms for Sustainable Crop Production (Dadarwal, K.R., Ed.), pp. 293–308. Scientific Publishers, Jodhpur.

Yang, Q., Li, Z., Li, W., Ku, L., Wang, C., Ye, J., ... & Li, J. (2013). CACTA-like transposable element in ZmCCT attenuated photoperiod sensitivity and accelerated the postdomestication spread of maize. *Proceedings of the National Academy of Sciences*, *110*(42), 16969-16974.

Ye, Z. H., Baker, A. J. M., Wong, M. H., & Willis, A. J. (1997). Zinc, lead and cadmium tolerance, uptake and accumulation by the common reed, Phragmites australis (Cav.) Trin. ex Steudel. *Annals of Botany*, *80*(3), 363-370.

Yu, J., Pressoir, G., Briggs, W. H., Bi, I. V., Yamasaki, M., Doebley, J. F., ... & Kresovich, S. (2006). A unified mixed-model method for association mapping that accounts for multiple levels of relatedness. *Nature genetics*, *38*(2), 203-208.

Zak, J. C., Willig, M. R., Moorhead, D. L., & Wildman, H. G. (1994). Functional diversity of microbial communities: a quantitative approach. *Soil Biology and Biochemistry*, *26*(9), 1101-1108.

Zhang, Z., Ersoz, E., Lai, C. Q., Todhunter, R. J., Tiwari, H. K., Gore, M. A., ... & Buckler, E. S. (2010). Mixed linear model approach adapted for genome-wide association studies. *Nature genetics*, *42*(4), 355-360.

Zhao, K., & Wu, Y. (2017). Effects of Zn Deficiency and Bicarbonate on the Growth and Photosynthetic Characteristics of Four Plant Species. *PloS one*, *12*(1), e0169812.

Zhao, K., Aranzana, M. J., Kim, S., Lister, C., Shindo, C., Tang, C., ... & Nordborg, M. (2007). An Arabidopsis example of association mapping in structured samples. *PLoS Genet*, *3*(1), e4.

Webpage & Programmes:

http://gwas.gmi.oeaw.ac.at

http://string-db.org : **Szklarczyk, D., Franceschini, A., Wyder, S., Forslund, K., Heller, D., Huerta-Cepas, J., ... & Kuhn, M.** (2014). STRING v10: protein–protein interaction networks, integrated over the tree of life. *Nucleic acids research*, *43*(D1), D447-D452.

http://www.chem.qmul.ac.uk/iubmb/enzyme/

http://www.ionomicshub.org/arabidopsis/piims/showIndex.action

http://www.medical-labs.net/wp-content/uploads/2014/03/Bacterial-colony-morphology.jpg

http://www.zinc.org

https://github.com/timeu/GWAPP

JMP: Version 12 (2013-2016) & Version 13 (2016-2017) SAS Institute Inc, Cary, NC

Meteocat: Servei Meteorològic de Catalunya. http://meteo.cat

phylogeny.lirmm.fr: **Dereeper, A., Guignon, V., Blanc, G., Audic, S., Buffet, S., Chevenet, F., ... & Claverie, J. M.** (2008). Phylogeny. fr: robust phylogenetic analysis for the non-specialist. *Nucleic acids research*, *36*(suppl_2), W465-W469.

8. Annex

1. Soil metal concentration of the different used soil.

	µg As/ g	µg Cd/ g	µg Pb/ g	µg Zn/ g	µg Cu/ g	µg Co/ g	µg Fe/ g
LPH (Les planes d'Hostoles)	0.0156 ± 0.003	0.077 ± 0.005	1.781 ± 0.094	2.077 ± 0.154	0.944 ± 0.044	0.388 ± 0.043	13.417 ± 1.364
SCF (Santa Coloma de Ferners)	0.049 ± 0.003	0.045 ± 0.003	4.424 ± 0.202	2.821 ± 0.152	1.122 ± 0.130	0.724 ± 0.040	174.162 ± 1.746
Mine	2.341 ± 0.386	4.167 ± 0.368	2920.456 ± 462.613	321.137 ± 22.115	54.986 ± 4.089	8.358 ± 0.983	189.410 ± 28.64
Mallorca	0.186 ± 0.006	0.277 ± 0.002	10.640 ± 0.36	4.558 ± 0.190	4.319 ± 0.110	5.419 ± 0.110	308.642 ± 13.390

2. Hap-map population

Barcode	ABRC_Stock_number	ecotypeid	native_name	stockparent	collector	lat	long	country
Fr1ALL1-2	CS76089	1	ALL1-2	NA	Roux	45,2667	1,48333	FRA
Fr2ALL1-3	CS76090	2	ALL1-3	NA	Roux	45,2667	1,48333	FRA
Fr55BUI	CS76104	15	BUI	NA	Roux	48,3667	0,933333	FRA
Fr77CAM16	CS76107	23	CAM-16	NA	Roux	48,2667	-4,58333	FRA
Fr116CAM	CS76108	66	CAM-61	NA	Roux	48,2667	-4,58333	FRA
Fr53CLE-6	CS76112	78	CLE-6	NA	Roux	48,9167	-0,48333	FRA
Fr16CUR	CS76115	81	CUR-3	NA	Roux	45	1,75	FRA
Fr58JEA	CS76148	91	JEA	NA	Roux	43,6833	7,333333	FRA
Fr48LAC-3	CS76157	94	LAC-3	NA	Roux	47,7	6,816667	FRA

Fr50LAC-5	CS76158	96	LAC-5	NA	Roux	47,7	6,81667	FRA
Fr234LDV	CS76160	104	LDV-14	NA	Roux	48,5167	-4,06667	FRA
Fr245LDV	CS76161	116	LDV-25	NA	Roux	48,5167	-4,06667	FRA
Fr254LDV	CS76162	126	LDV-34	NA	Roux	48,5167	-4,06667	FRA
Fr275LDV	CS76163	149	LDV-58	NA	Roux	48,5167	-4,06667	FRA
Fr154MIB	CS76181	166	MIB-15	NA	Roux	47,3833	5,31667	FRA
Fr160MIB	CS76182	173	MIB-22	NA	Roux	47,3833	5,31667	FRA
Fr165MIB	CS76183	178	MIB-28	NA	Roux	47,3833	5,31667	FRA
Fr209MIB	CS76184	223	MIB-84	NA	Roux	47,3833	5,31667	FRA
Fr132MOG	CS76189	242	MOG-37	NA	Roux	48,6667	-4,06667	FRA
Fr35PAR-3	CS76205	258	PAR-3	NA	Roux	46,65	-0,25	FRA
Fr36PAR-4	CS76206	259	PAR-4	NA	Roux	46,65	-0,25	FRA
Fr37PAR-5	CS76207	260	PAR-5	NA	Roux	46,65	-0,25	FRA
Fr42ROM-1	CS76221	267	ROM-1	NA	Roux	45,5333	4,85	FRA
Fr352TOU	CS76252	281	TOU-A1-115	NA	Roux	46,6667	4,11667	FRA
Fr353TOU	CS76253	282	TOU-A1-116	NA	Roux	46,6667	4,11667	FRA
Fr289TOU	CS76254	286	TOU-A1-12	NA	Roux	46,6667	4,11667	FRA
Fr307TOU	CS76255	321	TOU-A1-43	NA	Roux	46,6667	4,11667	FRA
Fr313TOU	CS76256	328	TOU-A1-62	NA	Roux	46,6667	4,11667	FRA
Fr319TOU	CS76257	333	TOU-A1-67	NA	Roux	46,6667	4,11667	FRA
Fr339TOU	CS76258	357	TOU-A1-96	NA	Roux	46,6667	4,11667	FRA

Fr373TOU	CS76259	362	TOU-C-3	NA	Roux	46,6667	4,11667	FRA
Fr379TOU	CS76260	366	TOU-E-11	NA	Roux	46,6667	4,11667	FRA
Fr386TOU	CS76261	373	TOU-H-12	NA	Roux	46,6667	4,11667	FRA
Fr387TOU	CS76262	374	TOU-H-13	NA	Roux	46,6667	4,11667	FRA
Fr391TOU	CS76263	378	TOU-I-17	NA	Roux	46,6667	4,11667	FRA
Fr389TOU	CS76264	379	TOU-I-2	NA	Roux	46,6667	4,11667	FRA
Fr390TOU	CS76265	380	TOU-I-6	NA	Roux	46,6667	4,11667	FRA
Fr392TOU	CS76266	383	TOU-J-3	NA	Roux	46,6667	4,11667	FRA
Fr397TOU	CS76267	386	TOU-K-3	NA	Roux	46,6667	4,11667	FRA
Fr26VOU	CS76299	390	VOU-1	NA	Roux	46,65	0,166667	FRA
Fr27VOU-2	CS76300	392	VOU-2	NA	Roux	46,65	0,166667	FRA
OF95	CS76165	641	LI-OF-095	NA	Bossdorf	40,7777	-72,9069	USA
S294BEL4	CS76095	957	Belmonte-4-94	NA	Ã…gren	42,1167	12,4833	ITA
KBSMAC8	CS76151	1716	KBS-Mac-8	NA	Byers	42,405	-85,398	USA
MNFPOT48	CS76187	1859	MNF-Pot-48	NA	Byers	43,595	-86,2657	USA
MNFPOT68	CS76188	1867	MNF-Pot-68	NA	Byers	43,595	-86,2657	USA
MNFCHE2	CS76185	1925	MNF-Che-2	NA	Byers	43,5251	-86,1843	USA
MNFJAC32	CS76186	1967	MNF-Jac-32	NA	Byers	43,5187	-86,1739	USA
MAP42	CS76180	2057	Map-42	NA	Byers	42,166	-86,412	USA
PAW3	CS76208	2150	Paw-3	NA	Byers	42,148	-86,431	USA

PENT1	CS76209	2187	Pent-1	NA	Byers	43,7623	-86,3929	USA
SLSP30	CS76228	2274	SLSP-30	NA	Byers	43,665	-86,496	USA
STE3	CS76232	2290	Ste-3	NA	Byers	42,03	-86,514	USA
UKCW06202	CS76292	4802	UKSW06-202	NA	Holub	50,4	-4,9	UK
UKKT06062	CS76280	4997	UKSE06-062	NA	Holub	51,3	0,5	UK
UKKT06192	CS76281	5056	UKSE06-192	NA	Holub	51,3	0,5	UK
UKKT06272	CS76282	5116	UKSE06-272	NA	Holub	51,3	0,4	UK
UKKT06278	CS76283	5122	UKSE06-278	NA	Holub	51,3	0,4	UK
UKKT06349	CS76284	5158	UKSE06-349	NA	Holub	51,3	0,4	UK
UKKT06351	CS76285	5160	UKSE06-351	NA	Holub	51,3	0,4	UK
UKKT06414	CS76286	5202	UKSE06-414	NA	Holub	51,3	0,4	UK
UKKT06429	CS76287	5207	UKSE06-429	NA	Holub	51,3	0,4	UK
UKKT06466	CS76288	5232	UKSE06-466	NA	Holub	51,2	0,4	UK
UKKT06482	CS76289	5245	UKSE06-482	NA	Holub	51,2	0,6	UK
UKKT06520	CS76290	5264	UKSE06-520	NA	Holub	51,3	1,1	UK
UKKT06628	CS76291	5341	UKSE06-628	NA	Holub	51,1	0,4	UK
UKLD06059	CS76275	5380	UKNW06-059	NA	Holub	54,4	-3	UK
UKLD06060	CS76276	5381	UKNW06-060	NA	Holub	54,4	-3	UK
UKLD06386	CS76277	5565	UKNW06-386	NA	Holub	54,6	-3,1	UK
UKLD06436	CS76278	5606	UKNW06-436	NA	Holub	54,7	-3,4	UK
UKLD06460	CS76279	5628	UKNW06-460	NA	Holub	54,7	-3,4	UK
UK22 Coe1	CS76271	5729	UKID22	NA	Holub	54,7	-3,4	UK

UK37 Frd1	CS76272	5742	UKID37	NA	Holub	51,3	1,1	UK
UK48 Laz1	CS76273	5753	UKID48	NA	Holub	54,7	-2,7	UK
UK80 Unt1	CS76274	5785	UKID80	NA	Holub	54,7	-2,9	UK
UK102H art	CS76270	5805	UKID101	NA	Holub	53,2	-1,4	UK
App 1-16	CS76092	5832	App1-16	NA	Nordborg	56,3333	15,9667	SWE
1*Bor-1	CS76099	5837	Bor-1	CS22590	Nordborg	49,4013	16,2326	CZE
DraIV 1-5	CS76120	5887	DraIV 1-5	NA	Nordborg	49,4112	16,2815	CZE
DraIV 1-7	CS76121	5889	DraIV 1-7	NA	Nordborg	49,4112	16,2815	CZE
DraIV1-14	CS76119	5896	DraIV 1-14	NA	Nordborg	49,4112	16,2815	CZE
DraIV6-16	CS76122	5987	DraIV 6-16	NA	Nordborg	49,4112	16,2815	CZE
DraIV6-35	CS76123	6005	DraIV 6-35	NA	Nordborg	49,4112	16,2815	CZE
2*DUK	CS76124	6008	Duk	<Null>	Nordborg	49,1	16,2	CZE
S*Fja 1-2	CS76131	6019	Fja1-2	NA	Nordborg	56,06	14,29	SWE
S*Fja 1-5	CS76132	6020	Fja1-5	NA	Nordborg	56,06	14,29	SWE
2*Hovdala	CS76143	6039	Hovdala-2	<Null>	Nordborg	56,1	13,74	SWE
2*Lom 1-1	CS76174	6042	Lom1-1	<Null>	Nordborg	56,09	13,9	SWE
1*Lov-5	CS76175	6046	Lav-5	CS22575	Nordborg	62,801	18,079	SWE
2*Or-1	CS76201	6074	a–r-1	<Null>	Nordborg	56,45	16,11	SWE
S*Rev-2	CS76219	6076	Rev-2	NA	Nordborg	55,7	13,4	SWE
S*Sparta 1	CS76229	6085	Sparta-1	NA	Nordborg	55,7097	13,0489	SWE
S*T1040	CS76233	6094	T1040	NA	Nordborg	55,6494	13,2147	SWE
S*T1060	CS76234	6096	T1060	NA	Nordborg	55,6472	13,2225	SWE
S*T1080	CS76235	6098	T1080	NA	Nordborg	55,6561	13,2178	SWE
S*T1110	CS76236	6100	T1110	NA	Nordborg	55,6	13,2	SWE
S*T1130	CS76237	6102	T1130	NA	Nordborg	55,6	13,2	SWE
S*T510	CS76238	6109	T510	NA	Nordborg	55,7936	13,1233	SWE
S*T540	CS76239	6112	T540	NA	Nordborg	55,7967	13,1044	SWE

S*T620	CS76240	6119	T620	NA	Nordborg	55,7	13,2	SWE
S*T690	CS76241	6124	T690	NA	Nordborg	55,8378	13,3092	SWE
S*Tad 01	CS76243	6169	TÃ…D 01	NA	Nordborg	62,8714	18,3447	SWE
S*TDR-01	CS76245	6188	TDr-1	NA	Nordborg	55,7683	14,1386	SWE
S*TDR-03	CS76248	6190	TDr-3	NA	Nordborg	55,7686	14,1381	SWE
S*TDR-08	CS76249	6194	TDr-8	NA	Nordborg	55,7706	14,1342	SWE
S*TDR-17	CS76246	6202	TDr-17	NA	Nordborg	55,7717	14,1206	SWE
S*TDR-18	CS76247	6203	TDr-18	NA	Nordborg	55,7714	14,1208	SWE
S*Tomegap	CS76250	6242	Tomegap-2	NA	Nordborg	55,7	13,2	SWE
2*Tottarp	CS76251	6243	Tottarp-2	<Null>	Nordborg	55,95	13,85	SWE
Udul 1-34	CS76269	6318	Udul 1-34	NA	Nordborg	49,2771	16,6314	CZE
S*Ull 3-4	CS76295	6413	Ull3-4	NA	Nordborg	56,06	13,97	SWE
Zdrl 2-24	CS76307	6448	Zdrl 2-24	NA	Nordborg	49,3853	16,2544	CZE
Zdrl 2-25	CS76308	6449	Zdrl 2-25	NA	Nordborg	49,3853	16,2544	CZE
CS28140	CS28140	6727	CIBC-2	CS22221	Crawley	51,4083	-0,6383	UK
CS28141	CS28141	6729	CIBC-4	CS22223	Crawley	51,4083	-0,6383	UK
CS28142	CS28142	6730	CIBC-5	CS22224	Crawley	51,4083	-0,6383	UK
CS28181	CS28181	6744	CSHL-5	CS22423	Weiss	40,8585	-73,4675	USA
CS28407	CS28407	6810	KNO-11	CS22411	Bergelson	41,2816	-86,621	USA
CS28550	CS28550	6847	NFC-20	CS22201	Crawley	51,4083	-0,6383	UK
CS28663	CS28663	6953	Pu2-24	CS22454	Cetl	49,42	16,36	CZE
CS28013	CS28013	6989	Alst-1	CS22550	Koornneef	54,8	-2,4333	UK

CS28014	CS28014	6990	Amel-1	CS22526	Koornneef	53,448	5,73	NED
CS28018	CS28018	6992	Ang-0	CS6605	Kranz	50,3	5,3	BEL
CS28049	CS28049	6994	Ann-1	CS22520	Koornneef	45,9	6,13028	FRA
CS28017	CS28017	6996	An-2	CS6604	Kranz	51,2167	4,4	BEL
CS28051	CS28051	6998	Arby-1	CS22547	Koornneef	59,4308	16,7999	SWE
CS28007	CS28007	7000	Aa-0	CS6600	Kranz	50,9167	9,57073	GER
CS28054	CS28054	7002	Baa-1	CS22529	Koornneef	51,3333	6,1	NED
CS28097	CS28097	7004	Bs-2	CS6628	Kranz	47,5	7,5	SUI
CS28064	CS28064	7008	Benk-1	CS22530	Koornneef	52	5,675	NED
CS28063	CS28063	7011	Be-1	CS6614	Kranz	49,6803	8,6161	GER
CS28053	CS28053	7014	Ba-1	CS6607	Kranz	56,5459	-4,79821	UK
CS28091	CS28091	7026	Boot-1	CS22551	Koornneef	54,4	-3,2667	UK
CS28099	CS28099	7031	Bsch-0	CS6630	Kranz	40,0167	8,6667	GER
CS28090	CS28090	7035	Blh-2	CS6657	Kranz	48	19	CZE
CS28108	CS28108	7056	Bu-8	CS6639	Kranz	50,5	9,5	GER
CS28128	CS28128	7062	Ca-0	CS6658	Kranz	50,2981	8,26607	GER
CS28160	CS28160	7064	Cnt-1	CS6921	Holub	51,3	1,1	UK
CS28133	CS28133	7069	Cha-0	CS6662	Kranz	46,0333	7,1167	SUI
CS28135	CS28135	7071	Chat-1	CS22521	Koornneef	48,0717	1,33867	FRA
CS28158	CS28158	7075	Cit-0	CS1080	Kranz	43,3779	2,54038	FRA
CS28163	CS28163	7078	Co-2	CS6670	Kranz	40,12	-8,25	POR
CS28165	CS28165	7080	Co-4	CS6672	Kranz	40,12	-8,25	POR
CS28193	CS28193	7092	Com-1	CS22522	Koornneef	49,416	2,823	FRA
CS28200	CS28200	7094	Da-0	CS6676	Kranz	49,8724	8,65081	GER
CS28208	CS28208	7098	Di-1	CS6681	Kranz	47	5	FRA
CS28202	CS28202	7100	Db-0	CS6677	Kranz	50,3055	8,324	GER

CS28210	CS28210	7102	Do-0	CS6683	Kranz	50,7224	8,2372	GER
CS28214	CS28214	7105	Dra-2	CS6687	Kranz	49,4167	16,2667	CZE
CS28217	CS28217	7110	Ede-1	CS22532	Koornneef	52,0333	5,66667	NED
CS28236	CS28236	7123	Ep-0	CS6697	Kranz	50,1721	8,38912	GER
CS28241	CS28241	7126	Es-0	CS6699	Kranz	60,1997	24,5682	FIN
CS28243	CS28243	7128	Est-0	CS6700	Kranz	58,3	25,3	RUS
CS28268	CS28268	7135	Fr-4	CS6710	Kranz	50,1102	8,6822	GER
CS28252	CS28252	7139	Fi-1	CS6705	Kranz	50,5	8,0167	GER
CS28274	CS28274	7141	Ga-2	CS6715	Kranz	50,3	8	GER
CS28279	CS28279	7143	Gel-1	CS22533	Koornneef	51,0167	5,86667	NED
CS28277	CS28277	7145	Ge-1	CS6718	Kranz	46,5	6,08	SUI
CS28280	CS28280	7147	Gie-0	CS6720	Kranz	50,584	8,67825	GER
CS28332	CS28332	7150	Gu-1	CS6731	Kranz	50,3	8	GER
CS28282	CS28282	7151	Go-0	CS6721	Kranz	51,5338	9,9355	GER
CS28326	CS28326	7158	Gr-5	CS6727	Hauser	47	15,5	AUT
CS28336	CS28336	7163	Ha-0	CS6733	Kranz	52,3721	9,73569	GER
CS28343	CS28343	7164	Hau-0	CS6734	Kranz	55,675	12,5686	DEN
CS28350	CS28350	7165	Hn-0	CS6739	Kranz	51,3472	8,28844	GER
CS28344	CS28344	7166	Hey-1	CS22534	Koornneef	51,25	5,9	NED
CS28345	CS28345	7169	Hh-0	CS6735	Kranz	54,4175	9,88682	GER
CS28373	CS28373	7178	Jm-1	CS6749	Kranz	49	15	CZE
CS28364	CS28364	7181	Je-0	CS6742	Kranz	50,927	11,587	GER
CS28395	CS28395	7186	Kn-0	CS6762	Kranz	54,8969	23,8924	LTU
CS28382	CS28382	7188	Kelsterbach-2	CS6102	Williams	50,0667	8,5333	GER
CS28394	CS28394	7199	Kl-5	CS6761	Kranz	50,95	6,9666	GER
CS28419	CS28419	7201	Kr-0	CS6764	Kranz	51,3317	6,55934	GER

CS28423	CS28423	7205	Krot-2	CS3888	Clauss	49,631	11,5722	GER
CS28420	CS28420	7206	Kro-0	CS6766	Kranz	50,0742	8,96617	GER
CS28454	CS28454	7224	Li-3	CS1316	Kranz	50,3833	8,0666	GER
CS28457	CS28457	7227	Li-5:2	CS6909	Kranz	50,3833	8,0666	GER
CS28459	CS28459	7229	Li-6	CS6777	Kranz	50,3833	8,0666	GER
CS28461	CS28461	7231	Li-7	CS6778	Kranz	50,3833	8,0666	GER
CS28495	CS28495	7244	Mnz-0	CS6794	Kranz	50,001	8,26664	GER
CS28490	CS28490	7252	Mc-0	CS1362	Kranz	54,6167	-2,3	UK
CS28492	CS28492	7255	Mh-0	CS6792	Kranz	50,95	7,5	POL
CS28573	CS28573	7258	Nw-0	CS6811	Kranz	50,5	8,5	GER
CS28575	CS28575	7260	Nw-2	CS6813	Kranz	50,5	8,5	GER
CS28578	CS28578	7263	Nz1	CS22661	Campanella	-37,7871	175,283	NZL
CS28568	CS28568	7270	Nok-1	CS6808	Kranz	52,24	4,45	NED
CS28564	CS28564	7275	No-0	CS3081	Kranz	51,0581	13,2995	GER
CS28580	CS28580	7277	Ob-1	CS6817	Kranz	50,2	8,5833	GER
CS28583	CS28583	7280	Old-1	CS6820	Kranz	53,1667	8,2	GER
CS28587	CS28587	7282	Or-0	CS6822	Kranz	50,3827	8,01161	GER
CS28848	CS28848	7283	Ors-1	CS22672	Butnaru	44,7203	22,3955	ROU
CS28849	CS28849	7284	Ors-2	CS22673	Butnaru	44,7203	22,3955	ROU
CS28595	CS28595	7291	Pa-2	CS6826	Kranz	38,07	13,22	ITA
CS28640	CS28640	7300	Pla-0	CS6834	Kranz	41,5	2,25	ESP
CS28650	CS28650	7306	Pog-0	CS6842	Kranz	-49,2655	-123,206	CAN
CS28645	CS28645	7307	Pn-0	CS6838	Kranz	-48,0653	-2,96591	FRA
CS28651	CS28651	7310	Pr-0	CS6841	Kranz	50,1448	8,60706	GER
CS28685	CS28685	7316	Rhen-1	CS22536	Koornneef	51,9667	5,56667	NED

CS28692	CS28692	7320	Rou-0	CS6847	Kranz	49,4424	1,09849	FRA
CS28724	CS28724	7330	Sapporo-0	CS22456	Hanzawa	43,0553	141,346	JPN
CS28734	CS28734	7331	Sh-0	CS6860	Kranz	51,6832	10,2144	GER
CS28729	CS28729	7333	Sei-0	CS6853	Kranz	46,5438	11,5614	ITA
CS28739	CS28739	7337	Si-0	CS6861	Kranz	50,8738	8,02341	GER
CS28725	CS28725	7340	Sav-0	CS6856	Kranz	49,1833	15,8833	CZE
CS28743	CS28743	7343	Sp-0	CS6862	Kranz	52,5339	13,181	GER
CS28732	CS28732	7344	Sg-1	CS6858	Kranz	47,6667	9,5	GER
CS28750	CS28750	7346	Ste-0	CS6864	Kranz	52,6058	11,8558	GER
CS28786	CS28786	7351	Ty-0	CS6878	Kranz	-56,4278	-5,23439	UK
CS28758	CS28758	7353	Tha-1	CS22537	Koornneef	52,08	4,3	NED
CS28759	CS28759	7354	Ting-1	CS22549	Koornneef	56,5	14,9	SWE
CS28760	CS28760	7355	Tiv-1	CS22525	Koornneef	41,96	12,8	ITA
CS28779	CS28779	7372	Tscha-1	CS22518	Koornneef	47,0748	9,9042	AUT
CS28780	CS28780	7373	Tsu-0	CS6874	Kranz	34,43	136,31	JPN
CS28787	CS28787	7378	Uk-1	CS6879	Kranz	48,0333	7,7667	GER
CS28788	CS28788	7379	Uk-2	CS6881	Kranz	48,0333	7,7667	GER
CS28795	CS28795	7382	Utrecht	CS6150	Willemsen	52,0918	5,1145	NED
CS28800	CS28800	7384	Ven-1	CS22538	Koornneef	52,0333	5,55	NED
CS28808	CS28808	7390	Wag-3	CS22542	Koornneef	51,9666	5,6666	NED
CS28809	CS28809	7391	Wag-4	CS22543	Koornneef	51,9666	5,6666	NED
CS28810	CS28810	7392	Wag-5	CS22544	Koornneef	51,9666	5,6666	NED
CS28804	CS28804	7394	Wa-1	CS6885	Kranz	52,3	21	POL
CS28823	CS28823	7397	Ws	CS915	Kranz	52,3	30	RUS

CS28814	CS28814	7405	Wc-2	CS6887	Kranz	52,6	10,0667	GER
CS28833	CS28833	7408	Wt-3	CS6894	Kranz	52,3	9,3	GER
CS28822	CS28822	7411	Wl-0	CS6920	Kranz	47,9299	10,8134	GER
CS28847	CS28847	7418	Zu-1	CS6903	Kranz	47,3667	8,55	SUI
CS28369	CS28369	7424	Jl-3	CS6745	Kranz	49,2	16,6166	CZE
CS28527	CS28527	7430	Nc-1	CS6802	Kranz	48,6167	6,25	FRA
CS28510	CS28510	7446	N4	CS22482	Savushkin	61,36	34,15	RUS
CS28513	CS28513	7449	N7	CS22485	Savushkin	61,36	34,15	RUS
CS28201	CS28201	7460	Da(1)-12	CS917	Vizir	<Null>	<Null>	CZE
CS28720	CS28720	7472	S96	CS914	Administrator	<Null>	<Null>	UNK
CS28812	CS28812	7477	WAR	CS8143	Pigliucci	41,7302	-71,2825	USA
CS28610	CS28610	7479	PHW-10	CS6055	Williams	51,2878	0,0565	UK
CS28613	CS28613	7482	PHW-13	CS6060	Williams	51,2878	0,0565	UK
CS28614	CS28614	7483	PHW-14	CS6061	Williams	51,2878	0,0565	UK
CS28620	CS28620	7490	PHW-20	CS6071	Williams	51,2878	0,0565	UK
CS28622	CS28622	7492	PHW-22	CS6075	Williams	51,4167	-1,7167	UK
CS28626	CS28626	7496	PHW-26	CS6081	Williams	50,6728	-3,8404	UK
CS28628	CS28628	7498	PHW-28	CS6083	Williams	50,35	-3,5833	UK
CS28631	CS28631	7502	PHW-31	CS6088	Williams	51,4666	-3,2	UK
CS28633	CS28633	7504	PHW-33	CS6092	Williams	52,25	4,5667	NED
CS28635	CS28635	7506	PHW-35	CS6096	Williams	48,6103	2,3086	FRA
CS28636	CS28636	7507	PHW-36	CS6098	Williams	48,6103	2,3086	FRA
CS28637	CS28637	7508	PHW-37	CS6099	Williams	48,6103	2,3086	FRA

CS28713	CS28713	7514	RRS-7	CS22564	Dritz	41,5609	-86,4251	USA
ME627-4Y1	CS76086	7571	627ME-4Y1	NA	Bergelson	42,093	-86,359	USA
2*Lis-2	CS76170	8222	Lis-2	<Null>	Nordborg	56	14,7	SWE
2*Bro 1-6	CS76102	8231	Bra1-6	<Null>	Nordborg	56,3	16	SWE
2*Gul 1-2	CS76138	8234	Gul1-2	<Null>	Nordborg	56,3	16	SWE
2*Hod	CS76141	8235	Hod	<Null>	Nordborg	48,8	17,1	CZE
2*HSm	CS76146	8236	HSm	<Null>	Nordborg	49,33	15,76	CZE
2*Koln	CS76155	8239	Kaln	CS6003	Williams	51	7	GER
2*Kulture	CS76156	8240	Kulturen-1	<Null>	Nordborg	55,705	13,196	SWE
2*Liarum	CS76166	8241	Liarum	<Null>	Nordborg	55,95	13,85	SWE
2*Lillo-1	CS76167	8242	Lilla-1	<Null>	Nordborg	56,1512	15,7844	SWE
2*cs6034	CS76212	8244	PHW-34	N6034	Williams	48,6103	2,3086	FRA
2*NC-6	CS76196	8246	NC-6	<Null>	Bergelson	35	-79,18	USA
1*Sha	CS76227	8248	Shahdara	CS22652	Vizir	38,35	68,48	TJK
1*Ag-0	CS76087	8251	Ag-0	CS22630	Kranz	45	1,3	FRA
2*Alc-0	CS76088	8252	Alc-0	N1656	Roldan	40,31	-3,22	ESP
1*An-1	CS76091	8253	An-1	CS22626	Kranz	51,2167	4,4	BEL
2*Ba 1-2	CS76093	8256	Ba1-2	<Null>	Nordborg	56,4	12,9	SWE
1*Bay-0	CS76094	8260	Bay-0	CS22633	Kranz	49	11	GER
2*Bg-2	CS76096	8261	Bg-2	CS22342	Winterer	47,6479	-122,305	USA
2*Bla-1	CS76097	8264	Bla-1	N971	Kranz	41,6833	2,8	ESP
2*Blh-1	CS76098	8265	Blh-1	N1031	Kranz	48	19	CZE
1*Bor-4	CS76100	8268	Bor-4	CS22591	Nordborg	49,4013	16,2326	CZE
1*Br-0	CS76101	8269	Br-0	CS22628	Kranz	49,2	16,6166	CZE
2*Bu-0	CS76103	8271	Bu-0	N1007	Kranz	50,5	9,5	GER
1*Bur-0	CS76105	8272	Bur-0	CS22656	Kranz	54,1	-6,2	IRL
1*C24	CS76106	8273	C24	CS22620	Kranz	41,25	-8,45	POR
2*Can-0	CS76109	8274	Can-0	N1065	Hauser	29,2144	-13,4811	ESP

2*Cen-0	CS76110	8275	Cen-0	N1067	Kranz	49	0,5	FRA
1*Cibc-17	CS76111	8276	CIBC-17	CS22603	Crawley	51,4083	-0,6383	UK
1*Col-0	CS76113	8279	Col-0	CS22625	Kranz	38,3	-92,3	USA
1*CT-1	CS76114	8280	Ct-1	CS22639	Kranz	37,3	15	ITA
1*Cvi-0	CS76116	8281	Cvi-0	CS22614	Kranz	15,1111	-23,6167	CPV
2*Dra 3-1	CS76117	8283	Dra3-1	<Null>	Nordborg	55,76	14,12	SWE
2*DraII-1	CS76118	8284	DraII-1	<Null>	Nordborg	49,4112	16,2815	CZE
1*Eden-2	CS76125	8287	Eden-2	CS22573	Nordborg	62,877	18,177	SWE
1*Edi-0	CS76126	8288	Edi-0	CS22657	Kranz	56	-3	UK
1*Est-1	CS76127	8291	Est-1	CS22629	Kranz	58,3	25,3	RUS
1*Fab-4	CS76128	8293	Fab-4	CS22577	Nordborg	63,0165	18,3174	SWE
1*Fei-0	CS76129	8294	Fei-0	CS22645	Alonso-Blanco	40,5	-8,32	POR
1*Ga-0	CS76133	8295	Ga-0	CS22634	Kranz	50,3	8	GER
2*Gd-1	CS76134	8296	Gd-1	N1185	Kranz	53,5	10,5	GER
2*Ge-0	CS76135	8297	Ge-0	N1187	Kranz	46,5	6,08	SUI
1*Got-7	CS76136	8299	Got-7	CS22608	RÃbbelen	51,5338	9,9355	GER
2*Gr-1	CS76137	8300	Gr-1	N1199	Hauser	47	15,5	AUT
1*Gy-0	CS76139	8302	Gy-0	CS22631	Kranz	49	2	FRA
2*Hi-0	CS76140	8304	Hi-0	N1227	Kranz	52	5	NED
2*Hov 4-1	CS76142	8306	Hov4-1	<Null>	Nordborg	56,1	13,74	SWE
1*HR-5	CS76144	8309	HR-5	CS22596	Crawley	51,4083	-0,6383	UK
2*Hs-0	CS76145	8310	Hs-0	N1237	Kranz	52,24	9,44	GER
2*In-0	CS76147	8311	In-0	N1239	Kranz	47,5	11,5	AUT
2*Ka-0	CS76149	8314	Ka-0	N1267	Kranz	47	14	AUT
1*Kin-0	CS76153	8316	Kin-0	CS22654	Kranz	44,46	-85,37	USA
1*Kno-18	CS76154	8318	Kno-18	CS22567	Bergelson	41,2816	-86,621	USA
2*Lc-0	CS76159	8323	Lc-0	N1307	Kranz	57	-4	UK
1*Ler-1	CS76164	8324	Ler-1	CS22618	Koornneef	47,984	10,8719	GER
2*Lip-0	CS76168	8325	Lip-0	N1337	Kranz	50	19,3	POL

2*Lis-1	CS76169	8326	Lis-1	<Null>	Nordborg	56	14,7	SWE
1*LL-0	CS76172	8328	LL-0	CS22650	Kranz	41,59	2,49	ESP
2*Lm-2	CS76173	8329	Lm-2	N1345	Kranz	48	0,5	FRA
1*LP2-2	CS76176	8332	Lp2-2	CS22594	Cetl	49,38	16,81	CZE
1*LP2-6	CS76177	8333	Lp2-6	CS22595	Cetl	49,38	16,81	CZE
2*Lund	CS76178	8335	Lund	<Null>	Nordborg	55,71	13,2	SWE
1*LZ-0	CS76179	8336	Lz-0	CS22615	Kranz	46	3,3	FRA
1*Mr-0	CS76190	8338	Mr-0	CS22640	Kranz	44,15	9,65	ITA
1*Mrk-0	CS76191	8339	Mrk-0	CS22635	Kranz	49	9,3	GER
1*Mt-0	CS76192	8341	Mt-0	CS22642	Kranz	32,34	22,46	LIB
1*Mz-0	CS76193	8342	Mz-0	CS22636	Kranz	50,3	8,3	GER
2*Na-1	CS76195	8343	Na-1	N1385	Kranz	47,5	1,5	FRA
1*Nd-1	CS76197	8344	Nd-1	CS22619	Kranz	50	10	SUI
1*NFA-10	CS76198	8345	NFA-10	CS22599	Crawley	51,4083	-0,6383	UK
1*NFA-8	CS76199	8346	NFA-8	CS22598	Crawley	51,4083	-0,6383	UK
1*Omo2-1	CS76200	8349	A–ma2-1	CS22584	Nordborg	56,14	15,78	SWE
2*Ost-0	CS76202	8351	Ost-0	N1431	Kranz	60,25	18,37	SWE
1*OY-0	CS76203	8352	Oy-0	CS22658	Kranz	60,23	6,13	NOR
2*Pa-1	CS76204	8353	Pa-1	N1439	Kranz	38,07	13,22	ITA
2*Per-1	CS76210	8354	Per-1	N1445	Kranz	58	56,3167	RUS
2*Petergo	CS76211	8355	Petergof	N926	Vizir	59	29	RUS
1*PNA-17	CS76213	8359	Pna-17	CS22570	Bergelson	42,0945	-86,3253	USA
1*Pro-0	CS76214	8360	Pro-0	CS22649	Bergelson	43,25	-6	ESP
1*Pu 2-23	CS76215	8361	Pu2-23	CS22593	Cetl	49,42	16,36	CZE
1*Ra-0	CS76216	8364	Ra-0	CS22632	Kranz	46	3,3	FRA
2*Rak-2	CS76217	8365	Rak-2	N1485	Kranz	49	16	CZE
1*REN-1	CS76218	8367	Ren-1	CS22610	RÃ¶bbeln	48,5	-1,41	FRA
1*RMXA180	CS76220	8371	Rmx-A180	CS22569	Bergelson	42,036	-86,511	USA
CS22689	CS22689	8372	RRS-10	<Null>	Dritz	41,5609	-86,4251	USA
2*Rsch-4	CS76222	8374	Rsch-4	CS1494	Holub	56,3	34	RUS

2*Sanna-2	CS76223	8376	Sanna-2	<Null>	Nordborg	62,69	18	SWE
2*Sap-0	CS76224	8378	Sap-0	N1507	Kranz	49,49	14,24	CZE
1*Se-0	CS76226	8379	Se-0	CS22646	Kranz	38,3333	-3,53333	ESP
1*SQ-8	CS76230	8385	Sq-8	CS22601	Crawley	51,4083	-0,6383	UK
2*St-0	CS76231	8387	St-0	N1535	Kranz	59	18	SWE
2*Ta-0	CS76242	8389	Ta-0	N1549	Kranz	49,5	14,5	CZE
1*TAMM-2	CS76244	8390	Tamm-2	CS22604	Savolainen	60	23,5	FIN
1*Ts-1	CS76268	8392	Ts-1	CS22647	Kranz	41,7194	2,93056	ESP
1*Ull 2-3	CS76293	8396	Ull2-3	CS22587	Nordborg	56,0648	13,9707	SWE
1*Ull 2-5	CS76294	8397	Ull2-5	CS22586	Nordborg	56,0648	13,9707	SWE
1*Uod 7	CS76296	8399	Uod-7	CS22613	Koch	48,3	14,45	AUT
1*Van-0	CS76297	8400	Van-0	CS22627	Kranz	49,3	-123	CAN
1*Var 2-1	CS76298	8401	Vayr2-1	CS22580	Nordborg	55,58	14,334	SWE
1*Wei-0	CS76301	8404	Wei-0	CS22622	Holub	47,25	8,26	SUI
1*Ws-0	CS76303	8405	Ws-0	CS22623	Kranz	52,3	30	RUS
1*Wt-5	CS76304	8407	Wt-5	CS22637	Kranz	52,3	9,3	GER
1*Yo-0	CS76305	8408	Yo-0	CS22624	Kranz	37,45	-119,35	USA
1*Zdr-6	CS76306	8410	Zdr-6	CS22589	Nordborg	49,3853	16,2544	CZE
2*Sav-0	CS76225	8412	Sav-0	CS1515	Kranz	49,1833	15,8833	CZE
2*Wil-1	CS76302	8419	Wil-1	N1595	Kranz	54,6833	25,3167	LTU
2*cs6041	CS76152	8420	Kelsterbach-4	CS6041	Williams	50,0667	8,5333	GER
2*Fja 1-1	CS76130	8422	Fja1-1	<Null>	Nordborg	56,06	14,29	SWE
1*Kas-1	CS76150	8424	Kas-1	CS6751	Somerville	35	77	IND
1*22491	CS76194	8429	N13	CS22491	Savushkin	61,36	34,15	RUS
2*Lisse	CS76171	8430	Lisse	CS6033	Williams	52,25	4,5667	NED
11ME1.32	CS76083	8610	11ME1.32	NA	Bergelson	42,093	-86,359	USA

328PNA054	CS76085	8692	328PNA054	NA	Bergelson	42,0945	-86,3253	USA
1PNA4.101	CS76084	8796	11PNA4.101	NA	Bergelson	42,0945	-86,3253	USA